STUDIES OF THE NEUROIMMUNE

RESPONSE IN CANCER-INDUCED PAIN

STUDIES OF THE NEUROIMMUNE

RESPONSE IN CANCER-INDUCED PAIN

By TANYA MILADINOVIC, M.Sc., H.B.A.

A Thesis

Submitted to the School of Graduate Studies

in Partial Fulfilment of the Requirements

for the Degree

Doctor of Philosophy

DOCTOR OF PHILOSOPHY (2019) McMaster University

Medical Sciences Hamilton, Ontario, Canada

TITLE: Studies of the neuroimmune response in cancer-induced pain

AUTHOR: Tanya Miladinovic, M.Sc. (Wilfrid Laurier University), B.A. (HONOURS; Wilfrid Laurier University)

SUPERVISOR: Professor Gurmit Singh, Ph.D.

NUMBER OF PAGES: xxvi, 239

LAY ABSTRACT

Cancer-induced pain (CIP) is a debilitating condition that accompanies late-stage metastatic cancer. Clinically, achieving analgesia often comes at the expense of patients' quality of life, as current therapeutics fail to adequately manage this pain and induce dose-dependent side effects. Cancer cells secrete excess amounts of glutamate, a signalling molecule involved in CIP, which can activate immune cells called microglia within the spinal cord. Mice that demonstrate tumour-induced pain exhibit an amplified immune response that manifests through the activation pattern and quantity of microglia within the spinal cord, as well as brain regions implicated in pain and distress. Pharmacologically blocking glutamate release from cancer cells limits this pain response, in addition to several physiological indicators of pain, including microglial activation in the central nervous system. Changes in microglia-related glutamate signalling may reflect the emotional problems reported by patients with CIP. Better understanding the mechanisms of CIP will help generate more comprehensive treatment approaches.

ABSTRACT

Cancer-induced pain (CIP) is a debilitating condition that accompanies late-stage cancer for the majority of patients. The work presented in this dissertation addresses the multifaceted role of glutamate in cancer cell-induced pain signalling and provides several potential therapeutic directions. Several cell types, including breast cancer cells and microglia, release glutamate via the system x_C^- antiporter. To limit the excitotoxic tendency of breast cancer cells to release glutamate in excess, we first indirectly inhibited xCT, the active subunit of system x_C^-, with the TrkA inhibitor AG879. We demonstrated that the system x_C^- antiporter is functionally influenced by the actions of nerve growth factor on its cognate receptor, TrkA, and that inhibiting this complex reduced CIP via downstream actions on xCT. Co-culture studies then demonstrated the direct effect of glutamate released by wildtype MDA-MB-231 carcinoma cells on microglial activation, as well as functional system x_C^- activity, while knockdown of xCT in MDA-MB-231 cells mitigated microglial activation and cystine uptake. Blockade of system x_C^- with sulfasalazine attenuated nociception in an immunocompetent murine model of CIP and inhibited tumour-induced microglial activation in the dorsal horn of the spinal cord. Finally, tumour-induced nociceptive behaviors appeared to progress in parallel with microglial activation in the hippocampus, and ablating microglia delayed the onset and severity of tumour-induced nociceptive behaviours, confirming that microglia are implicated

in CIP and regional microglia are influenced by this pain. This is the first experimental evidence to demonstrate the effects of peripheral tumour on hippocampal microglial activation in relation to cancer-related nociception. These data collectively demonstrate that the system x_C^- antiporter is functionally implicated in CIP and may be particularly relevant to pain progression through spinal microglia. Upregulated xCT in chronically activated microglia may be one pathway to central glutamate cytotoxicity. Therefore, microglial xCT may therefore be a valuable target for mitigating CIP.

PREFACE

This dissertation is presented as a sandwich thesis. Each manuscript is presented as a separate chapter and includes a preface detailing each author's contributions, as well as a description of the underlying context for the manuscript. Chapter 1 provides a conceptual overview and comprehensive background information on the pathophysiology of pain, the effect of peripheral tumour cells in the context of nociception, and the role of glutamate in mediating this pain state. The three chapters that follow (Chapters 2, 3, and 4) detail experiments that were performed during the author's Ph.D. candidacy. A concluding chapter (Chapter 5) summarizes the major findings of this dissertation and discusses future directions to be considered in the study of cancer-induced pain.

Literature cited within each manuscript (Chapters 2-4) are independent and consistent with the requirements of their respective journals. Literature cited elsewhere (Chapters 1 and 5) use the American Psychological Association (6th edition) style and appear in a separate References section at the end of the dissertation. Note that as per corresponding journal requirements, Chapters 3 and 4 use American spelling and grammatical conventions, while text used elsewhere conforms to Canadian English standards. Appendices are included following the body of this dissertation, which provide detailed protocols and describe relevant optimization experiments used in this research in cases where journal length

restrictions did not allow for such detailed methodological description (Appendix 1), as well as details of co-authored papers not included in the body of this dissertation (Appendix 2).

ACKNOWLEDGEMENTS

Firstly, I would like to express my deepest gratitude to my supervisor, Dr. Gurmit Singh, for enthusiastically accepting me into his lab and providing a platform to explore my scientific curiosities. Dr. Singh has refined the art of generating scientists from students. I can say with confidence that his mentorship has shaped my approach to scientific inquiry. His counsel to “remain focused” has been instrumental to this body of work and is a lesson I will carry with me beyond his lab. I would also like to thank Dr. Snezana Popovic and Dr. Laurie Doering for serving on my Supervisory Committee. I have had the pleasure of collaborating with Dr. Popovic, and she has provided invaluable clinical input on the histological component of the manuscripts within this dissertation. Dr. Doering has provided incredibly constructive feedback and asked challenging questions to guide and refine my project. I am grateful for the presence of each of my committee members in my academic career, as well as for their candor throughout the development of this dissertation. Their coaching has contributed to the evolution of this thesis and made me a better scientist.

To Katja Linher-Melville, thank you for sharing your unparalleled expertise and for finding the patience to explain theoretical and technical intricacies to me. To the ever-glowing Natalie Zacal, thank you for your unyielding optimism and for spending endless hours troubleshooting with me over histological techniques. To Robert Ungard, My Ph.D. experience would have

been an entirely different four years without you. You have managed to not only keep me sane during this degree, but genuinely happy and eager to spend long days in the lab. You have made a dramatic impact on this dissertation and my life. I would also like to thank the entire Singh Lab family, past and present; Jennifer Fazzari, Yong Fang Zhu, Manu Sharma, Jesse Sidhu, Kimberly Young, Mina Nashed, Natalka Parzei, Franziska Miller, Hana Geres, Andy Phan, and all the amazing undergraduate students that I have had the pleasure of working with, thank you for making the last four years some of my very best. My appreciation also extends to the entire staff of McMaster's Central Animal Facility and the McMaster University support staff – without your dedication this work would not have been possible.

To my fantastically supportive and wildly enthusiastic friends beyond the lab, thank you for your words of encouragement, for all the love and support you have shared with me leading up to this point, for entertaining my long-winded answers about the world of scientific research, and for providing escape in the form of exclusively non-lab-related escapades and laughing ourselves to tears. Thank you for sharing your beautiful souls with me.

To my forever-a-kid sister, Elana, you are a ray of sunshine to anyone privileged enough to know you. Thank you for sharing so much of your shine with me. My forever bestie, my confidant, my other other half, thank you for being my sister lobster. To my parents, who have shown me what it means to love

what you do, thank you for the sacrifices you have made to provide opportunity for Elana and I. Mama Nadj and Papa Ron, your commitment to your values and your drive to work hard is something I am proud to model. Thank you for giving me the fundamentals to make the journey to where I am today.

Lastly, I would like to thank my darling husband, Rastko. Endless love, appreciation, and gratitude for your continued encouragement, patience, and acceptance throughout this extended period of madness in our lives. Your unyielding support over the past four years has been the backbone of my perseverance through this degree. Your determination to excel in everything you choose to, your words of encouragement, and your interest in the minute details of this dissertation continue to amaze me. Thank you, Sweetness. You are my inspiration, my rock, my everything. I am so excited to write our next chapter together.

TABLE OF CONTENTS

Lay Abstract ..... *iii*

Abstract ..... *iv*

Preface ..... *vi*

Acknowledgements ..... *viii*

List of Figures and Tables ..... *xix*

List of Abbreviations and Symbols ..... *xxii*

Declaration of Academic Achievement ..... *xxv*

Chapter 1 ..... *1*

Preface **2**

Context and Background Information **2**

Cancer-induced Pain **4**

Role of Glutamate in CIP **5**

Glutamate Receptors **7**

Glutamate Transporters **8**

Glutamate Dysregulation in CIP **9**

System x_C^- 9

Nerve Growth Factor..... 10

Microglia in the Naïve CNS 12

Microglia in the Diseased CNS 14

Microglial Glutamate 15

The Affective Component of Pain Perception..... 17

Hypothesis and Objectives 19

Chapter 2 25

Preface..... 26

Context and Background Information 27

Abstract..... 30

Keywords 31

Introduction..... 32

Materials and Methods..... 35

In Vitro 35

In vivo..... 40

Ex Vivo 45

Statistical Analyses 46

Results 49

In Vitro 49

In vivo 51

Ex Vivo 51

Discussion 53

Acknowledgements 59

Conflict of Interest 59

References 60

Chapter 3 87

Preface 88

Context and Background Information 88

Abstract 92

Introduction 94

Methods 96

Cell cultures 96

Animals 97

Behavioural Test of Nociception 97

Tumour Allografts 98

Drug Treatments 99

Transcardial Perfusion and Tissue Collection 99

Immunofluorescence 99

Co-cultures 100

In Vitro Cell Treatments 101

Co-culture Cystine Uptake 101

Immunocytochemistry 102

Western Blotting 102

Statistical Analyses 103

Results 104

Blockade of System xC- with SSZ attenuates CIP 104

Peripheral Tumour Alters Spinal Microglial Activity 105

MDA-MB-231-released Glutamate Activates Microglia *In Vitro* 105

MDA-MB-231-released Glutamate Increases Microglial Cystine Uptake 106

MDA-MB-231 Carcinoma Cells Alter Microglial Protein Expression *In Vitro*....106

Discussion 107

Acknowledgements 114

Disclosure..... 114

References..... 115

Chapter 4 134

Preface..... 135

Context and Background Information 135

Abstract..... 139

Keywords 141

Introduction..... 142

Materials and methods 145

Cell Culture 145

Crystal Violet 145

Mice 146

Experimental Design..... 146

Spontaneous Nociception..... 148

Evoked Nociception 148

Transcardial Perfusion and Tissue Collection 149

Radiographic Analysis 150

Hematoxylin and Eosin 151

Immunofluorescence 151

RNA Isolation 151

Quantitative Real-time PCR 152

Statistical Analyses 153

Results 154

Pexidartinib Does Not Significantly Alter Tumor Cell Growth 155

Peripheral Tumor Increases Activated Microglia in DG and CA1 155

Peripheral Tumor Decreases Hippocampal Neural Activity 156

Pexidartinib Attenuates Tumor-induced Nociceptive Behaviors 156

Pexidartinib Does Not Significantly Alter Tumor Invasion 157

Peripheral Tumor Alters Hippocampal mRNA 157

Discussion 159

Conclusions 165

Acknowledgements **166**

Disclosure **166**

References **167**

Chapter 5 ..... ***191***

Summary **192**

Future Directions **202**

Conclusions **206**

References **208**

Appendix 1: General Materials and Methods ***240***

Preface **241**

Cell Cultures and Treatments **242**

Co-cultures **245**

^{14}C-Cystine Uptake **246**

Bio-Rad Protein Assay **249**

Amplex Red **251**

Co-Culture ^{14}C-Cystine Uptake **254**

Quantitative Real-Time RT-PCR..... 256

Fluorescent Immunocytochemistry..... 258

Tissue Collection and Preservation / *Ex Vivo* Immunofluorescence..... 260

Appendix 2: Co-authored Papers and Other Published Works..... 269

Oncodynamics: Effects of Cancer Cells on the Body 270

Glutamate Dysregulation in Central Pathologies 271

Preparation of tetrazine-containing [2 + 1]… Diels-Alder chemistry..... 272

LIST OF FIGURES AND TABLES

CHAPTER 1

Figure 1. Schematic summarizing mechanisms of cancer-induced pain 23

CHAPTER 2

Figure 2.1. System x_C^--mediated glutamate is regulated by TrkA signalling. 73

Figure 2.2. β-NGF and AG879 do not affect 4T1 carcinoma cell metabolism ... 74

Figure 2.3. AG879 attenuates β-NGF-induced increase in xCT in 4T1 cells..... 75

Figure 2.4. AG879 inhibits β-NGF-induced xCT mRNA in 4T1 cells 77

Figure 2.5. AG879 inhibits β-NGF-induced functional system x_C^- activity..... 78

Figure 2.6. AG879 delays the onset and severity of nociceptive behaviours 79

Figure 2.7. AG879 delays time until behavioural decline 80

Figure 2.8. AG879 attenuates tumour-induced femoral osteolysis..... 82

Figure 2.9. AG879 inhibits xCT expression in 4T1 murine carcinoma cells 83

Table 2.1. AG879 concentration-dependently decreases cancer cell number..... 85

Table 2.2. xCT primers used for relative qPCR. 86

CHAPTER 3

Figure 3.1. Blockade of System xC- with SSZ attenuates CIP..... 127

Figure 3.2. Dorsal horn microglial xCT increases in tumour-bearing mice 128

Figure 3.3. Immunocytochemical staining of xCT and Iba1 in microglia..... 130

Figure 3.4. Glutamate increases microglial functional system x_C^- activity..... 131

Figure 3.5. LPS alters microglial protein levels..... 132

Table 3.1. Antibodies Utilized for Western Blotting 133

CHAPTER 4

Figure 4.1. Timeline of in vivo experiments..... 177

Figure 4.2. Hippocampal Microdissection Methodology 178

Figure 4.3. CSF1R inhibition does not alter 4T1 breast cancer cell number..... 179

Figure 4.4. Peripheral Tumors Increase Activated Microglia in Hippocampus 180

Figure 4.5. Double-label immunofluorescent staining of Iba1 and xCT 182

Figure 4.6. Pexidartinib decreases spontaneous nociceptive behaviors..... 183

Figure 4.7. Pexidartinib decreases evoked nociceptive behaviors..... 184

Figure 4.8. Pexidartinib does not alter tumor-induced femoral osteolysis 185

Figure 4.9. Intrafemoral tumors increase hippocampal microglial markers 186

Figure 4.10. Peripheral tumors alter select hippocampal mRNA 188

Table 4.1. Primers used for relative qPCR analysis..... 189

Table 4.2. Housekeeping gene primers used for relative qPCR analysis..... 190

LIST OF ABBREVIATIONS AND SYMBOLS

AMPA	α-amino-3-hydroxy-5-methyl-4-isoxazolepropionic acid
APA	American Psychiatric Association
AREB	Animal Research Ethics Board
BBB	Blood brain barrier
BDNF	Brain-derived neurotrophic factor
CA1	Cornu Ammonis 1
CIBP	Cancer-induced bone pain
CIP	Cancer-induced pain
CNS	Central nervous system
CTCF	Corrected total cell fluorescence
DG	Dentate gyrus
DMSO	Dimethyl sulfoxide
DNA	Deoxyribonucleic acid
DPA	Dynamic Plantar Aesthesiometer

DWB	Dynamic Weight Bearing
EDTA	Ethylenediaminetetraacetic acid
FBS	Fetal bovine serum
GluR	Glutamate receptor
GSH	Glutathione
HBSS	Hanks' Balanced Salt solution
NaOH	Sodium hydroxide
NBF	Neutral buffered formalin
NGF	Nerve growth factor
NH_4OH	Ammonium hydroxide
NMDA	N-methyl-D-aspartate
PBS	Phosphate buffered saline
PFA	Paraformaldehyde
Polr2b	Polymerase II polypeptide B
PVDF	Polyvinylidene difluoride
qPCR	Quantitative real-time PCR

RNA	Ribonucleic acid
ROS	Reactive oxygen species
RPMI	Roswell Park Memorial Institute medium
SDHA	Succinate Dehydrogenase Complex Flavoprotein Subunit A
SNI	Spared nerve injury
SSZ	sulfasalazine
Taf1b	TATA box binding protein-associated factor
TLR-4	Toll like receptor 4
TrkA	Tropomyosin receptor kinase A

DECLARATION OF ACADEMIC ACHIEVEMENT

This doctoral dissertation is presented as a sandwich thesis and consists of three manuscripts that were prepared for publication during the author's Ph.D. candidacy. Chapter 1 provides a general introduction to this collection of studies. Of the chapters that follow, two manuscripts have been published (Chapters 2 and 4), and one manuscript has been accepted for publication and is *in press* (Chapter 3), as follows:

Miladinovic T, Ungard RG, Linher-Melville K, Popovic S, Singh G. (2018). Functional effects of TrkA inhibition on system x_C^--mediated glutamate release and cancer-induced bone pain. *Molecular Pain, 14*(1), 1–15.

Miladinovic T, Singh G. (2019). Spinal Microglia Contribute to Cancer-induced Pain Through System x_C^--mediated Glutamate Release. *In Press.*

Miladinovic T, Sharma M, Phan A, Geres H, Ungard RG, Linher-Melville K, Singh G. (2019). Activation of hippocampal microglia in a murine model of cancer-induced pain. *Journal of Pain Research*, *12:* 1003–1016.

Additionally, I co-authored the following three publications (shared first authorship of one review paper, first author to one book chapter, and co-author to one peer-reviewed paper, respectively) during my Ph.D. candidacy:

Miladinovic T, Nashed MG, Singh G. (2015). Overview of Glutamatergic Dysregulation in Central Pathologies. *Biomolecules*, 5(4), 3112- 3141.

Miladinovic T, Singh, G. (2016).Cancer-induced Neurogenesis. In G. Singh (Ed.), Oncodynamics: Effects of Cancer Cells on the Body (pp. 55-71). Cham: Springer International Publishing, Switzerland.

Yazdani A1, Janzen N, Czorny S, Ungard RG, **Miladinovic T**, Singh G, Valliant JF. (2017). Preparation of tetrazine-containing [2 + 1] complexes of ^{99}mTc and in vivo targeting using bioorthogonal inverse electron demand Diels-Alder chemistry. *Dalton Trans*., 46(42), 14691-14699.

CHAPTER 1

Introduction

Preface

In this chapter, I introduce the concepts underlying the main thesis through a comprehensive review of the relevant literature and provide the rationale to the work generated within this dissertation. For this chapter, I performed a literature review inclusive of all topics discussed. I wrote this chapter of the thesis, generated the figures within, and modified the material based on editorial suggestions. Dr. Gurmit Singh provided constructive feedback and academic direction.

Context and Background Information

This chapter begins with an introduction highlighting the prevalence of pain in the cancer patient population and the failure of current therapeutic options to manage this pain. A current understanding of cancer-related pain is discussed, with several potential underlying mechanisms considered, including inflammatory, neuropathic, and bone-specific fundamental processes. This discussion covers the involvement of glutamate in the pain state, including a comprehensive discussion of glutamate receptors and the exchange of glutamate for cystine through the system x_C^- antiporter, as well as neurotrophic influences as they relate to cancer pain. I then discuss the involvement of the neuroimmune response in this pain state, with emphasis on microglial signalling within specific regions of the spinal cord relevant to several pain states, including neuropathic

and cancer-induced nociception. The chapter closes with a discussion of the affective component of pain, also described as the perceptive complement to sensation, with specific reference to the role of hippocampal brain regions in this affective response.

The final section of this chapter outlines the remaining chapters of this thesis, in brief, and introduces the overall implications of each scholarly work, as they pertain to the overall thesis herein presented.

Cancer-induced Pain

Breast cancer has a propensity to metastasize to the bone, causing severe CIP and reduced quality of life. Bone is one of the most common sites of metastases, particularly in lung, breast, and prostate cancer (Mundy, 2002), occurring in approximately 70% of metastatic breast and prostate cancers (Coleman, 1997; Guise, 2010). Accordingly, the effective management of CIP is essential to improving quality of life for cancer patients. Clinically, achieving analgesia often comes at the expense of patients' quality of life; current treatment options often induce severe dose-dependent side effects and fail to adequately manage advanced breast CIP, as this pain manifests in highly heterogeneous ways as a cumulative result of varied pathological mechanisms. The complexity of CIP is partly due to the unique properties of the affected tissue; osteoclastogenesis (Lozano-Ondoua, Symons-Liguori, & Vanderah, 2013), inflammation (Asai *et al*., 2005; Breese, George, Pauers, & Stucky, 2005), increased neurotrophic activity (W. G. Mantyh *et al*., 2010; Sevcik *et al*., 2005), demyelination (Inoue *et al*., 2004), and extracellular acidification (Asai *et al*., 2005) created by the presence of bone tumours have been implicated in the sensitization of surrounding nociceptors and may cumulatively contribute to cancer-induced hyperalgesia. Bone is highly vascularized, and supports a rich neuronal network beneath its surface, among cells that regulate its formation and degradation. Furthermore, increased osteoclastogenesis results in severe bone destruction and increased exposure of

neurovascular beds, leaving them vulnerable to amplified excitatory stimulation. Several contributing abnormalities may culminate in the experience of chronic pain. Of these underlying mechanisms, glutamate dysregulation is particularly pertinent to the development of CIP and is discussed at length below.

Role of Glutamate in CIP

Glutamate is an important signalling molecule and a major excitatory neurotransmitter in the mammalian central nervous system (CNS) (Fonnum, 1984). Central and peripheral glutamate signalling involves several transporters, as well as ionotropic and metabotropic receptors (Eulenburg & Gomeza, 2010; Kew & Kemp, 2005; H Sato, Tamba, Ishii, & Bannai, 1999). In addition to its critical role in the CNS, glutamate also contributes to autocrine and paracrine signalling in peripheral tissues such as bone, testis, pancreas, and the adrenal, pituitary and pineal glands (Hinoi, Takarada, Ueshima, Tsuchihashi, & Yoneda, 2004). Glutamate also plays an import role in peripherally-mediated nociceptive signalling to the CNS (Jang, Kim, Sang Nam, Se Paik, & Leem, 2004). Considering glutamate's widespread role in important central and peripheral processes, it is unsurprising that glutamate release, uptake, metabolism, and signalling are tightly regulated processes. Disturbances in these processes are often aetiologically associated with central pathologies (Meldrum, 2000).

Glutamate receptors (GluRs) are located on neuronal and non-neuronal cell types and regulate a broad range of processes. Under normal physiological conditions, glutamate is released as a neurotransmitter into the synaptic cleft and initiates the propagation of action potentials. Glutamate is largely found intracellularly, with relatively little (up to one million-fold less) found in the extracellular environment, which establishes the steep concentration gradient required for rapid synaptic transmission (Fonnum, 1984; Nicholls & Attwell, 1990; Schousboe, 1981).

Considerable metabolic commitment is devoted to regulating glutamate metabolism, uptake, and release (Reissner & Kalivas, 2010). Glutamate levels are tightly regulated by sodium-dependent glutamate transporters, which remove excess glutamate molecules from the extracellular fluid, and are predominantly present on surrounding astrocytes at the synapse (Danbolt, 2001; Grewer & Rauen, 2005; Tzingounis & Wadiche, 2007; Vandenberg & Ryan, 2013). Glutamate transporters maintain low concentrations of synaptic and extrasynaptic glutamate by using the established electrochemical gradients as the driving force for uptake to protect against excitotoxicity. At elevated extracellular concentrations, glutamate becomes neurotoxic and capable of degenerating target neurons. Under pathological conditions, extracellular glutamate exceeds normal levels and ionotropic glutamate receptors are overactive, triggering excitotoxicity

and cell death in surrounding postsynaptic neurons (Choi, 1994; Choi, Maulucci-Gedde, & Kriegstein, 1987).

Glutamate Receptors

Several types of GluRs have been identified through molecular cloning. Glutamate-gated ion channels comprise the ionotropic glutamate receptors (iGluRs). These ligand-gated ion channels include *N*-methyl-D-aspartate receptors (NMDARs), α-amino-3-hydroxy-5-methyl-4-isoxazole propionic acid receptors (AMPARs), and kainate receptors, named after the synthetic agonists that activate them. Like other ligand-gated channel receptors, iGLuRs are formed from the association of several protein subunits that combine in various ways to produce a large number of receptor isoforms.

In addition to the iGluRs, metabotropic glutamate receptors (mGluRs) indirectly modulate postsynaptic ion channels, consist of G-protein coupled receptors (mGluR1 – 8), which are further subdivided according to their activation by either (±)1-amino-cyclopentane-trans-1,3-dicarboxylic acid (trans-ACPD) or L(+)-2-amino-4-phosphonobutyric acid (L-AP4), and cause slower synaptic responses that can either increase or decrease postsynaptic potentials (Borges & Dingledine, 1998; Hollmann & Heinemann, 1994; Schoepfer *et al*., 1994).

Glutamate Transporters

To date, five plasma membrane glutamate transporter subtypes have been cloned: the excitatory amino acid transporters (EAATs) GLAST/EAAT1, GLT1/EAAT2, EAAC1/EAAT3, EAAT4, and EAAT5 (Arriza, Eliasof, Kavanaugh, & Amara, 1997; Kanai & Hediger, 1992; Pines *et al*., 1992; Storck, Schulte, Hofmann, & Stoffel, 1992). GLAST/EAAT1 is found primarily on astrocytes and oligodendrocytes and is the major glutamate transporter in the forebrain (Bar-Peled *et al*., 1997); GLT1/EAAT2 is found on astrocytes throughout the CNS (Bar-Peled *et al*., 1997); EAAC1/EAAT3 is found primarily on neurons in the hippocampus, basal ganglia, and cerebellum (Bar-Peled *et al*., 1997; Furuta, Martin, Lin, Dykes-Hoberg, & Rothstein, 1997); EAAT4 is found on Purkinje cells (Bar-Peled *et al*., 1997; Furuta *et al*., 1997); and EAAT5 on photoreceptors and bipolar cells (Arriza *et al*., 1997).

The cystine/glutamate antiporter system x_C^- is predominantly expressed on glial cells and is a critical regulator of non-synaptic extracellular glutamate levels (Baker, Xi, Shen, Swanson, & Kalivas, 2002). System x_C^-, a transporter that catalyses the release of glutamate in exchange for cystine uptake, is composed of two subunits: the 4F2 heavy chain glycoprotein *SLC3A2* and the specific xCT light chain subunit *SLC7A11* (McBean, 2002; H Sato *et al*., 1999). Imported cystine is reduced to cysteine, which is used in the intracellular production of the antioxidant glutathione (GSH) (Sagara, Miura, & Bannai, 1993). GSH plays an

important role in neutralizing reactive oxygen species (ROS), which are a by-product of oxidative metabolism in the CNS (Lo, Wang, & Gout, 2008).

Glutamate Dysregulation in CIP

Among other influences, it is clear that glutamate dysregulation (Seidlitz, Sharma, & Singh, 2010) and aberrant neurotrophic activity (Bloom *et al*., 2011; Juan Miguel Jimenez-Andrade, Ghilardi, Castañeda-Corral, Kuskowski, & Mantyh, 2011) may contribute to CIP through pathological osteoclastogenesis and sensitization. Considerable evidence suggests that glutamate released through system x_C^- is involved in multiple physiological and pathological processes, including CIP (Reviewed in (Miladinovic, Nashed, & Singh, 2015)); when glutamate efflux becomes excessive, its character within the nervous system switches from an excitatory transmitter to a well-characterized and pathologically-relevant excitotoxin (Choi, 1994; Choi *et al*., 1987). Glutamate dysregulation has been linked to pain in cancer patients, an effect which is supported by animal models of CIP (Slosky *et al*., 2016; Ungard, Seidlitz, & Singh, 2014).

System x_C^-

System x_C^- is a membrane-bound, sodium-independent, chloride-dependent antiporter of cystine and glutamate. The antiporter mediates the release of glutamate from the cell in exchange for cystine into the cell, where it is reduced

to cysteine, which is key to the synthesis of GSH. Given the exchange of cystine for glutamate, system x_C^- is a major determinant of ambient CNS glutamate, thereby activating metabotropic and ionotropic GluRs (Baker *et al*., 2002; Hardingham & Bading, 2010).

Pre-clinical data demonstrates that the absence of system x_C^- in mice decreases anxiety and depressive-like behavior (Bentea *et al*., 2015). Furthermore, genetic deletion of xCT attenuates peripheral and central inflammation and mitigates lipopolysaccharide (LPS)-induced sickness and depressive-like behavior in mice (Albertini *et al*., 2018).

Nerve Growth Factor

The neurotrophin nerve growth factor (NGF) acts via its cognate receptor Tropomyosin receptor kinase A (TrkA), through which it activates several downstream signaling pathways that regulate neuronal survival and differentiation. While breast epithelial tissue does not depend on NGF-TrkA signalling, breast cancer cells express the TrkA receptor (Descamps *et al*., 2001; Descamps, Lebourhis, Delehedde, Boilly, & Hondermarck, 1998), and NGF is a potent activator of the survival and proliferation of breast cancer cells (Descamps *et al*., 2001). Furthermore, biologically active NGF is excessively synthesized and released by breast cancer cells, an effect which is blocked by the TrkA inhibitor

K252, indicating the existence of an NGF autocrine loop (Dollé, El Yazidi-Belkoura, Adriaenssens, Nurcombe, & Hondermarck, 2003).

In humans, endogenous NGF levels are elevated in pain states associated with chronic conditions (Aloe, Tuveri, Carcassi, & Levi-Montalcini, 1992; Friess *et al*., 1999; Halliday, Zettler, Rush, Scicchitano, & McNeil, 1998; Lowe *et al*., 1997), and NGF appears to be an important driver of the increased pain sensitivity characteristic of late stage metastatic cancer. Correspondingly, in animal models of nociception, NGF- and TrkA-knockout mice are hypoalgesic (Crowley *et al*., 1994; Smeyne *et al*., 1994), while transgenic animals that overexpress NGF exhibit hyperalgesic behaviours (Davis, Lewin, Mendell, Jones, & Albers, 1993; Stucky *et al*., 1999). Preclinical research suggests that anti-NGF treatment may be particularly effective in pain that originates in bone (Halvorson, 2005; Juan M. Jimenez-Andrade *et al*., 2007; Juan M Jimenez-Andrade *et al*., 2010; W. G. Mantyh *et al*., 2010; McNamee *et al*., 2010; Sevcik *et al*., 2005), as more than half of the nerve fibers that innervate bone are responsive to NGF (Castañeda-Corral *et al*., 2011).

To date, research on the neurotrophic consequences of metastatic cancer has largely focused on pathological nerve sprouting of sensory and sympathetic nerve fibers that innervate the tumor-bearing host tissue (Bloom *et al*., 2011; Juan M. Jimenez-Andrade *et al*., 2007; P. W. Mantyh, Koltzenburg, Mendell, Tive, & Shelton, 2011; W. G. Mantyh *et al*., 2010). In Chapter 2, I propose an alternative

consideration and complementary explanation of the role of NGF-TrkA in CIP and the influence of this neurotrophin-receptor complex on system x_C^-.

There is considerable evidence for bi-directional signalling between glutamate and neurotrophins. Glutamate stimulates neurotrophic expression (Taylor, Srinivasan, Wordinger, & Roque, 2003; Xiong *et al*., 2002) and select neurotrophins have been implicated in the functional upregulation of system x_C^- (X. Liu, Resch, Rush, & Lobner, 2012). Glutamate plays a key role in several neurodevelopmental and neurodegenerative disorders, and overexpression of system x_C^- has been shown to have neuroprotective effects in conditions of oxidative stress (Shih *et al*., 2006). Furthermore, NGF (Dollé *et al*., 2003), TrkA (Lagadec *et al*., 2009), and xCT (Seidlitz, Sharma, Saikali, Ghert, & Singh, 2009; Sharma, Seidlitz, & Singh, 2010) are upregulated in breast cancer cells, supporting the notion that a functional relationship exists. These overlapping actions suggest that system x_C^- may be influenced by neurotrophic activity.

Microglia in the Naïve CNS

Microglia comprise 5–12% of the cells in the CNS and are heterogeneously distributed (Lawson, Perry, Dri, & Gordon, 1990). These cells are the resident macrophages of the CNS and their activation is one of the first steps in the inflammatory response. In healthy organisms, activated microglia release neurotrophic and anti-inflammatory factors to clear toxins and pathogens

in an effort to maintain and support neuronal survival (Streit, 2002). However, rising attention is given to chronically activated microglia, which release substances inherent to several neurodegenerative disorders, leading to cytotoxicity and neuronal degeneration (reviewed in (Tang & Le, 2016)). Accumulating pre-clinical studies demonstrate that spinal microglial activation is a hallmark of nociception. A growing body of evidence indicates that peripheral nerve injury induces substantial changes in microglia and astrocytes within the spinal cord (Abbadie *et al*., 2003; Myers, Heckman, & Rodriguez, 1996; Tofaris, Patterson, Jessen, & Mirsky, 2002; Zhuo, Wu, & Wu, 2011), and several glia modifying drugs have been shown to alter pain sensitivity (Raghavendra, Tanga, & DeLeo, 2003; Sweitzer, Schubert, & DeLeo, 2001; Watkins, Martin, Ulrich, Tracey, & Maier, 1997). Mounting evidence has suggested that the immune response may play a significant role in the development of CIP, especially through the chronic activation of microglia and astrocytes in the spinal cord (Bu *et al*., 2014; J.-H. Hu *et al*., 2012; Jin, Yang, Hu, Wang, & Zuo, 2015; Yang *et al*., 2015).

Microglia become activated by various stimuli (Colburn *et al*., 1997; Stoll & Jander, 1999; Watkins *et al*., 1997). Proliferation in the spinal cord is an important feature of microglial activation, as in resting state very few of these cells divide. Microglia proliferation has been shown to occur in response to nerve injury (Graeber, Tetzlaff, Streit, & Kreutzberg, 1988), is found in diverse models of neuropathic pain (Peng *et al*., 2016; Stoll & Jander, 1999), and is suggested to

be responsible for the initiation of neuropathic pain induced by peripheral nerve injury (Cao & Zhang, 2008). Activation of microglia leads to increased production of inflammatory mediators and has been widely implicated in neuroinflammation in the CNS, leading to neurodegeneration and abnormal nociceptive signalling.

Microglia in the Diseased CNS

Several *in vitro* studies have demonstrated that microglia may be involved in the neuropathogenesis of various diseases within the CNS. The majority of this research explores to role of spinal microglia (Reviewed in (Cao & Zhang, 2008; Tsuda, Inoue, & Salter, 2005)); however, early studies are beginning to explore alternative areas of processing within the CNS, including the hippocampus, as discussed in Chapter 4. The toll like receptor 4 (TLR-4) is widely expressed in cells of macrophage lineage (reviewed in (Vaure & Liu, 2014)). Intraperitoneal injections of the TLR-4 agonist LPS increases hippocampal transcription of proinflammatory factors (Rigillo *et al*., 2018). While LPS does not cross the blood brain barrier (BBB), microglia-secreted factors, including interleukin 1β (IL-1β) and tumor necrosis factor α (TNF-α), for instance, are able to cross the BBB, where they affect functional neural activity and contribute to the release of cytokines and neurotoxic factors in the CNS (Banks *et al*., 2015; Qin *et al*., 2007; Skelly, Hennessy, Dansereau, & Cunningham, 2013).

Microglial Glutamate

Activated microglia are known to release glutamate via system x_C^- (Piani & Fontana, 1994), and the vast majority of glutamate exported from activated microglia can be attributed to the system x_C^- exchange mechanism (S W Barger & Basile, 2001; Piani & Fontana, 1994). Microglia express high levels of the system x_C^- transporter due to a marked need for oxidative protection and are therefore a major source of excitotoxic glutamate.

One pathway to neurotoxicity involves the release of glutamate by microglia (Piani, Frei, Do, Cuénod, & Fontana, 1991). In support of this hypothesis, inhibitors of cystine uptake in macrophages have been shown to inhibit the cytotoxic effects of microglia through the suppression of glutamate release (Bannai, 1986; Watanabe & Bannai, 1987). Neurons of the CNS have limited capacity for cystine uptake through system x_C^-, and are reliant primarily on glial cells for the provision of cysteine for neuronal GSH production (Dringen, Pfeiffer, & Hamprecht, 1999). This mechanism becomes extremely active in microglia because it is the primary route of internalizing cystine for the production of GSH. As activated microglia produce abundant ROS, they place themselves under severe oxidative stress. Thus, the microglial oxidative burst creates a GSH shortage that is alleviated by cystine influx through xCT, the functional subunit of system x_C^-, extruding glutamate in the balance (Steven W Barger, Goodwin, Porter, & Beggs, 2007).

The relationship between microglia and glutamate is dynamic in that microglia are activated by exogenous glutamate (reviewed in (Murugan, Ling, & Kaur, 2013)) and also secrete glutamate upon activation (S W Barger & Basile, 2001; Steven W Barger *et al*., 2007; Kigerl *et al*., 2012; Piani & Fontana, 1994). The presence of GluRs on microglia has therefore been presented as a potential link between inflammation and excitotoxic CNS damage (Pocock & Kettenmann, 2007; Tahraoui *et al*., 2001). Given that microglia express various metabotropic and ionotropic GluRs, glutamate released by microglia may act in an autocrine fashion by activating neighboring microglial GluRs (reviewed in (Milligan & Watkins, 2009)), thus exacerbating the pain response.

Physiological, molecular, and biochemical evidence cumulatively indicate the presence of functional GluR on microglia (Murugan *et al*., 2013), including NMDA (G. J. Liu, Kalous, Werry, & Bennett, 2006) and AMPA receptors (Hagino *et al*., 2004). However, the significance of GluR activation in microglia remains largely unknown. Given the presence of functional GluRs on microglia, these neuroimmune cells are believed to be a putative synaptic candidate. That is, microglial processes may be involved in forming a neuron-glial synapse. Thus, the presence of glutamate receptors on microglia is a potential link between inflammation and excitotoxic brain damage (Pocock & Kettenmann, 2007; Tahraoui *et al*., 2001). Microglia are capable of secreting various factors that induce cell proliferation, including NGF, brain-derived neurotrophic factor

(BDNF), and other growth factors (Dougherty, Dreyfus, & Black, 2000). In the naïve CNS, resting microglia express negligible amounts of xCT (Ottestad-Hansen *et al*., 2018), but several reports have implicated activated microglia in CIP (X.-F. Hu *et al*., 2017; Huo *et al*., 2018; M. Liu *et al*., 2017; Mao-Ying *et al*., 2012; Wang *et al*., 2012; Yang *et al*., 2015), and emerging evidence suggests that microglial xCT protein levels increase in the activated state (Domercq *et al*., 2016; H Sato *et al*., 1999). Chapter 4 outlines the role of xCT on activated microglia in CIP conditions, with specific focus on microglia activated by glutamate released from cancer cells.

The Affective Component of Pain Perception

Pain is a complex, heterogeneous phenomenon resulting from integration of sensory, affective, and cognitive experiences. Emerging evidence suggests that the hippocampus may be involved in nociceptive processing, particularly with respect to the affective aspect of pain perception (Al Amin, Atweh, Jabbur, & Saadé, 2004; Echeverry, Guimarães, & Del Bel, 2004; Favaroni Mendes & Menescal-de-Oliveira, 2008; Khanna, Chang, Jiang, & Koh, 2004; McEwen, 2001; McKenna & Melzack, 1992, 2001; E Soleimannejad, Semnanian, Fathollahi, & Naghdi, 2006; Elaheh Soleimannejad, Naghdi, Semnanian, Fathollahi, & Kazemnejad, 2007; Yamamotová *et al*., 2007; Zhao *et al*., 2009). A growing body of literature suggests that chronic pain conditions may be linked to aberrant functioning of neural circuits implicated in mood and motivation. The

hippocampus is a brain region involved in multiple cognitive and emotional processes, including the initiation and maintenance of anxiety and depression (Eisch & Petrik, 2012; Murray, Smith, & Hutson, 2008).

Clinical studies suggest that such mood conditions are among the factors that prevent recovery from pain, and may significantly reduce the efficacy of analgesic medications (Legrain, Iannetti, Plaghki, & Mouraux, 2011). Accordingly, development of pharmacologic interventions for the treatment of chronic pain ought to extend beyond circuits which control sensory transmission, to those which mediate affect.

The inflammatory response within the hippocampus has been implicated in the perception of pain (Fasick, Spengler, Samankan, Nader, & Ignatowski, 2015) through the processing and modification of nociceptive stimuli (Bushnell, Ceko, & Low, 2013; M.-G. Liu & Chen, 2009; Simons, Elman, & Borsook, 2014). Models of neuropathic pain show hippocampal abnormalities with persistent pain. Thus, spinal nerve injury (SNI) mice had reduced extracellular signal-related kinase expression, decreased neurogenesis, and altered short-term synaptic plasticity (Mutso *et al*., 2012). Several experimental studies have found that direct manipulation of the hippocampus alters the perception of noxious stimuli. For example, lesion of the ventral hippocampus partially alleviates acute thermal and mechanical nociception in rat pups and adults (Al Amin *et al*., 2004), while injection of the local anesthetic and sodium channel blocker lidocaine

directly into the dentate gyrus (DG) region of the hippocampus produces analgesia (McEwen, 2001; McKenna & Melzack, 1992). Chapter 4 presents a collection of studies which were collectively designed to assess the role of the central immune response and higher-order processing in cancer-related nociception through hippocampal microglia.

The cystine-glutamate antiporter represents the main glial provider of extracellular glutamate in mouse hippocampus (Albertini *et al*., 2018). Inhibition of system x_C^- may modulate microglial functioning in the CNS toward a protective state. Indeed, immunohistochemical studies have confirmed the up-regulation of system x_C^- in microglia of rats in states of inflammation, and system x_C^- inhibition with sulfasalazine (SSZ) and (S)-4-Carboxyphenylglycine (S4-CPG) resulted in increases and decreases of the anti- and pro-inflammatory markers, respectively (Domercq *et al*., 2016; Mesci *et al*., 2015), cumulatively suggesting that xCT is intimately involved in the inflammatory response.

Hypothesis and Objectives

The studies that constitute this thesis collectively test the hypothesis that:

Cancer can induce pain through definable mechanisms, including activated microglia. Chronically-activated microglia release excess glutamate through system x_C^-. *Therefore, pharmacologically targeting microglia will reduce cancer pain through xCT-mediated glutamate release.*

From this hypothesis, several experimentally testable objectives were formulated that represent the main body of the experimental work presented. Each of these specific objectives will be addressed individually in the following chapters, and key results from each objective will then be summarized with major conclusions drawn in the final chapter. To facilitate understanding of this dissertation, a general outline of the manuscript follows, organized by specific objectives, which are also outlined in Fig. 1.1.

Objective 1. Examine the effects of TrkA inhibition on functional system x_C^- activity and CIP.

Objective 1 is further detailed in Chapter 2. Briefly, I investigated the prominent and complex condition of metastatic bone pain and proposed a novel approach to pharmacologically modulating system x_C^--mediated glutamate release from cancer cells for the treatment of cancer pain. This research was an important contribution to the understanding of cancer pain signalling, as it illustrated the connection between increases in glutamate release with previously unrelated increases in NGF. This content was published in *Molecular Pain* and suggests that the actions of NGF extend beyond its conventionally-recognized roles of neuronal survival and differentiation in cancer cells. These data therefore indicate that indirectly inhibiting system x_C^- through the pharmacological modulation of TrkA presents a valuable target for therapeutic intervention in the treatment of cancer pain.

Objective 2. Examine the nociceptive relationship between peripherally-released glutamate and microglial xCT.

Objective 2 is further detailed in Chapter 3. Briefly, I employed a co-culture system to model the influence of peripheral (carcinoma-released) glutamate on microglial activation and functional system x_C^- activity. This work outlines important discoveries in microglia-mediated glutamate signalling and builds on the growing body of literature that implicates microglia in the pain state associated with peripheral tumour. To my knowledge, this is the first study to explore the relationship between tumour cell-released glutamate and microglial xCT. As such, this is an important contribution to appreciating system x_C^- as a key driver of the immune component of cancer pain.

Objective 3. Evaluate the activation pattern of hippocampal microglia in a syngeneic model of CIP and the anti-nociceptive effects of microglial inhibition.

Objective 3 is further detailed in Chapter 4. Briefly, I investigated the role of hippocampal microglia in tumour-bearing mice in the context of the affective component of pain. Through this final manuscript, I have demonstrated that microglial activation increases in the hippocampi of intrafemoral tumor-bearing

mice, and that globally abolishing microglia with the CSF1R inhibitor Pexidartinib effectively attenuates cancer-induced nociception in this specific immunocompetent murine model. This manuscript outlines a preliminary account of hippocampal immune cells in CIP and notes parallels between CIP and cancer-induced depression. The discovery that hippocampal microglia temporally increase in tumor-bearing mice suggests a novel approach to targeting regional microglia for metastatic cancer pain relief.

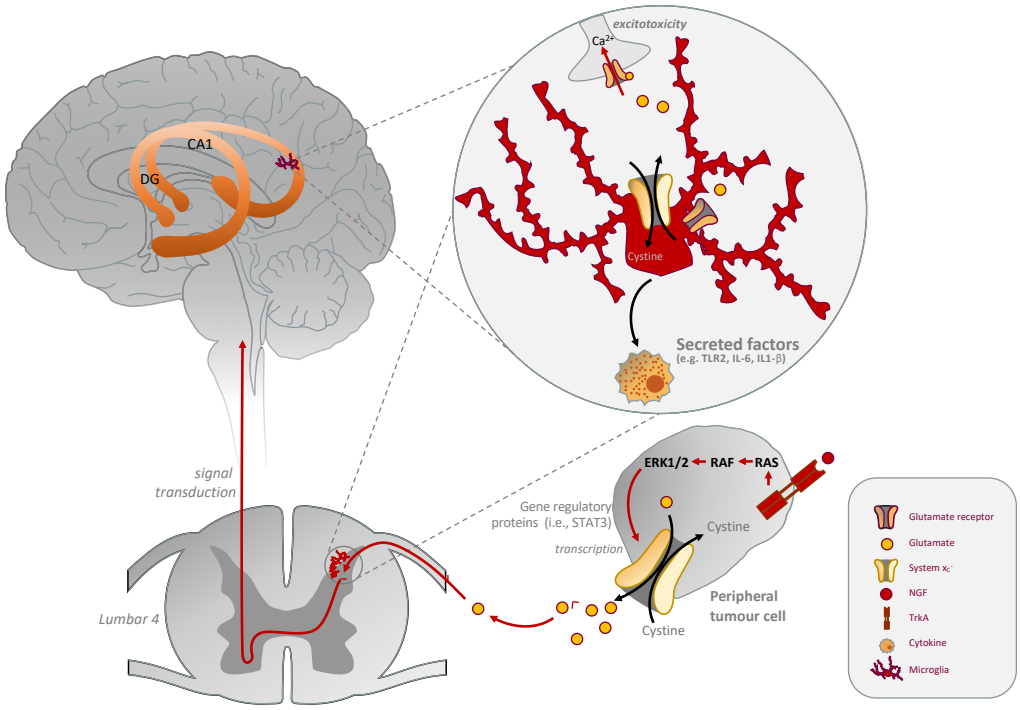

Figure 1. Schematic summarizing proposed mechanisms of cancer-induced pain.

Peripheral tumour cells release excess amounts of glutamate (Glu) through the system x_C^- antiporter. Secreted glutamate may act on the spinal cord through signal transduction pathways that project to brain regions which mediate the pain response. The neurotrophin nerve growth factor (NGF) may contribute to increased system x_C^- transcription through acting on its cognate receptor, TrkA to activate mitogen-activated protein kinase (MAPK) signaling pathways. Tumour burden has also been shown to influence microglial activation in the spinal cord. Once activated, microglia secrete several soluble factors, including glutamate, which may then act on spinal microglial glutamate receptors (GluRs) to

exacerbate activation patterns of these immune cells. Microglial activation patterns within hippocampal regions associated with pain perception (Cornu Ammonis 1, CA1; dentate gyrus, DG) are also altered with tumour burden.

CHAPTER 2

Functional effects of TrkA inhibition on system x_C^--mediated glutamate release and cancer-induced bone pain

Tanya Miladinovic, Robert G Ungard, Katja Linher-Melville,

Snezana Popovic, & Gurmit Singh

(2018). *Molecular Pain, 14,* 1–15

Preface

In this chapter, the author-generated version of the manuscript entitled "Functional effects of TrkA inhibition on system x_C^--mediated glutamate release and cancer-induced bone pain," published in *Molecular Pain* May 2018, is presented. This paper is reproduced, with written permission from Dr. Min Zhuo, Editor-in-chief of *Molecular Pain*.

For this paper, I performed all drug preparations, behavioural assays, and animal drug treatments. I also conducted all in vitro assays, including cell culture, cell drug treatment, ^{14}C-cystine uptake and glutamate release quantification, Western blotting, and qPCR. I also developed and optimized all immunofluorescent staining protocols through several rounds of troubleshooting and performed photomicroscopy and fluorescent image capture. I completed all statistical analyses, wrote and revised the manuscript and created all figures and tables therein. Robert Ungard was instrumental to the behavioural data collection through his teaching of several techniques. He also performed tumour cell inoculation surgeries. Dr. Snezana Popovic provided insightful feedback on histological imaging interpretation. Dr. Katja Linher-Melville provided expertise on qPCR and ^{14}C-cystine uptake techniques. Dr. Gurmit Singh and Dr. Katja Linher-Melville provided intellectual direction and guidance in initial experimental design, writing and revising the manuscript.

Context and Background Information

In an effort to elucidate the relationship between NGF and system x_C^- with respect to CIP, the present chapter explores the cellular and *in vivo* response of xCT to TrkA inhibition in an immunocompetent model of CIP utilizing murine 4T1 carcinoma cells and BALB/c mice. As such, the functional effects of the selective TrkA inhibitor AG879 on system x_C^--mediated glutamate release in human and murine mammary carcinoma cell lines were first characterized. The effects of TrkA inhibition on tumour-induced nociceptive responses was then demonstrated using a syngeneic mouse model of CIP. TrkA inhibition appeared to significantly reduce functional system x_C^- activity *in vitro* and relevant behavioural and physiological responses *in vivo*.

This manuscript explores the hypothesis that the system x_C^- antiporter is functionally influenced by the actions of the neurotrophin NGF on its cognate receptor tyrosine kinase, TrkA, and that inhibiting this complex may reduce cancer-induced bone pain via its downstream actions on xCT, the functional subunit of system x_C^-. Through this manuscript, I have demonstrated the ability of TrkA to functionally inhibit system x_C^-, as revealed by the marked reduction of both cystine uptake and glutamate release from breast cancer cells. This paper also demonstrates that chronic administration of AG879 has antinociceptive effects in our behavioural model of metastatic cancer pain. The role of glutamate in cancer cell metabolism and the effects of neurotrophins on system x_C^--mediated

glutamate output suggest that this connection may be vital to the progression of cancer pain.

This manuscript outlines key advances in the field of cancer pain research through the discovery that NGF and system x_C^- are functionally interconnected, and provides a novel approach to targeting system x_C^- for metastatic cancer pain relief.

Functional effects of TrkA inhibition on system x_C^--mediated glutamate release and cancer-induced bone pain

Tanya Miladinovic[1,2], Robert G Ungard[1,2], Katja Linher-Melville[1,2], Snezana Popovic[2], & Gurmit Singh[1,2]

[1] Michael G. DeGroote Institute for Pain Research and Care, Medicine, McMaster University, 1280 Main St. West, Hamilton, ON L8S 4M1, Canada

[2] Department of Pathology and Molecular Medicine, McMaster University, 1280 Main St. West, Hamilton, ON L8S 4M1, Canada

Corresponding Author: Dr. Gurmit Singh

Department of Pathology & Molecular Medicine, McMaster University, 1280 Main Street West, Hamilton, ON L8N 3Z5, Canada.

Tel.: +1 905 525 9140 x28144.

E-mail address: singhg@mcmaster.ca (G. Singh).

URL: http://www.singhlab.ca (G. Singh).

Abstract

Breast cancer cells release the signalling molecule glutamate via the system x_C^- antiporter, which is up-regulated to exchange extracellular cystine for intracellular glutamate to protect against oxidative stress. Here, we demonstrate that this antiporter is functionally influenced by the actions of the neurotrophin NGF on its cognate receptor tyrosine kinase, TrkA, and that inhibiting this complex may reduce cancer-induced bone pain (CIBP) via its downstream actions on xCT, the functional subunit of system x_C^-. We have characterized the effects of the selective TrkA inhibitor AG879 on system x_C^- activity in murine 4T1 and human MDA-MB-231 mammary carcinoma cells, as well as its effects on nociception in our validated immunocompetent mouse model of CIBP, in which BALB/c mice are intrafemorally inoculated with 4T1 murine carcinoma cells. AG879 decreased functional system x_C^- activity, as measured by cystine uptake and glutamate release, and inhibited nociceptive and physiologically relevant responses in tumour-bearing animals. Cumulatively, these data suggest that the activation of TrkA by NGF may have functional implications on system x_C^--mediated cancer pain. System x_C^--mediated TrkA activation therefore presents a promising target for therapeutic intervention in cancer pain treatment.

Keywords

Cancer

Pain

System x_C^-

Glutamate

Neurotrophin

NGF

Introduction

Breast cancer has a propensity to metastasize to the bone, causing severe cancer-induced bone pain (CIBP) and reduced quality of life. Accordingly, the effective management of CIBP is essential to improving quality of life for cancer patients. Our group has demonstrated that breast cancer cells secrete the signalling molecule glutamate via system x_C^- and overexpress the gene encoding this antiporter [1,2]. When glutamate efflux becomes excessive, its character within the central nervous system switches from an excitatory transmitter to a well-characterized and pathologically-relevant excitotoxin [3,4]. Considerable evidence suggests that glutamate released through system x_C^- is involved in multiple physiological and pathological processes (Reviewed in [5]). Its dysregulation has been linked to chronic pain, an effect which is supported by animal models of CIBP [6,7]. Exogenous glutamate released from peripheral metastases may then sensitize surrounding nerves, directly acting on adjacent nociceptors within the bone environment.

The neurotrophin nerve growth factor (NGF) acts via its cognate receptor TrkA, through which it activates several downstream signaling pathways that regulate neuronal survival and differentiation. While normal breast epithelial tissue does not rely on NGF-TrkA signalling, breast cancer cells express the TrkA receptor [8,9], and NGF is a potent activator of the survival and proliferation of breast cancer cells [8]. Furthermore, biologically-active NGF is excessively

synthesized and released by breast cancer cells, an effect which is blocked by the TrkA inhibitor K252, indicating the existence of an NGF autocrine loop [10].

In humans, endogenous NGF levels are elevated in pain states associated with chronic conditions [11–14], and NGF appears to be an important driver of the increased pain sensitivity characteristic of late stage metastatic cancer (reviewed in [15]). Correspondingly, in animal models of nociception, NGF- and TrkA-knockout mice are hypoalgesic [16,17], while transgenic animals that overexpress NGF exhibit hyperalgesic behaviours [18,19]. Preclinical research suggests that anti-NGF treatment may be particularly effective in pain that originates in bone [20–25], as more than half of the nerve fibers that innervate bone are responsive to NGF [26].

To date, research on the neurotrophic consequences of metastatic cancer has largely focused on pathological nerve sprouting of sensory and sympathetic nerve fibers that innervate the tumour-bearing host tissue [20,24,27,28]. Below, we propose an alternative consideration and complementary explanation of the role of NGF-TrkA in CIBP (See Fig. 2.1 for schematic).

There is considerable evidence for bi-directional signalling between glutamate and neurotrophins. Glutamate stimulates neurotrophic expression [29,30] and the neurotrophin FGF-2 has been implicated in the functional upregulation of system x_C^- in mixed neuronal and glial cultures [31]. Glutamate plays a key role in several neurodevelopmental and neurodegenerative disorders,

and overexpression of system x_C^- has been shown to have neuroprotective effects in conditions of oxidative stress [32]. Furthermore, NGF [10], TrkA [33], and xCT [1,2] are upregulated in breast cancer cells, supporting the notion that a functional relationship exists. The overlapping actions of xCT and NGF suggest that system x_C^- may be influenced by neurotrophic activity. To further elucidate the underlying pathophysiology of glutamate-related cancer pain, we have focused on the NGF-TrkA complex as a therapeutic target to reduce aberrant system x_C^--meditated glutamate release that accompanies CIBP. Here, we test the hypothesis that systematically inhibiting the actions of NGF on TrkA may reduce CIBP by decreasing functional system x_C^- activity.

Materials and Methods

In Vitro

Cell culture

4T1 triple-negative murine mammary gland carcinoma cells (American Type Culture Collection, ATCC) were maintained in high glucose RPMI (Life Technologies); MDA-MB-231 triple-negative human breast carcinoma cells (ATCC) were maintained in high glucose DMEM (Life Technologies). All cells were supplemented with 10 % fetal bovine serum (FBS) and 1 % antibiotic/antimycotic (Life Technologies) incubated at 37 °C and 5 % CO_2 and verified to be mycoplasma free before experimental use.

Effect of TrkA Inhibition on Breast Cancer Cell Number

The selective TrkA inhibitor Tyrphostin AG879 (Sigma Aldrich), a validated and specific inhibitor of TrkA [34], was dissolved in DMSO for preparation of a 79 mM stock. 4T1 and MDA-MB-231 cells were seeded at 5×10^3 cells/well in 96-well plates and treated with serial doses of AG879 from 50 μM through 3.125 μM dissolved in dimethyl sulfoxide (DMSO, maximum final concentration: 0.1 %) or 0.1 % DMSO alone (negative control).

Effect of NGF-TrkA on Breast Cancer Cell Number

Cell lines were seeded at 5×10^3 cells/well in 96-well plates, treated with various concentrations (0, 10, or 100 ng) of the recombinant human β-NGF protein (R&D Systems) in the presence of AG879 (6 μM) or control (DMSO) for 24 h, fixed with 10 % neutral buffered formalin (NBF) and quantified using 0.1 % Crystal Violet stain in 80 % EtOH based on standard curves for each cell line. Absorbance was read on a spectrophotometer optical plate reader (BioTek) at λ = 570 nm.

Effects of NGF-TrkA on Breast Cancer Cell Metabolism

Cell lines were seeded and treated with serial doses of β-NGF (or PBS) in the presence or absence of AG879, as above, and incubated in 0.5 mg/mL MTT labelling reagent (3-[4,5-dimethylthiazol-2-yl]-2,5-diphenyl tetrazolium bromide (Sigma Aldrich) for the final 2 h of the 24 h treatment period. Absorbance was read on a spectrophotometer optical plate reader at λ = 650 nm.

Effects of NGF-TrkA on xCT Protein Level

Cells were treated with 100 ng β-NGF (or PBS) and 6 μM AG879 (or DMSO) for 24 h to determine the effects of NGF-TrkA activity on xCT protein levels, as quantified by Western blot analysis. Total protein concentrations were first determined using the Bio-Rad protein assay (Bio-Rad Laboratories) to ensure equal protein loading of whole cell lysates on 10 % SDS-PAGE gels and

subsequent electrophoretic transfer to PVDF membranes (Immobilon-P, Millipore Corporation). Expression of xCT was evaluated using respective primary antibody (Novus Biologicals), at a concentration of 1:1000, applied overnight at 4 °C, with blocking in 5 % skim milk in TBS-T. After washing, membranes were incubated in horseradish peroxidase-conjugated goat anti-rabbit secondary antibody (Santa Cruz) for 2 h at RT and visualized by enhanced chemiluminescence using an ECL-plus kit (GE Healthcare Ltd.) on Amersham Hyperfilm (GE Healthcare). Calnexin (90 kDa) was used as a loading control. Processed blots were scanned and quantified using densitometry with ImageJ software (US National Institutes of Health). Values were normalized to loading controls and compared to DMSO-treated control plates of the same cell line.

Effects of NGF-TrkA on xCT mRNA

mRNA was quantified using qualitative real-time PCR (qPCR) as previously described [35]. Briefly, 10^6 4T1 cells were seeded in 10 cm dishes, treated with 100 ng β-NGF in the presence (6 μM) or absence (DMSO) of the TrkA inhibitor AG879 for 24 h. Total RNA isolation from cell pellets was conducted using the Qiagen RNeasy kit (Qiagen Inc.). cDNA was then synthesized via reverse transcription using Superscript III and oligo DTs (Thermo Fisher Scientific) and qPCR assays were performed in duplicate using xCT primers (detailed in Table 2) and SsoAdvanced Universal SYBR Green Supermix (BioRad). Readings were normalized to the loading control Succinate

Dehydrogenase Complex Flavoprotein Subunit A (SDHA). Relative quantification analysis of gene expression data was conducted according to the $2^{-\Delta\Delta CT}$ method.

Effects of NGF-TrkA on ^{14}C-Cystine Uptake

The cellular uptake of radiolabeled ^{14}C-cystine was quantified, as cystine uptake is mediated by an exchange with glutamate via system x_C^-. The cystine uptake protocol was adapted from previous reports [32,36]. Briefly, 2×10^5 4T1 and MDA-MB-231 cells were seeded in 6-well plates, treated with 100 ng β-NGF, with or without 6 μM AG879 for 24 h. Media was then collected and stored at 4 °C to quantify glutamate release (see below). Cultures were washed with Hank's Buffered Salt Solution (HBSS) and exposed to ^{14}C-Cystine (0.015 mCi/mL) for 20 min at 37 °C. Following ^{14}C-cystine exposure, cultures were washed with ice cold HBSS to wash away excess extracellular cystine and dissolved in 220 μL of lysis buffer (0.1 % Triton-X in 0.1 N NaOH) for 30 min. A 100 μL aliquot of each cell lysate was added to 1 mL Ecoscint-H scintillation fluid for quantification. Values were normalized to mg of total protein using the Bradford protein assay (BioRad) and compared to ^{14}C-cystine uptake in DMSO-treated controls on the same experimental plate.

Effects of NGF-TrkA on Glutamate Release

Immediately prior to ^{14}C-cystine uptake quantification, growth media samples from 6-well plates were collected and stored at 4 °C. Glutamate release was quantified using the AMPLEX Red glutamic acid assay kit (Invitrogen/Molecular Probes, Eugene, OR, USA). This assay quantitates the fluorescent reaction product resorufin, which is produced in proportion to glutamate, for analysis on a CytoFluor Series 4000 Fluorescence Multi-Well Plate Reader (PerSeptive Biosystems, Framingham, MA, USA). To optimize this assay for measurement of media glutamate concentrations beyond 0.5 μM and eliminate the repeated cycling of glutamate and α-ketoglutarate, L-alanine and L-glutamate pyruvate transaminase were omitted from the reaction mixture [55]. Background glutamate from a media-only control well was subtracted from extracellular glutamate levels in culture media and values were normalized to total protein using the Bradford protein assay, as above.

Immunocytochemistry

Immunocytochemistry was performed to confirm the presence of xCT on cultured 4T1 cells. Cells were seeded at 10^4 cells/well in 8-well chamber slides, fixed with 10 % NBF, permeabilized with 0.1 % Triton X-100, blocked with 1 % BSA, incubated in rabbit polyclonal anti-xCT primary antibody (Novus, 1:1000) for 1 h at RT, and visualized using AlexaFluor-488 goat anti-rabbit secondary antibody (Life Technologies, 1:500) with DAPI counterstain using EVOS FL Cell Imaging System.

In vivo

Mice

Experimentally naïve immunocompetent female BALB/c mice (Charles River Laboratories) aged 4-6 weeks old upon arrival were group housed in cages maintained at 24 °C with a 12-h light/dark cycle and provided *ad libitum* access to food and water. All animal procedures were performed according to guidelines established by the Canadian Council on Animal Care under a protocol reviewed and approved by the *Animal Research Ethics Board* (AREB) of McMaster University.

Experimental Groups

Mice (N = 26) were randomly assigned to three treatment groups: sham surgery + vehicle control (n = 9), tumour + vehicle control (n = 9), and tumour + AG879 (n = 8). Mice were inoculated with either 2×10^4 4T1 cells (n = 17) or an equal number of frozen/heat killed 4T1 cell sham controls (n = 9) injected percutaneously into the right distal femur to establish tumours. Drug treatment was delayed until 7 days post 4T1 cell inoculation to allow sufficient time for the implanted cells to reliably establish a bone tumour without drug interference, more accurately mimicking clinical conditions. Osmotic pump loading and implantation were performed in accordance with the manufacturer's

specifications. AG879 was dissolved in DMSO and administered via intraperitoneally-implanted Alzet model 1002 mini-osmotic pumps (Durect) in a volume of 0.25 µL/h for a total of 5 mg/kg/day, based on the mean weight of the mice on the day of surgical implantation (20 g). Pumps were intraperitoneally implanted under isofluorane anaesthesia and animals were systemically treated with AG879 from Day 7 post-cell inoculation through to endpoint.

All behavioural testing was performed with the groups being blinded, during the animals' light cycle. Animals were randomly assigned to systemic therapy or control groups and were acclimated to the behavioural testing environment and equipment one week prior to commencing data recording and were tested twice weekly for the duration of the experiment. The progression of spontaneous and evoked pain pre- and post-4T1 cell inoculation was monitored using a battery of tests for nociceptive behaviours: The Dynamic Weight Bearing system (DWB; BioSeb), the Dynamic Plantar Aesthesiometer (DPA; Ugo Basile), and open field observations, including Spontaneous Guarding time and Limb Use. Three behavioural tests were performed prior to experiment day 0 which served to establish a stable baseline for the animals' normal behaviour; results are expressed for each animal as a percentage of these baseline scores. Behavioural testing occurred on days 6, 9, 13, 16, and 20 post inoculation, and animals that had not yet reached endpoint were sacrificed on day 21.

Spontaneous Pain

Open Field tests, including Spontaneous Guarding of the affected limb and Limb Use, were used to visually assess ongoing and ambulatory nociception using previously-validated tests [37]. The time (s) spent spontaneously guarding the hindpaw represented ongoing pain and was recorded during a five-minute open field observation period using a stopwatch. Guarding Time was defined as the time the hindpaw was held aloft while ambulatory. During the five-minute spontaneous ambulation period, normal hindlimb use was observed and scored on a scale of 4 to 0: (4) normal use, (3) slight limp, (2) limp and guarding behavior, (1) partial non-use of the limb in locomotor activity, and (0) complete lack of limb use.

The DWB quantitates spontaneous pain-related discomfort and postural disequilibrium [38] by recording the weight distribution of each point of contact of freely moving animals via a sensor pad covering the entire floor surface of the testing chamber. Weight-bearing data was directly captured at a sampling rate of 10 Hz, and the animals' position on the sensor was manually validated following data collection using respective software (DWB v.1.3.4.36). To reduce experimenter bias and ensure spatial and temporal objectivity, a video camera recorded the animals' position within the testing chamber over the capture period. Postural disequilibrium was defined as favouring the tumour-bearing limb and a

compensatory shift of weight-bearing to other body parts, and was considered indirect evidence of nociception. Data for each test day were calculated as a mean weight recorded for all points of weight bearing and expressed as a single measurement of the weight borne by the affected limb as a ratio of the total weight recorded at each frame within the capture period. Data were normalized to the baseline scores prior to cancer cell inoculation for each mouse. A relative reduction in weight borne by the ipsilateral paw was considered evidence of postural disequilibrium.

Evoked Pain

The DPA test, which is a semi-automated version of the classic von Frey test [145], was used to quantify mechanical allodynia and hyperalgesia in mice pre- and post-tumour cell inoculation. A mechanical metal filament was raised by an electrical actuator with variable force and acceleration. The filament stimulated the plantar surface of the affected hindpaw and contralateral hindlimb, and the threshold force and time at which each animal withdrew its paw were recorded. The average force of four independent measurements collected from each paw on each test day was calculated, and mean values were normalized to individual animal's baseline DPA values. A reduction of force required to elicit paw withdrawal in the tumour-bearing limb was considered indicative of hypersensitivity manifested as deliberate withdrawal of the affected paw from the filament pressure.

Tumour Xenografts

The 4T1 mammary carcinoma cell line is highly tumourigenic and invasive; the growth and metastatic spread of these cells in BALB/c mice very closely mimic human breast cancer in its proliferative and metastatic characteristics [40]. Thus, this tumour was used as an animal model for stage IV human breast cancer. On experimental day 0, mice were anaesthetized by isoflurane inhalation and injected with buprenorphine (0.05 mg/kg, subcutaneous; Schering-Plough) to mitigate surgically-induced discomfort. Animals were inoculated with 2×10^4 4T1 cells suspended in 25 µL sterile PBS percutaneously into the right distal femur. Mice were laid supine with the ipsilateral stifle joint bent to 90 º to clear the patella and minimize tissue damage. A 26-gauge needle was then manually inserted between the medial and lateral condyles of the distal epiphysis by delicate rotation parallel to the longitudinal axis of the femur to breach the cortical bone. Once within the bone epiphysis, the injectate was slowly infused over the course of approximately 1 min. The contralateral hind limb served as a negative control specific to each animal. This method of intrafemoral injection was selected to minimize damage to the surrounding tissues, and has been successfully applied in mouse [41] and rat [42] models of bone cancer-induced nociceptive behaviour.

Transcardial Perfusion and Tissue Collection

Throughout tumour development, each animal was monitored daily for limb use, overall health status, and body weight. Animals were euthanized by transcardial perfusion when they no longer bore weight on the affected hindlimb. This experimental endpoint occurred on or before day 21 post tumour cell inoculation for all animals. Under sodium pentobarbital anesthetic (90 mg/kg, ip.), animals were perfused with 100 mL cold PBS, immediately followed by 100 mL cold 4 % paraformaldehyde (PFA). Tumour-bearing femurs and surrounding tissues were dissected, X-rayed, post-fixed in 4 % PFA for 48 h, decalcified in 10 % Ethylenediaminetetraacetic acid (EDTA) for 14 days, and paraffin-embedded for histological analyses.

Ex Vivo

Radiographic Analysis

High-resolution radiographic analysis was used to establish the extent of bone degradation in ipsilateral hindlimbs immediately following perfusion, with substantial bone degradation considered to be evidence of tumour invasion. X-ray scans of all mice were collected using a Faxitron MX-20 X-ray system (Faxitron X-ray Co., Wheeling, IL, USA) on Kodak MIN-R 2000 Mammography film

(Eastman Kodak, Rochester, NY, USA). Affected hindlimbs were scored on a scale of 0-3: (0) Normal bone, no visible lesion; (1) Minor loss of bone density, minimal lesion; (2) Moderate to substantial loss of bone density, lesion limited to bone trabecula and cortex; (3) Substantial loss of bone density, lesion includes clear periosteal involvement or fracture.

Hematoxylin and Eosin

Ipsilateral hindlimbs were stained with hematoxylin and eosin to confirm the degree of intrafemoral tumour in animals that demonstrated lytic lesions on X-rays. Following decalcification, femurs and surrounding tissues were paraffin-embedded, sagittally sectioned at 5 μm, slide mounted, stained, and xylene-cleared for microscopy.

Immunofluorescence

Immediately adjacent serial hindlimb sections from the same paraffin block were processed for immunofluorescence; following antigen retrieval in EDTA (pH 8, 95 °C) for 30 min, sections were incubated in respective primary antibodies (xCT: Novus, 1:1000; cytokeratin 7: Santa Cruz, 1:500) overnight at 4 °C, washed in PBS, incubated in 1:500 fluorescent secondary antibodies (Life Technologies AlexaFluor-488 goat anti-rabbit, and AlexaFluor-647 goat anti-mouse, respectively) for 2 h at RT, counterstained with DAPI, and coverslipped.

Statistical Analyses

In vitro

For each cell line, a one-way ANOVA with Bonferroni post hoc comparisons was used to assess the dose response of AG879 on cell number. A two-way ANOVA with Bonferroni post hoc comparisons was then used to assess the effect of serial dilutions of β-NGF for each cell line, in the presence and absence of 6 μM AG879, on cell number and metabolism. Separate two-way ANOVAs with Bonferroni post hoc comparisons were used to assess the effect of β-NGF and AG879 on xCT protein levels and mRNA levels for each cell line. One-way ANOVAs with Bonferroni post hoc comparisons were used to assess the dose effect of β-NGF on functional system x_C^- activity, as measured by cystine uptake and glutamate release. Independent t-tests were then used to assess the effect of AG879 on cystine uptake relative to cells treated with each β-NGF dose.

In vivo

DWB and DPA datasets were analyzed to derive survival curves comparing the time until respective behavioural scores fell irreversibly below 50 % of the animals' baseline nociceptive responses. For Kaplan-Meier curve analyses of 50 % threshold pain data (time to behavioural decline) in DWB and DPA behavioural tests, chi square analyses were used.

Ex vivo

Chi square analysis of the proportion of scores within each treatment group was used to assess radiographic analysis of osteolysis. Immunocytochemical staining of xCT in 4T1 cells and immunofluorescent staining of xCT within ipsilateral hindlimbs were qualitatively considered.

All analyses were performed using GraphPad Prism 5.0a software (GraphPad Software, Inc., La Jolla, CA, USA) and GraphPad QuickCals; α was set at 0.05. Data are expressed as means ± SEM from three independent experiments, unless otherwise stated.

Results

In Vitro

AG879 Influences Breast Cancer Cell Number

Selective TrkA inhibition appeared to concentration-dependently decrease cell number in 4T1 and MDA-MB-231 triple-negative cells, such that higher doses of AG879 (*i.e.*, 12.5, 25, and 50 μM AG879) decreased cell number relative to DMSO-treated controls after 24 h treatment (See Table 1). Treatment with 6 μM AG879 did not significantly alter 4T1 or MDA-MB-231 cell growth or metabolism as measured by Crystal Violet and MTT assays. Thus, this dose was selected for all further *in vitro* studies.

Selected AG879 and NGF Doses Do Not Affect 4T1 Cell Metabolism

Treatment with β-NGF (0.01-100 ng) or AG879 (6 μM) for 24 h did not significantly affect breast cancer cell number (data not shown) or metabolism (Fig. 2.2).

AG879 attenuates β-NGF-induced increases in xCT protein in 4T1 cells

Western blotting analysis confirmed the presence of TrkA on 4T1 and MDA-MB-231 cells (data not shown). Blots also demonstrated a marked increase in xCT bands at 37 kDa in cells treated with 100 ng β-NGF in both 4T1 and MDA-MB-231 cell lines, an effect which was attenuated by AG879 in 4T1 murine carcinoma cells, with a similar, albeit modest, trend observed in MDA-MB-231 cells (Fig. 2.3).

AG879 attenuates β-NGF-induced increases in xCT mRNA in 4T1 cells

qPCR analysis demonstrated a marked increase in xCT mRNA in 4T1 cells treated with 100 ng β-NGF, an effect which was attenuated by treatment with 6 μM AG879 (Fig. 2.4).

AG879 Decreases Functional System x_C^- Activity

In 4T1 cells, ^{14}C-cystine uptake was markedly reduced in cells treated with 6 μM AG879 for 24 h relative to DMSO- and 10 ng β-NGF-treated cells. Treatment with β-NGF appeared to marginally increase ^{14}C-cystine uptake relative to DMSO control, however this effect was not statistically significant (Fig. 2.5A & B). Accordingly, glutamate release was increased in cells treated with 10 ng and 100 ng β-NGF (Fig. 2.5C). Treatment with 6 μM AG879 did not

significantly affect this (Fig. 2.5D). A similar trend was observed in triple-negative human MDA-MB-231 cells (data not shown).

In vivo

AG879 Attenuates Tumour-induced Nociceptive Behaviours

The TrkA inhibitor AG879 appeared to delay the onset of nociception, as measured by progressively impaired Limb Use and increased Spontaneous Guarding scores (Fig. 2.6A & B, respectively). In both the DWB (Fig. 2.7A) and the DPA (Fig. 2.7B), tumour-bearing mice exhibited significantly greater pain behaviours compared to their sham controls from day nine post-tumour cell inoculation until endpoint. AG879 significantly delayed behavioural decline, as measured by postural disequilibrium in the DWB, indicating that significantly fewer tumour-bearing animals fell below 50 % of their individual baseline nociceptive score when treated with AG879 (Fig. 2.7A). In the DPA, a similar trend was observed, with fewer AG879-treated animals falling below 50 % of their individual baseline scores, but this effect was not statistically significant (Fig. 2.7B).

Ex Vivo

AG879 Impedes Tumour Invasion *In Vivo*

Radiographic analysis confirmed the presence of bone degradation in cancer cell-inoculated mice at endpoint and AG879 appeared to partially attenuate tumour-induced osteolysis (Fig. 2.8A). Hematoxylin and eosin staining of ipsilateral hindlimbs confirmed the presence of tumour cells in femurs of animals that demonstrated lytic lesions in radiographic X-rays; tumour invasion was most frequently observed in the distal epiphysis and diaphysis of ipsilateral femurs. AG879-treated mice demonstrated marginally less osteolytic activity, with generally smaller tumours observed in drug-treated animals (See Fig. 2.8B & C for representative images), in accordance with radiographic lesion scores.

AG879 Inhibits xCT Expression *In Vivo*

Immunocytochemistry confirmed the presence of xCT on 4T1 murine carcinoma cells *in vitro* (Fig. 2.9A) and immunofluorescent staining of ipsilateral femurs demonstrated the presence of the epithelial marker cytokeratin 7 (Fig. 2.9B), confirming the presence of breast cancer cells within the bone environment at endpoint. Double-label immunofluorescence demonstrated the overlapping distribution of xCT with breast cancer cells in ipsilateral femurs (Fig. 2.9C), confirming the expression of xCT on 4T1 cells *in vivo*. AG879 appeared to markedly inhibit xCT expression by tumour cells (Fig. 2.9D).

Discussion

Cancer pain is highly heterogeneous and is thought to be the result of varied pathological mechanisms. Current treatment options often induce severe dose-dependent side effects and fail to adequately manage advanced breast CIBP. Clinically, achieving analgesia often comes at the expense of patients' quality of life. The complexity of CIBP is partly due to the unique properties of the affected tissue; osteoclastogenesis [43], inflammation [44,45], increased neurotrophic activity [20,23], demyelination [46], and extracellular acidification [45] created by the presence of bone tumours have been implicated in the sensitization of surrounding nociceptors and may cumulatively contribute to cancer-induced hyperalgesia. Among other influences, it is clear that glutamate dysregulation [47] and aberrant neurotrophic activity [27,48] may contribute to CIBP through pathological osteoclastogenesis and sensitization. The production and vesicular secretion of NGF drives the autocrine stimulation and proliferation of breast cancer cells through its cognate receptor, TrkA [10]. In the present study, we have demonstrated that inhibiting the NGF-TrkA complex may limit CIBP, conceivably through downstream effects on system x_C^-. Extensive research supports the hypothesis that NGF drives cancer pain through pathological nerve sprouting [20,24,27,28]; this study provides evidence that the effects of NGF on breast cancer cells and surrounding cells in the tumour microenvironment may not be limited to its conventionally-accepted neurotrophic actions. The discovery that

NGF and system x_C^- may be functionally interconnected provides a novel approach to indirectly targeting system x_C^- for CIBP relief.

In vitro, AG879 dose-dependently reduced breast cancer cell growth, in accord with previous findings [49]. More importantly, however, a dose which did not effectively alter cell number or metabolism significantly inhibited the functional activity of system x_C^-. That is, AG879 markedly reduced cystine uptake in 4T1 carcinoma cells in the presence and absence of β-NGF. One possible explanation for the relationship between NGF and system x_C^- is through changes that occur at the level of xCT by activation of the MAPK/ERK signalling pathway. Through TrkA, NGF is known to activate RAS-MAPK signalling (reviewed in [50]). Interestingly, serine kinases, including MAPK, phosphorylate STAT3, which then homo- or heterodimerizes and translocates into the nucleus [35,51,52], where it then binds specific DNA recognition elements to regulate expression of genes, including xCT [51]. In MDA-MB-231 breast cancer cells, for example, the MAPK inhibitor PD098059 abolishes basal xCT transcriptional activity [51]. Furthermore, STAT3 activation is coupled with increased system x_C^- activity. Accordingly, sustained treatment with the STAT3 inhibitor SH-4-54 decreases xCT expression and system x_C^- activity in MDA-MB-231 cells [51]. It is therefore plausible that phosphorylated TrkA contributes to xCT expression through MAPK and/or STAT3 signalling, although further research is required to explore the specific pathways involved in this relationship.

A consistent trend was observed across both cell lines assayed *in vitro*; AG879 influenced functional system x_C^- activity in murine 4T1 and human MDA-MB-231 carcinoma cells. Thus, to mitigate the number of animals employed and avoid the complexity of using human cancer cells in an immunocompromised animal model, a syngeneic mouse model was utilized to characterize the effects of TrkA on cancer progression and CIBP *in vivo*. The battery of tests for nociceptive behaviours was cumulatively selected to reflect what is observed in patients who protect or suspend their afflicted limb.

Inhibition of TrkA delayed the onset of nociceptive behaviours in tumour-bearing mice, as demonstrated by Spontaneous Guarding and Limb Use scores, as well as time until behavioural decline in the DWB. No significant reduction of evoked pain was observed in the DPA, suggesting that either NGF-TrkA signalling or functional system x_C^- activity may be more implicated in spontaneous than evoked pain. Previous work has shown that early, but not late administration of an NGF sequestering antibody can prevent the onset of tumour-induced nerve sprouting in a mouse model of CIBP [20]. Here, pharmacological TrkA inhibition began on Day 7 after intrafemoral cancer cell inoculation, corresponding with initial behavioural indications of CIBP. This time point represents a relative late administration regimen to mimic what is seen clinically, as patients are often not diagnosed until metastases have progressed to an advanced, often painful, state. The ability of AG879 to partially mitigate, but not

abolish, nociceptive behaviours when administered relatively late, with the onset of pain, suggests that irreversible damage to the bone microenvironment may have already occurred, but that this inhibitor nevertheless had subsequent effects on additional targets implicated in nociception.

The cystine-coupled export of glutamate through system x_C^- bears additional significance within the nervous system, as it represents a non-vesicular route by which this excitatory neurotransmitter can activate glutamate receptors on sympathetic nerve fibers, particularly those present in extrasynaptic locales. While glutamate is recognized as a ubiquitous cell signalling molecule and critical intercellular neurotransmitter, excessive glutamate efflux produces an excitotoxic environment. One means by which glutamate may directly contribute to nociception is by acting on adjacent afferent nociceptive neurons within the bone. Another means by which glutamate evokes nociception is by influencing many aspects of metabolic homeostasis during normal bone remodeling [47,53,54], affecting the communication between osteoblasts and osteoclasts, which maintain a delicate balance of bone formation and resorption, respectively [54,55]. The disruption of glutamatergic signalling within the bone microenvironment influences cell differentiation [56,57] and function [47,58,59]. In the presence of bone metastases, the balance between bone formation and degradation is disturbed [60]. Disruption of this homeostasis by the aberrant increase in glutamate released from breast cancer cells into the bone microenvironment leads to excessive

osteoclastogenesis [61–63] and reduced bone mineralization [64]. Given that glutamate released by system x_C^- can directly stimulate adjacent afferent nociceptors, disrupt normal bone remodeling, and inhibit bone mineralization, the observed delay until the time of onset of nociception is a logical consequence of inhibiting system x_C^-. Accordingly, the reduced osteolysis seen in AG879-treated animals, relative to untreated tumour-bearing animals, is reflective of the observed delay in nociceptive behaviours and reduction of functional system x_C^- activity seen in the *in vivo* and *in vitro* data, respectively, and cumulatively suggest that TrkA may be implicated in the osteolytic contribution to cancer pain.

Our group has reported on the antinociceptive effects of the steric system x_C^- inhibitor, sulfasalazine (SSZ) in a validated model of CIBP in which SSZ delayed the onset of tumour-induced nociception [41], an outcome which has since been validated in a syngeneic mouse model [7]. However, despite its efficacy in animal models of CIBP, SSZ has limited translational capacity given the poor bioavailability of the parent drug relative to its metabolites. Furthermore, side effects of SSZ mirror many of the symptoms already observed in cancer patients, including nausea, vomiting, and anorexia, symptoms which ought to be controlled, not exacerbated. Therefore, although system x_C^- is a promising pharmacological target for the treatment of CIBP, novel inhibitors are needed to better manage this pain without the negative side effects that accompany SSZ.

The present study corroborates the role of aberrant glutamate secretion through system x_C^- in breast CIBP and suggests the possibility of a feedback loop between NGF and system x_C^-. The role of glutamate in cancer cell metabolism and the effects of NGF on system x_C^--mediated glutamate output suggest that this connection may be vital to the progression of cancer pain. The relationship between TrkA and system x_C^- is an important link in elucidating breast cancer-induced pain signalling. The present study supports the pharmacological inhibition of glutamate release to limit nociception and connects increases in glutamate release to previously unrelated increases in NGF. This study suggests that the actions of NGF extend beyond its conventionally-recognized roles of neuronal survival and differentiation. Indirectly inhibiting system x_C^- through the pharmacological modulation of TrkA therefore presents a valuable target for therapeutic intervention in the treatment of cancer pain.

Acknowledgements

The authors wish to thank Dr. Mark Inman for his expert advice in statistical analyses. This work was supported by the Canadian Institute of Health Research to G.S.

Conflict of Interest

The authors declare no conflict of interest.

References

1. Seidlitz EP, Sharma MK, Saikali Z, Ghert M, Singh G. Cancer cell lines release glutamate into the extracellular environment. Clin. Exp. Metastasis. 2009;26:781–7.

2. Sharma MK, Seidlitz EP, Singh G. Cancer cells release glutamate via the cystine/glutamate antiporter. Biochem. Biophys. Res. Commun. 2010;391:91–5.

3. Choi DW. Glutamate receptors and the induction of excitotoxic neuronal death. Prog. Brain Res. 1994;100:47–51.

4. Choi DW, Maulucci-Gedde M, Kriegstein AR. Glutamate neurotoxicity in cortical cell culture. J. Neurosci. 1987;7:357–68.

5. Miladinovic T, Nashed MG, Singh G. Overview of Glutamatergic Dysregulation in Central Pathologies. Biomolecules. 2015;5:3112–41.

6. Ungard RG, Seidlitz EP, Singh G. Inhibition of breast cancer-cell glutamate release with sulfasalazine limits cancer-induced bone pain. Pain. 2014;155:28–36.

7. Slosky LM, BassiriRad NM, Symons AM, Thompson M, Doyle T, Forte BL, *et al*. The cystine/glutamate antiporter system x_C^- drives breast tumour

cell glutamate release and cancer-induced bone pain. Pain. Wolters Kluwer Health; 2016;157:2605–16.

8. Descamps S, Toillon RA, Adriaenssens E, Pawlowski V, Cool SM, Nurcombe V, *et al*. Nerve growth factor stimulates proliferation and survival of human breast cancer cells through two distinct signaling pathways. J. Biol. Chem. 2001;276:17864–70.

9. Descamps S, Lebourhis X, Delehedde M, Boilly B, Hondermarck H. Nerve growth factor is mitogenic for cancerous but not normal human breast epithelial cells. J. Biol. Chem. 1998;273:16659–62.

10. Dollé L, El Yazidi-Belkoura I, Adriaenssens E, Nurcombe V, Hondermarck H. Nerve growth factor overexpression and autocrine loop in breast cancer cells. Oncogene. 2003;22:5592–601.

11. Lowe EM, Anand P, Terenghi G, Williams-Chestnut RE, Sinicropi D V, Osborne JL. Increased nerve growth factor levels in the urinary bladder of women with idiopathic sensory urgency and interstitial cystitis. Br. J. Urol. 1997;79:572–7.

12. Aloe L, Tuveri MA, Carcassi U, Levi-Montalcini R. Nerve growth factor in the synovial fluid of patients with chronic arthritis. Arthritis Rheum. 1992;35:351–5.

13. Halliday DA, Zettler C, Rush RA, Scicchitano R, McNeil JD. Elevated nerve growth factor levels in the synovial fluid of patients with inflammatory joint disease. Neurochem. Res. 1998;23:919–22.

14. Friess H, Zhu ZW, di Mola FF, Kulli C, Graber HU, Andren-Sandberg A, *et al*. Nerve growth factor and its high-affinity receptor in chronic pancreatitis. Ann. Surg. 1999;230:615–24.

15. Wang W, Chen J, Guo X. The role of nerve growth factor and its receptors in tumourigenesis and cancer pain. Biosci. Trends. 2014;8:68–74.

16. Crowley C, Spencer SD, Nishimura MC, Chen KS, Pitts-Meek S, Armanini MP, *et al*. Mice lacking nerve growth factor display perinatal loss of sensory and sympathetic neurons yet develop basal forebrain cholinergic neurons. Cell. 1994;76:1001–11.

17. Smeyne RJ, Klein R, Schnapp A, Long LK, Bryant S, Lewin A, *et al*. Severe sensory and sympathetic neuropathies in mice carrying a disrupted Trk/NGF receptor gene. Nature. 1994;368:246–9.

18. Davis BM, Lewin GR, Mendell LM, Jones ME, Albers KM. Altered expression of nerve growth factor in the skin of transgenic mice leads to changes in response to mechanical stimuli. Neuroscience. 1993;56:789–92.

19. Stucky CL, Koltzenburg M, Schneider M, Engle MG, Albers KM, Davis BM. Overexpression of nerve growth factor in skin selectively affects the survival and functional properties of nociceptors. J. Neurosci. 1999;19:8509–16.

20. Mantyh WG, Jimenez-Andrade JM, Stake JI, Bloom AP, Kaczmarska MJ, Taylor RN, *et al*. Blockade of nerve sprouting and neuroma formation markedly attenuates the development of late stage cancer pain. Neuroscience. 2010;171:588–98.

21. Halvorson KG. A Blocking Antibody to Nerve Growth Factor Attenuates Skeletal Pain Induced by Prostate Tumour Cells Growing in Bone. Cancer Res. 2005;65:9426–35.

22. Jimenez-Andrade JM, Bloom AP, Stake JI, Mantyh WG, Taylor RN, Freeman KT, *et al*. Pathological sprouting of adult nociceptors in chronic prostate cancer-induced bone pain. J. Neurosci. 2010;30:14649–56.

23. Sevcik MA, Ghilardi JR, Peters CM, Lindsay TH, Halvorson KG, Jonas BM, *et al*. Anti-NGF therapy profoundly reduces bone cancer pain and the accompanying increase in markers of peripheral and central sensitization. Pain. 2005;115:128–41.

24. Jimenez-Andrade JM, Martin CD, Koewler NJ, Freeman KT, Sullivan LJ, Halvorson KG, *et al*. Nerve growth factor sequestering therapy attenuates non-malignant skeletal pain following fracture. Pain. 2007;133:183–96.

25. McNamee KE, Burleigh A, Gompels LL, Feldmann M, Allen SJ, Williams RO, *et al*. Treatment of murine osteoarthritis with TrkAd5 reveals a pivotal role for nerve growth factor in non-inflammatory joint pain. Pain. 2010;149:386–92.

26. Castañeda-Corral G, Jimenez-Andrade JM, Bloom AP, Taylor RN, Mantyh WG, Kaczmarska MJ, *et al*. The majority of myelinated and unmyelinated sensory nerve fibers that innervate bone express the tropomyosin receptor kinase A. Neuroscience. 2011;178:196–207.

27. Bloom AP, Jimenez-Andrade JM, Taylor RN, Castañeda-Corral G, Kaczmarska MJ, Freeman KT, *et al*. Breast cancer-induced bone remodeling, skeletal pain, and sprouting of sensory nerve fibers. J. Pain. 2011;12:698–711.

28. Mantyh PW, Koltzenburg M, Mendell LM, Tive L, Shelton DL. Antagonism of nerve growth factor-TrkA signaling and the relief of pain. Anesthesiology. 2011;115:189–204.

29. Taylor S, Srinivasan B, Wordinger RJ, Roque RS. Glutamate stimulates neurotrophin expression in cultured Müller cells. Mol. Brain Res. 2003;111:189–97.

30. Xiong H, Futamura T, Jourdi H, Zhou H, Takei N, Diverse-Pierluissi M, *et al*. Neurotrophins induce BDNF expression through the glutamate receptor pathway in neocortical neurons. Neuropharmacology. 2002;42:903–12.

31. Liu X, Resch J, Rush T, Lobner D. Functional upregulation of system x_C^- by fibroblast growth factor-2. Neuropharmacology. 2012;62:901–6.

32. Shih AY, Erb H, Sun X, Toda S, Kalivas PW, Murphy TH. Cystine/glutamate exchange modulates glutathione supply for neuroprotection from oxidative stress and cell proliferation. J. Neurosci. 2006;26:10514–23.

33. Lagadec C, Meignan S, Adriaenssens E, Foveau B, Vanhecke E, Romon R, *et al*. TrkA overexpression enhances growth and metastasis of breast cancer cells. Oncogene. 2009;28:1960–70.

34. Ohmichi M, Pang L, Ribon V, Gazit A, Levitzki A, Saltiel AR. The tyrosine kinase inhibitor tyrphostin blocks the cellular actions of nerve growth factor. Biochemistry. 1993;32:4650–8.

35. Linher-Melville K, Nashed MG, Ungard RG, Haftchenary S, Rosa DA, Gunning PT, *et al*. Chronic Inhibition of STAT3/STAT5 in Treatment-Resistant Human Breast Cancer Cell Subtypes: Convergence on the ROS/SUMO Pathway and Its Effects on xCT Expression and System x_C^- Activity. Tan M, editor. PLoS One. 2016;11:e0161202.

36. Lutgen V, Qualmann K, Resch J, Kong L, Choi S, Baker DA. Reduction in phencyclidine induced sensorimotor gating deficits in the rat following increased system xc^- activity in the medial prefrontal cortex. Psychopharmacology (Berl). 2013;226:531–40.

37. Luger NM, Honore P, Sabino MA, Schwei MJ, Rogers SD, Mach DB, *et al*. Osteoprotegerin diminishes advanced bone cancer pain. Cancer Res. 2001;61:4038–47.

38. Robinson I, Sargent B, Hatcher JP. Use of dynamic weight bearing as a novel end-point for the assessment of Freund's Complete Adjuvant induced hypersensitivity in mice. Neurosci. Lett. 2012;524:107–10.

39. Nirogi R, Goura V, Shanmuganathan D, Jayarajan P, Abraham R. Comparison of manual and automated filaments for evaluation of neuropathic pain behavior in rats. J. Pharmacol. Toxicol. Methods. 2012;66:8–13.

40. Pulaski BA, Ostrand-Rosenberg S. Mouse 4T1 Breast Tumour Model. Curr. Protoc. Immunol. Hoboken, NJ, USA: John Wiley & Sons, Inc.; 2001. p. Unit 20.2.

41. Ungard RG, Seidlitz EP, Singh G. Inhibition of breast cancer-cell glutamate release with sulfasalazine limits cancer-induced bone pain. Pain. 2014;155:28–36.

42. De Ciantis K, Henry J, Yashpal G, Singh G. Characterization of a rat model of metastatic prostate cancer bone pain. J. Pain Res. 2010;3:213.

43. Lozano-Ondoua AN, Symons-Liguori AM, Vanderah TW. Cancer-induced bone pain: Mechanisms and models. Neurosci. Lett. 2013;557 Pt A:52–9.

44. Breese NM, George AC, Pauers LE, Stucky CL. Peripheral inflammation selectively increases TRPV1 function in IB4-positive sensory neurons from adult mouse. Pain. 2005;115:37–49.

45. Asai H, Ozaki N, Shinoda M, Nagamine K, Tohnai I, Ueda M, *et al*. Heat and mechanical hyperalgesia in mice model of cancer pain. Pain. 2005;117:19–29.

46. Inoue M, Rashid MH, Fujita R, Contos JJA, Chun J, Ueda H. Initiation of neuropathic pain requires lysophosphatidic acid receptor signaling. Nat. Med. 2004;10:712–8.

47. Seidlitz EP, Sharma MK, Singh G. Extracellular glutamate alters mature osteoclast and osteoblast functions. Can. J. Physiol. Pharmacol. 2010;88:929–36.

48. Jimenez-Andrade JM, Ghilardi JR, Castañeda-Corral G, Kuskowski MA, Mantyh PW. Preventive or late administration of anti-NGF therapy attenuates tumour-induced nerve sprouting, neuroma formation, and cancer pain. Pain. 2011;152:2564–74.

49. Larsson L-I. Novel actions of tyrphostin AG 879: inhibition of RAF-1 and HER-2 expression combined with strong antitumoural effects on breast cancer cells. Cell. Mol. Life Sci. 2004;61:2624–31.

50. Huang EJ, Reichardt LF. Trk receptors: roles in neuronal signal transduction. Annu. Rev. Biochem. 2003;72:609–42.

51. Linher-Melville K, Haftchenary S, Gunning P, Singh G. Signal transducer and activator of transcription 3 and 5 regulate system x_C^- and redox balance in human breast cancer cells. Mol. Cell. Biochem. Springer US; 2015;405:205–21.

52. Linher-Melville K, Singh G. The complex roles of STAT3 and STAT5 in maintaining redox balance: Lessons from STAT-mediated xCT expression in cancer cells. Mol. Cell. Endocrinol. 2017;

53. Skerry TM. The role of glutamate in the regulation of bone mass and architecture. J. Musculoskelet. Neuronal Interact. 2008;8:166–73.

54. Takarada T, Yoneda Y. Pharmacological topics of bone metabolism: glutamate as a signal mediator in bone. J. Pharmacol. Sci. 2008;106:536–41.

55. Chenu C. Glutamatergic regulation of bone remodeling. J. Musculoskelet. Neuronal Interact. 2002;2:282–4.

56. Merle B, Itzstein C, Delmas PD, Chenu C. NMDA glutamate receptors are expressed by osteoclast precursors and involved in the regulation of osteoclastogenesis. J. Cell. Biochem. 2003;90:424–36.

57. Peet NM, Grabowski PS, Laketic-Ljubojevic I, Skerry TM. The glutamate receptor antagonist MK801 modulates bone resorption in vitro by a mechanism predominantly involving osteoclast differentiation. FASEB J. 1999;13:2179–85.

58. Itzstein C, Espinosa L, Delmas PD, Chenu C. Specific antagonists of NMDA receptors prevent osteoclast sealing zone formation required for bone resorption. Biochem. Biophys. Res. Commun. 2000;268:201–9.

59. Taylor AF. Osteoblastic glutamate receptor function regulates bone formation and resorption. J. Musculoskelet. Neuronal Interact. 2002;2:285–90.

60. Rose AAN, Siegel PM. Breast cancer-derived factors facilitate osteolytic bone metastasis. Bull. Cancer. 2006;93:931–43.

61. Coleman RE, Lipton A, Roodman GD, Guise TA, Boyce BF, Brufsky AM, *et al*. Metastasis and bone loss: advancing treatment and prevention. Cancer Treat. Rev. 2010;36:615–20.

62. Boyle WJ, Simonet WS, Lacey DL. Osteoclast differentiation and activation. Nature. 2003;423:337–42.

63. Dougall WC, Chaisson M. The RANK/RANKL/OPG triad in cancer-induced bone diseases. Cancer Metastasis Rev. 2006;25:541–9.

64. Wang L, Hinoi E, Takemori A, Nakamichi N, Yoneda Y. Glutamate inhibits chondral mineralization through apoptotic cell death mediated by retrograde operation of the cystine/glutamate antiporter. J. Biol. Chem. 2006;281:24553–65.

65. Rende M, Brizi E, Conner J, Treves S, Censier K, Provenzano C, *et al*. Nerve growth factor (NGF) influences differentiation and proliferation of myogenic cells in vitro via TrKA. Int. J. Dev. Neurosci. 2000;18:869–85.

66. Holtzman DM, Kilbridge J, Li Y, Cunningham ET, Lenn NJ, Clary DO, *et al*. TrkA expression in the CNS: evidence for the existence of several novel NGF-responsive CNS neurons. J. Neurosci. NIH Public Access; 1995;15:1567–76.

67. Zhou Y, Brattain MG. Synergy of epidermal growth factor receptor kinase inhibitor AG1478 and ErbB2 kinase inhibitor AG879 in human colon carcinoma cells is associated with induction of apoptosis. Cancer Res. 2005;65:5848–56.

68. He H, Hirokawa Y, Gazit A, Yamashita Y, Mano H, Kawakami Y, *et al*. The Tyr-kinase inhibitor AG879, that blocks the ETK-PAK1 interaction, suppresses the RAS-induced PAK1 activation and malignant transformation. Cancer Biol. Ther. 2004;3:96–101.

69. He H, Hirokawa Y, Manser E, Lim L, Levitzki A, Maruta H. Signal therapy for RAS-induced cancers in combination of AG 879 and PP1, specific inhibitors for ErbB2 and Src family kinases, that block PAK activation. Cancer J. 2001;7:191–202.

70. Yu H, Zou B, Wang X, Li M. Effect of tyrphostin AG879 on Kv 4.2 and Kv 4.3 potassium channels. Br. J. Pharmacol. 2015;172:3370–82.

71. Barry DM, Trimmer JS, Merlie JP, Nerbonne JM. Differential expression of voltage-gated K+ channel subunits in adult rat heart. Relation to functional K+ channels? Circ. Res. 1995;77:361–9.

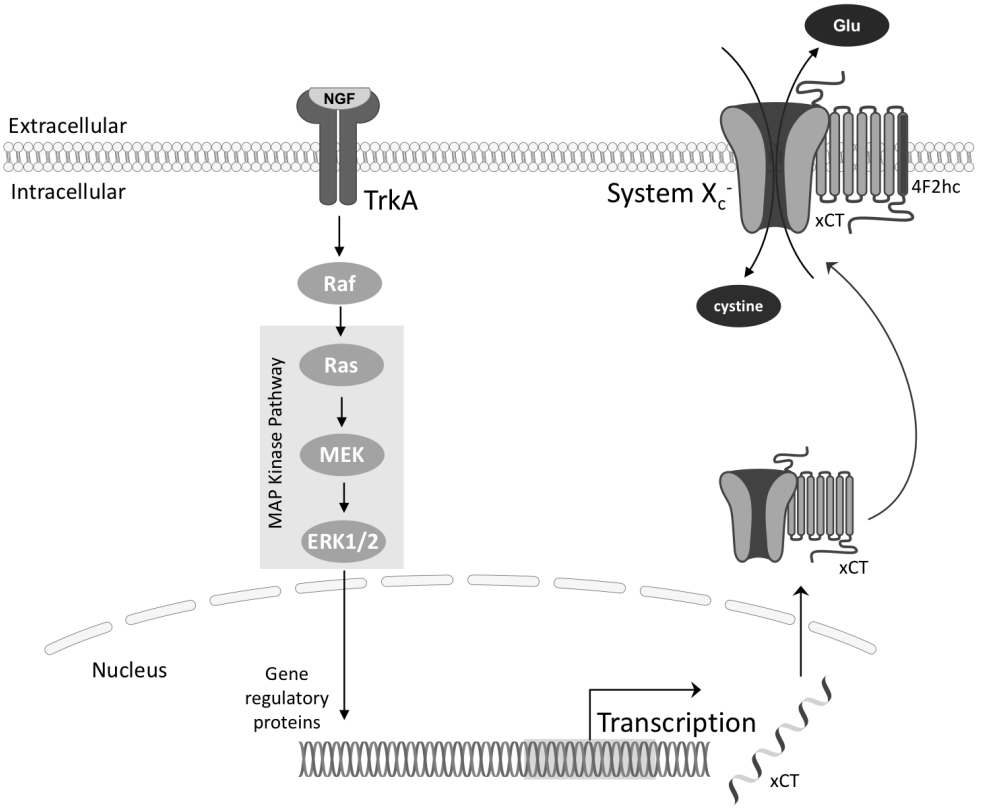

Figure 2.1. Proposed mechanism by which system x_C^--mediated glutamate release is regulated by TrkA-activated signalling pathways.

NGF activates RAS-MAPK signalling through its tyrosine kinase receptor TrkA, which regulates xCT gene expression.

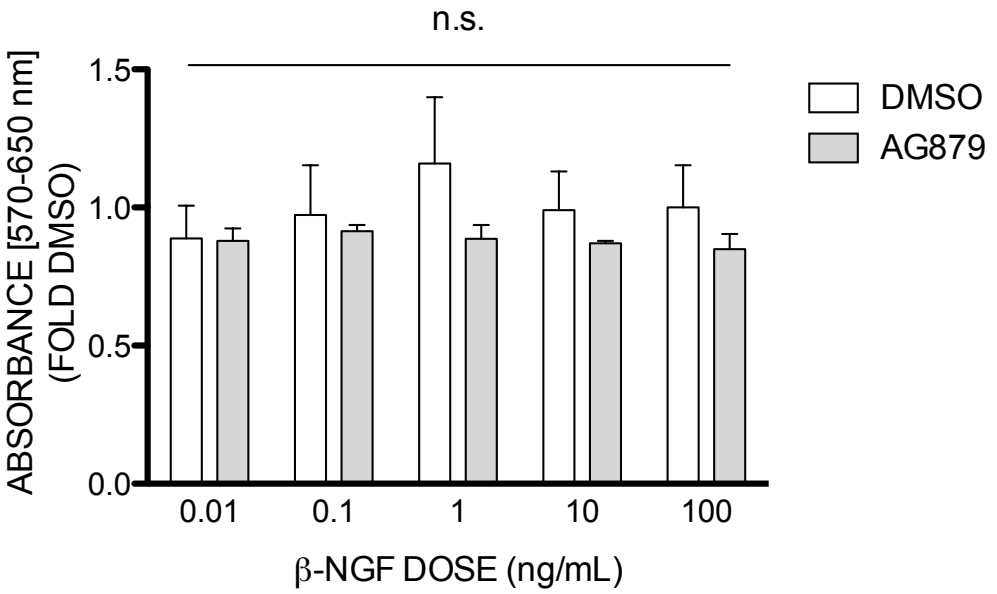

Figure 2.2. Treatment with β-NGF or AG879 does not significantly affect 4T1 carcinoma cell metabolism.

4T1 murine carcinoma cells were seeded and treated with 0.01 – 100 ng β-NGF in the presence or absence of 6 μM AG879 and the MTT assay was utilized during the last 2 h of the 24 h drug treatment period to quantitate cellular metabolic activity. Bars indicate mean ± SEM fold change compared to DMSO negative control. Data are from three independent experiments, $\alpha = 0.05$.

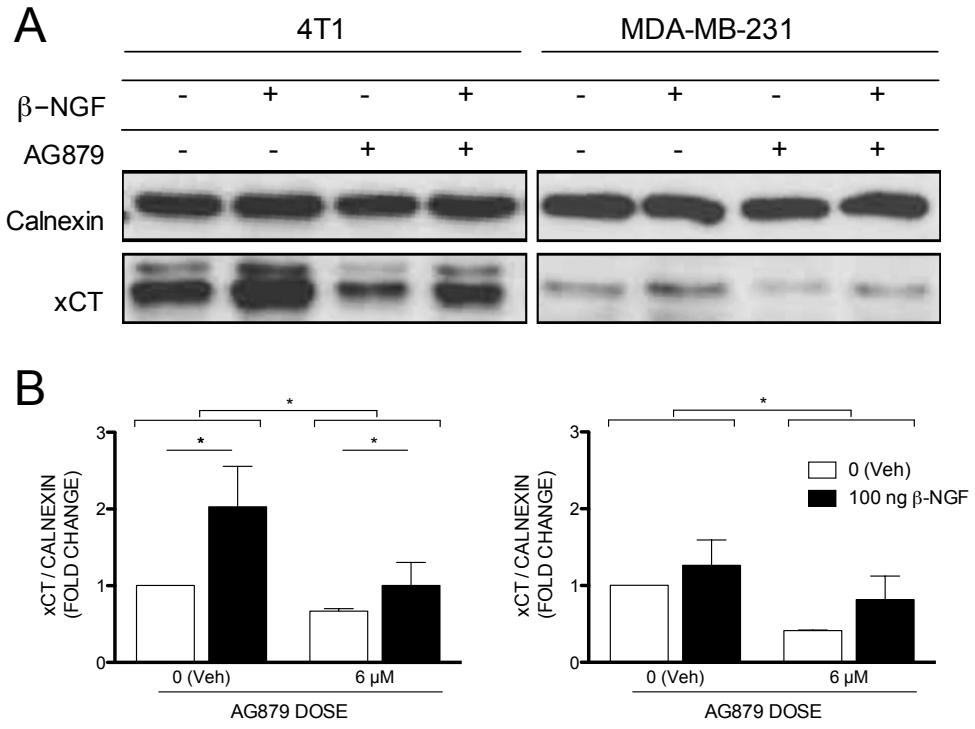

Figure 2.3. AG879 attenuates β-NGF-induced increase in xCT protein in carcinoma cells.

xCT is expressed by murine 4T1 and human MDA-MB-231 breast cancer cells. Treatment with AG879 (6 μM, 24 h) reduces xCT protein levels in 4T1 and MDA-MB-231 cells relative to vehicle-treated cells, and significantly attenuates β-NGF-induced increase in xCT protein levels in murine 4T1 cells. (A) Representative xCT protein levels in cells treated with 6 μM AG879 (or DMSO) and 100 ng β-NGF (or PBS) for 24 h. (B) Relative expression of xCT (37 kDa) compared to DMSO-treated control plates of the same cell line, as determined by

densitometry analysis. Data are from three independent experiments, normalized to Calnexin (90 kDa) and are expressed as means ± SEM, $\alpha = 0.05$.

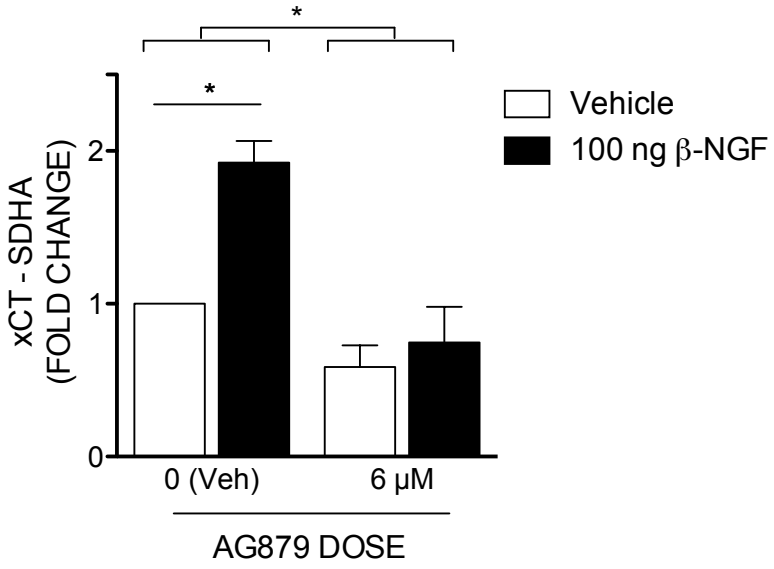

Figure 2.4. AG879 attenuates β-NGF-induced increase in xCT mRNA in carcinoma cells.

xCT mRNA in murine 4T1 carcinoma cells treated with DMSO and β-NGF, relative to negative control. Data are from three independent experiments, normalized to SDHA, and are expressed as means ± SEM, $\alpha = 0.05$.

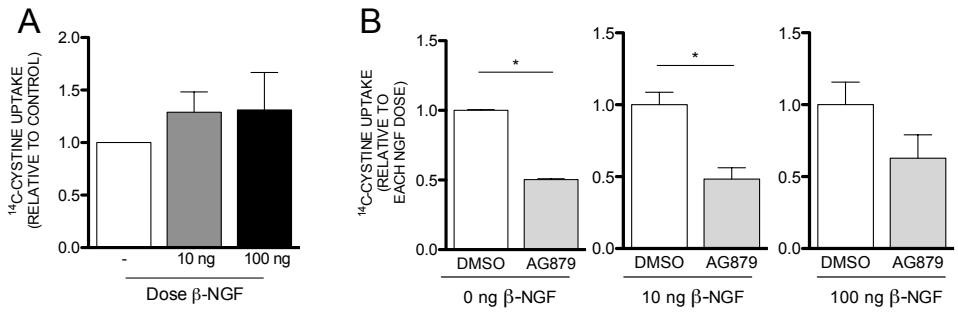

Figure 2.5. Functional system x_C^- activity is increased by β-NGF and attenuated by TrkA inhibition in murine 4T1 carcinoma cells.

Treatment with β-NGF for 24 h did not significantly increase ^{14}C-cystine uptake in 4T1 cells relative to DMSO control in 4T1 cells (A); cells treated with 6 μM AG879 for 24 h demonstrated a relative decrease in ^{14}C-cystine uptake compared to corresponding doses of β-NGF (B). Data are from three independent experiments, normalized to protein level, and are expressed as means ± SEM relative to DMSO, *significantly different from DMSO control, $\alpha = 0.05$.

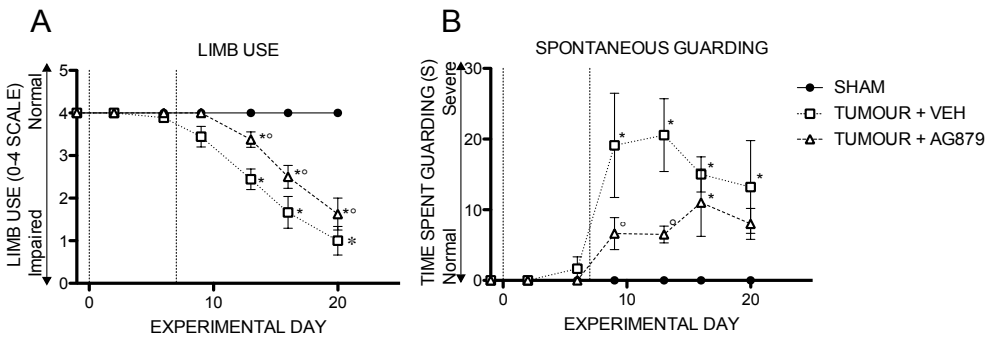

Figure 2.6. AG879 significantly delays the onset and severity of spontaneous nociceptive behaviours.

Open Field tests, including time spent spontaneously guarding the affected limb and scaled limb use, were used to visually assess ongoing and ambulatory nociception. (A) Quantification of limb use in the ipsilateral femurs throughout tumour progression. Normal hindlimb use during spontaneous ambulation was observed and scored on a scale of 4 to 0: Points indicate mean ± SEM of each stage of bone destruction as quantified by this scale. Limb Use numbers represent: (4) normal use, (3) pronounced limp, (2) limp and guarding behaviour, (1) partial non-use of the limb in locomotor activity, and (0) complete lack of limb use. (B) Time spent spontaneously guarding the hindpaw represented ongoing pain and was recorded during an open field observation period. Guarding Time was defined as the time (s) the hindpaw was held aloft while ambulatory. Points indicate means ± SEM; *significantly different from SHAM, °significantly different from TUMOUR, $\alpha = 0.05$; Vertical dashed lines indicate intrafemoral injections (DAY 0) and start of treatment (DAY 7).

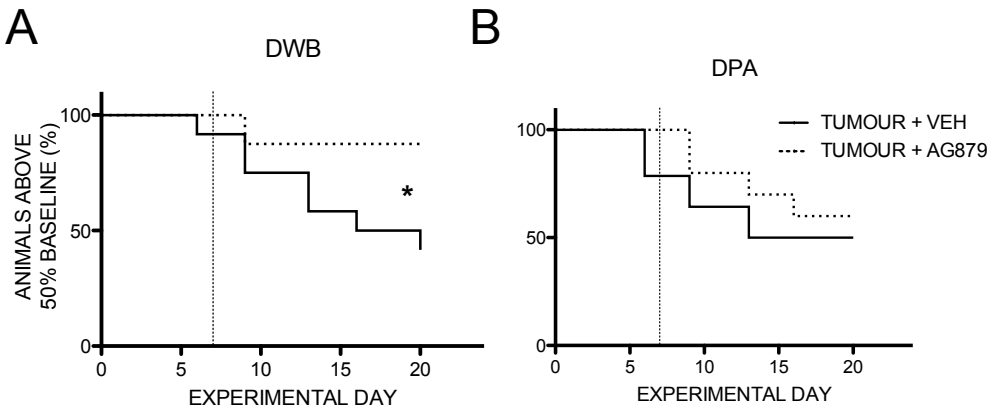

Figure 2.7. AG879 delays time until behavioural decline.

(A) The DWB quantitates the weight borne by the affected limb as a percentage of total recorded weight, standardized to baseline scores. Thus, 100 % on the y-axis represents behaviour prior to tumour inoculation; less than 100% indicates a decrease in weight borne by the tumour-afflicted limb and is indicative of nociceptive behaviour. Kaplan-Meier curve analysis of the time until behavioural decline, expressed as a percentage of animals above the 50 % of baseline cut-off, shows AG879 significantly delays time until the onset of postural disequilibrium in the DWB (Chi square = 0.018, p = 0.724). (B) The DPA test quantitates the threshold force at which the animal withdraws from a progressive stimulus applied to the plantar surface of the affected hindpaw. Thus, 100 % on the y-axis is equivalent to baseline behaviour prior to tumour inoculation; less than 100 % indicates a decrease in the force withstood by the tumour-bearing limb. Kaplan-Meier curve analysis of the time until behavioural decline shows AG879 did not

significantly affect time until decline in the DPA (Chi square = 4.465, p = 0.1). Vertical dashed lines indicate start of treatment (DAY 7).

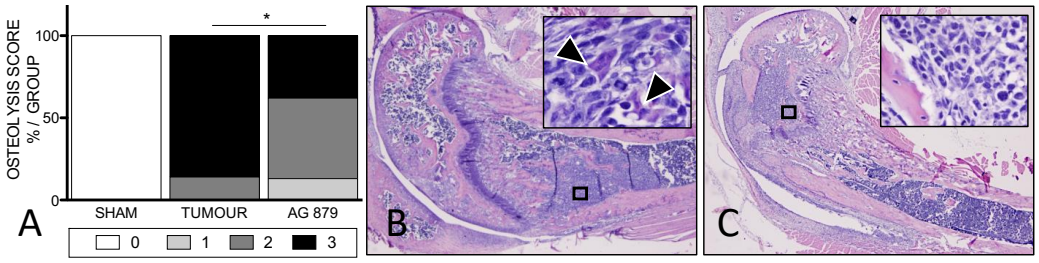

Figure 2.8. AG879 attenuates tumour-induced femoral osteolysis.

(A) Quantification of bone osteolysis in the ipsilateral femurs at endpoint of all treatment groups on 0–3 radiographic analysis scale. Numbers represent: (0) Normal bone, no visible lesion; (1) Minor loss of bone density, marginal lesion; (2) Considerable loss of bone density, lesion limited to bone trabeculae and cortex; (3) Substantial loss of bone density, lesion suggests periosteal involvement and/or fracture. Osteolytic scores are expressed as total percent per treatment group in each score category at endpoint, *significantly different from sham, $\alpha = 0.05$. Representative hematoxylin and eosin staining of ipsilateral femurs in vehicle- (D) and PLX3397-treated (F) tumour-inoculated mice at endpoint, 10× magnification. Boxed areas indicate areas of tumour invasion, inserts depict enlarged tumour cell boxes at 60× magnification, arrow heads indicate osteoclasts.

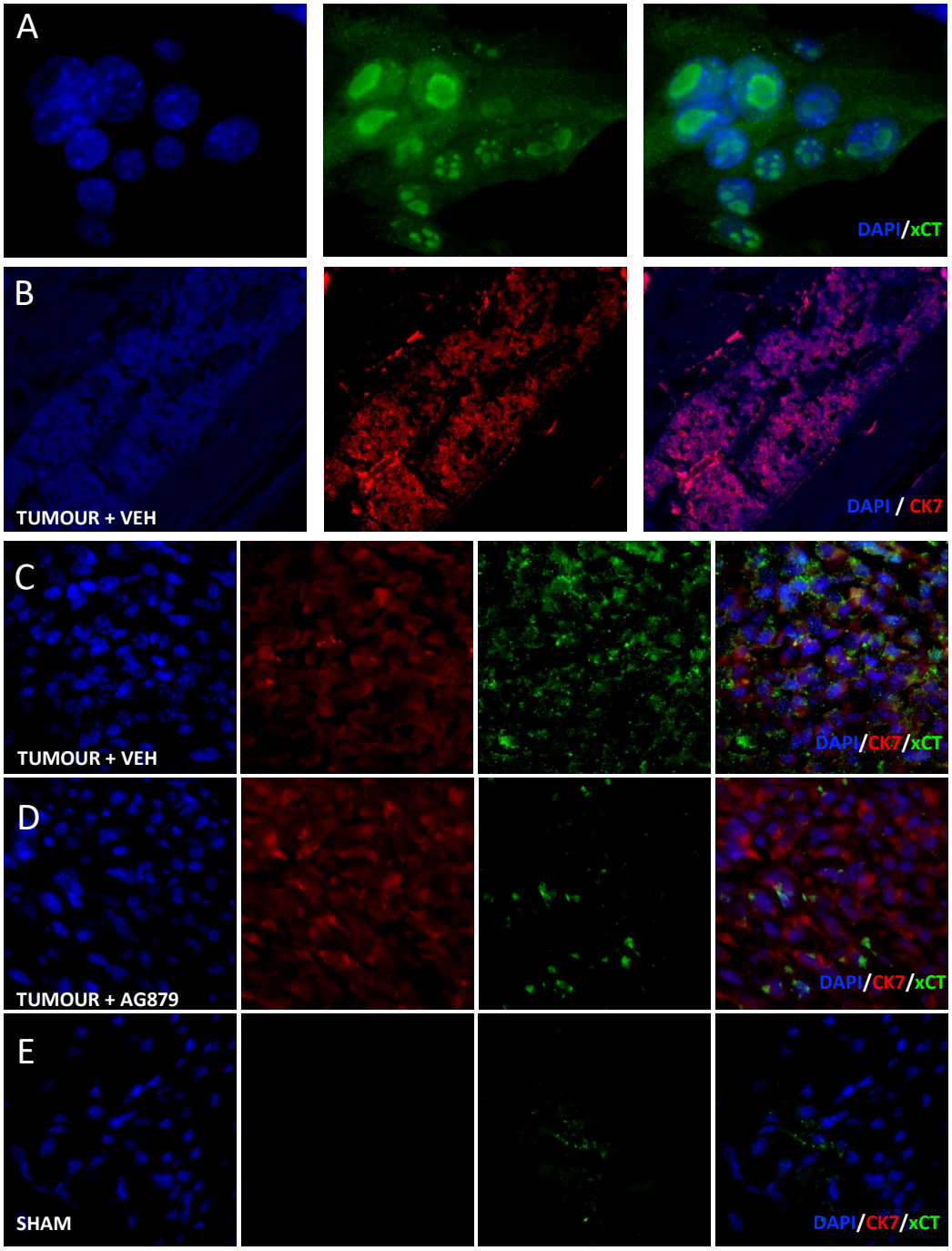

Figure 2.9. AG879 inhibits xCT expression in 4T1 murine carcinoma cells.

Immunocytochemical staining of xCT in murine 4T1 mammary carcinoma cells *in vitro* at 60× magnification (A). Immediately adjacent serial sections to hematoxylin and eosin-stained femurs were stained for nuclei (blue), cytokeratin 7 (CK7), and xCT (green) and imaged using EVOS FL Cell Imaging System at 10× dry (B) and 60× oil (C-E) immersion lenses: double-label immunofluorescent staining of epithelial marker CK7 and xCT in representative tumour-inoculated animals (B), vehicle- (C) and AG879-treated (D) tumour-bearing femurs (D) and sham control (E).

	3 µM	6 µM	12 µM	25 µM	50 µM
4T1	1.08 ± 0.04	0.87 ± 0.07	0.8 ± 0.04*	0.66 ± 0.07**	0.35 ± 0.02**
MDA-MB-231	0.75 ± 0.06*	0.85 ± 0.06	0.65 ± 0.11*	0.55 ± 0.05*	0.39 ± 0.05*

Table 2.1. AG879 concentration-dependently decreases breast cancer cell number.

Murine 4T1 and human MDA-MB-231 carcinoma cells were seeded and treated with serial doses of AG879 for 24 h and cell number was quantified using Crystal Violet staining. Values indicate mean ± SEM fold change in cell number compared to DMSO negative control (0 µM AG879), data are from three independent experiments, *significantly different from DMSO control, *$p < 0.05$, **$p < 0.005$.

Gene Symbol	Primer Sequences (5' to 3')	Reference Gene	Product Size (bp)	Melt Peak (◦C)
SLC7A11 (xCT)	FOR: CCTCTATTCGGACCCATTTAG	SDHA	99	80.0–80.5
	REV: CTGGGTTTCTTGTCCCATATA			

Table 2.2. xCT primers used for relative qPCR.

Melt peaks were obtained on a BioRad CFX Connect Real-TimeSystem.

CHAPTER 3

Spinal Microglia Contribute to Cancer-induced Pain Through System x_C^--mediated Glutamate Release

Tanya Miladinovic & Gurmit Singh

(In press) PAIN Reports

Preface

In this chapter, the author-generated version of the manuscript entitled "Spinal Microglia Contribute to Cancer-induced Pain Through System x_C^--mediated Glutamate Release" accepted February 27, 2019 to *PAIN Reports* (manuscript ID: PAINREPORTS-D-18-0092), is presented. This paper is reproduced, with written permission from Dr. David Yarnitsky, Editor-in-chief of *PAIN Reports*.

For this paper, I performed the drug preparations, cell culturing and treatments, as well as co-culture systems, ^{14}C-cystine uptake assay, immunocytochemistry, Western blotting, animal drug treatments, endpoint tissue collection, processing, and embedding, microtome sectioning of brain tissue, immunofluorescent histology, and photomicroscopy. I also performed all statistical analyses, wrote and revised the manuscript and created all figures and tables therein. Dr. Gurmit Singh provided intellectual direction and guidance in revising the manuscript.

Context and Background Information

Microglial activation within the superficial laminae of the dorsal horn has been repeatedly established in animal models of chronic pain (Cao & Zhang, 2008; Ji, Berta, & Nedergaard, 2013; Shan *et al*., 2007; Sun *et al*., 2008), and has recently been demonstrates in cancer pain states (X.-F. Hu *et al*., 2017; Huo *et al*.,

2018; M. Liu *et al*., 2017; Mao-Ying *et al*., 2012; Wang *et al*., 2012; Yang *et al*., 2015). In healthy organisms, activated microglia promote recovery through the release of trophic and anti-inflammatory factors to clear toxins and pathogens and support neuronal survival. However, chronically activated microglia produce and release harmful substances, including excess glutamate, driving cytotoxicity (S W Barger & Basile, 2001; Steven W Barger *et al*., 2007; Piani & Fontana, 1994; Walter & Neumann, 2009).

The relationship between microglia and glutamate is multidimensional. That is, microglia secrete glutamate via system x_C^- upon activation (Steven W Barger *et al*., 2007; Kigerl *et al*., 2012), but are also activated by exogenous glutamate (reviewed in (Murugan *et al*., 2013)). The presence of glutamate receptors (GluRs) on microglia has therefore been presented as a potential link between inflammation and excitotoxic CNS damage (Pocock & Kettenmann, 2007; Tahraoui *et al*., 2001). Microglia express GluRs (Pocock & Kettenmann, 2007; Tahraoui *et al*., 2001) and are activated by exogenous glutamate (Murugan *et al*., 2013), Therefore, it has been suggested that glutamate released by microglia may act in an autocrine fashion by activating neighboring microglial GluRs (reviewed in (Milligan & Watkins, 2009)).

The following manuscript explores the nociceptive relationship between glutamate released from carcinoma cells and microglial activation and functional system x_C^- activity. This paper employs the use of a co-culture system, in which

wildtype or xCT knockdown (KD) MDA-MB-231 carcinoma cells generated in our lab (Ungard *et al*., 2019) are introduced to microglial cultures. The physiological and functional effects of these low-glutamate-releasing carcinoma cells and their wildtype counterparts was then quantified in microglial cultures.

Spinal Microglia Contribute to Cancer-induced Pain Through System x_C^--mediated Glutamate Release

Tanya Miladinovic[1,2] & Gurmit Singh[1,2]

[1] Michael G. DeGroote Institute for Pain Research and Care, Medicine, McMaster University, 1280 Main St. West, Hamilton, ON L8S 4M1, Canada

[2] Department of Pathology and Molecular Medicine, McMaster University, 1280 Main St. West, Hamilton, ON L8S 4M1, Canada

Corresponding Author: Dr. Gurmit Singh

Department of Pathology & Molecular Medicine, McMaster University, 1280 Main Street West, Hamilton, ON L8N 3Z5, Canada.

Tel.: +1 905 525 9140 x28144.

E-mail address: singhg@mcmaster.ca (G. Singh).

URL: http://www.singhlab.ca (G. Singh).

Abstract

Introduction: Microglial cells, the resident macrophages of the central nervous system (CNS), are a key contributor to the generation and maintenance of cancer-induced pain (CIP). In healthy organisms, activated microglia promote recovery through the release of trophic and anti-inflammatory factors to clear toxins and pathogens and support neuronal survival. Chronically-activated microglia, however, release toxic substances, including excess glutamate, causing cytotoxicity. Accordingly, rising attention is given to microglia for their role in abnormal physiology and in mediating neurotoxicity.

Methods: A validated murine model of 4T1 carcinoma cell-induced nociception was utilized to assess the effect of peripheral tumour on spinal microglial activation and xCT expression. Co-culture systems were then used to investigate the direct effect of glutamate released by wildtype and xCT knockdown MDA-MB-231 carcinoma cells on microglial activation, functional system x_C^- activity, and protein levels of interferon regulatory factor 8 (IRF8), a transcription factor implicated in microglia-mediated nociception.

Results: Blockade of system x_C^- with sulfasalazine (SSZ) *in vivo* attenuated nociception in a 4T1 murine model of CIP and attenuates tumour-induced microglial activation in the dorsal horn of the spinal cord. Furthermore, knockdown

of xCT in MDA-MB-231 cells mitigated tumour cell-induced microglial activation and functional system x_C^- activity *in vitro*.

Conclusions: These data collectively demonstrate that the system x_C^- antiporter is functionally implicated in CIP and may be particularly relevant to pain progression through microglia. Upregulated xCT in chronically-activated spinal microglia may be one pathway to central glutamate cytotoxicity. Microglial xCT may therefore be a valuable target for mitigating CIP.

Introduction

Cancer-induced pain (CIP) is a debilitating condition that accompanies late-stage cancer for the vast majority of patients. As the resident macrophages of the central nervous system (CNS), microglia are a key contributor to the generation and maintenance of pain. In healthy organisms, activated microglia promote recovery, clear pathogens, and support neuronal survival [51]. Chronically-activated microglia, however, release harmful substances, including excess glutamate, causing cytotoxicity [60]. Accordingly, rising attention is given to microglia for their role in abnormal physiology and mediating neurotoxicity. A growing body of evidence indicates that spinal microglial activation is a hallmark of neuroinflammation and is well-documented in chronic pain [9,20,46,52] (reviewed in [56,57]). Peripheral nerve injury has been shown to induce substantial changes in microglia within the spinal cord [1,34,55], and several glia-modifying drugs have been shown to alter pain sensitivity [42,53,63]. Accumulating evidence also suggests that microglial activation plays a definitive roll in CIP [17,18,23,27,61,64].

In their activated state, microglia produce soluble factors, including the ubiquitous cell signalling molecule and major excitatory neurotransmitter glutamate [4,5,37]. Glutamate dysregulation has been linked to various pathologies by its excitotoxic property, and is exchanged with cystine through xCT, the active subunit of the system x_C^- antiporter (reviewed in [11,30]). System

x_C^- activity and xCT expression are constitutively low in the naïve CNS [43], however, one pathway to neurotoxicity involves the release of glutamate by microglia via system x_C^- [3,37–39,62]. The system x_C^- transporter is upregulated in microglia in the presence of oxidative stress as a compensatory mechanism for neurons' limited capacity to upregulate this antiporter [5]. Accordingly, inhibitors of cystine uptake have been shown to inhibit the cytotoxic effects of macrophages through the suppression of glutamate release [62]. Activation of spinal microglia is associated with elevated cerebral spinal fluid (CSF) glutamate concentrations in rats with sciatic nerve injury [10] and reduction of CSF glutamate levels through inhibition of glutamate transporter 1 (GLT-1) and glutamate aspartate transporter (GLAST) inhibits formalin-induced nociception [35,36].

The relationship between microglia and glutamate is multidimensional. Activated microglia secrete glutamate via system x_{C-} [5,21], but are also activated by exogenous glutamate (reviewed in [33]). The presence of glutamate receptors (GluRs) on microglia has therefore been presented as a potential link between inflammation and excitotoxic CNS damage [40,54]. Given that microglia express various metabotropic and ionotropic GluRs, glutamate released by microglia may act in an autocrine fashion by activating neighboring microglial GluRs (reviewed in [32]).

Our lab previously demonstrated the involvement of glutamate in a murine model of CIP [44,59], and has recently developed a human MDA-MB-231

carcinoma cell line that features a stable shRNA-induced knockdown of *SLC7A11*, the gene which encodes xCT [58]. To explore the role of xCT in the inflammatory immune response to peripheral tumours, our validated murine model of CIP was used to quantify spinal microglial activation and xCT expression in relation to nociceptive behaviours. We then employed an isolated *in vitro* co-culture system to confirm that the observed *in vivo* effects represented a direct relationship between peripherally-released glutamate and reactive spinal microglia.

Methods

Cell cultures

HMC3 human microglia cells (American Type Culture Collection; ATCC, Manassas, VA) were maintained in EMEM (Life Technologies, Carlsbad, CA). Wildtype MDA-MB-231 triple-negative human mammary gland carcinoma cells (ATCC, Manassas, VA, USA), shRNA-generated C6 xCT knockdown clones (xCT KD), and pLK01 empty vector control cells [58] were maintained in high glucose DMEM (Life Technologies, Carlsbad, CA). To maintain xCT knockdown, growth media for xCT KD clones (and empty vector controls) were supplemented with Puromycin (1 μg/mL) daily. As per supplier instructions, microglia were supplemented with 10 % fetal bovine serum (FBS). 4T1 triple-negative murine carcinoma cells (ATCC) were maintained in RPMI (Life

Technologies). All carcinoma cells were supplemented with 10 % FBS and 1 % antibiotic/antimycotic, incubated at 37 °C and 5 % CO_2, and verified to be mycoplasma free before experimental use.

Animals

Experimentally naïve immunocompetent female BALB/c mice (Charles River Laboratories, Quebec) aged 4-6 weeks old upon arrival were group-housed at 24 °C with a 12-h light/dark cycle, and provided *ad libitum* access to food and water. All procedures were performed according to guidelines established by the Canadian Council on Animal Care under a protocol reviewed and approved by the Animal Research Ethics Board (AREB) of McMaster University.

Behavioural Test of Nociception

A validated syngeneic mouse model of CIP [31] was utilized to characterize the effects of intrafemoral tumour on nociceptive behaviours and spinal microglial xCT. The progression of spontaneous nociception pre- and post-tumour cell inoculation was monitored using the Dynamic Weight Bearing system (DWB; BioSeb, France), a test for pain-related discomfort and postural equilibrium, as previously described [31]. Briefly, mice (N = 24) were randomly assigned to treatment groups (4T1 tumour (treated with SSZ or vehicle, n = 8/group) or frozen/heat killed 4T1 cell sham controls, n = 8) and acclimated to

testing environment prior to data collection. Three behavioural tests were performed prior to experimental day 0 to establish a stable baseline for normal behaviour, and a video camera provided user-independent spatiotemporal references. Postural disequilibrium was defined as a favouring of the tumour-bearing limb and the resultant shift of weight-bearing to other body parts and was considered indirect evidence of nociception; results are expressed for each animal as a percentage of respective baseline scores.

Tumour Allografts

The 4T1 carcinoma cell line was selected as a model for stage IV human breast cancer, as it is highly tumourigenic and invasive, with the growth and metastatic spread of these cells in BALB/c mice closely mirroring human MDA-MB-231 breast cancer in its proliferative and metastatic properties [41]. Mice were inoculated with 4T1 cells or an equal number of frozen/heat killed 4T1 sham controls injected percutaneously into the right distal femur to establish tumours, as previously described [31,59]. Briefly, on experimental Day 0, mice were anaesthetized by isoflurane inhalation and injected with buprenorphine (0.05 mg/kg, subcutaneous; Schering-Plough, Kenilworth, NJ) to mitigate surgically-induced nociceptive discomfort. Animals were inoculated with 4T1 cells (2×10^4, suspended in 25 μL sterile PBS). The contralateral hindlimb served as a negative control specific to each animal. This method of intrafemoral

injection was selected to minimize damage to the surrounding tissues and has been successfully applied in mouse [31,59] and rat [12] models of bone CIP.

Drug Treatments

Mice were systemically treated with SSZ or vehicle from Day 7 post-cell inoculation through end point. Drug treatment was delayed until Day 7 to allow sufficient time for the implanted cells to reliably establish a bone tumour without drug interference, more accurately mimicking clinical conditions. SSZ was dissolved in 1 M NH_4OH and administered via intraperitoneally-implanted mini-osmotic pumps (Alzet model 1002, Durect) at a maximum soluble dose of 6.6 mg/kg/day, based on the mean weight of the mice on Day 0 (20 g).

Transcardial Perfusion and Tissue Collection

Mice were euthanized by transcardial perfusion by Day 20 post-tumour cell inoculation, when they no longer bore weight on the afflicted limb. Under sodium pentobarbital anesthetic (90 mg/kg, i.p.), animals were perfused with 100 mL cold PBS, immediately followed by 100 mL cold 4 % paraformaldehyde (PFA). Spinal cords were immediately dissected and lumbar vertebrae 4 (L4) sections were isolated and post-fixed in fresh 4 % PFA for 48 h, then processed for immunofluorescent analyses.

Immunofluorescence

The L4 region of the spinal cords were decalcified in 10 % Ethylenediaminetetraacetic acid (EDTA; Sigma-Aldrich) for 14 days, dehydrated, and paraffin-embedded for histological analyses. Spinal cords were then coronally sectioned at 5 µm, deparaffinized and rehydrated, exposed to antigen retrieval in EDTA (pH 8, 95 °C) for 20 min, blocked (Dako protein block) for 2 h, incubated in respective primary and fluorescent secondary antibodies (see Table 1), counterstained with DAPI, coverslipped, and imaged using EVOS FL Cell Imaging System. Serial sections were stained, with primary antibodies replaced by isotype control to serve as a negative control specific to each animal.

Co-cultures

HMC3 human microglia were cultured with or without wildtype, xCT KD, or empty vector control MDA-MB-231 carcinoma cells as an *in vitro* model of peripheral tumour-released glutamate on microglial activation. HMC3 and MDA-MB-231 cells were seeded at 5 x 10^5 cells/well in 6-well plates and 4 µM pore transwell inserts (Corning, Tewksbury, MA), respectively. Cells adhered to inserts or wells in respective media for 2 h, then MDA-MB-231 transwell inserts were added to HMC3 plates and co-cultured for 24 h, with EMEM+ and DMEM+/+ media-only negative controls.

In Vitro Cell Treatments

Lipopolysaccharide (LPS; Sigma- Aldrich), the system x_C^- inhibitor SSZ (Sigma-Aldrich, St. Louis, MO), and L-glutamic acid (Sigma-Aldrich) were prepared in accordance with manufacturer's recommendations in PBS, 1 M NH_4OH, and PBS, respectively, and administered at doses of 1 µg/mL (LPS), 200 µM (SSZ), and 300 mM (L-glutamic acid).

Co-culture Cystine Uptake

The cellular uptake of radiolabeled ^{14}C-cystine was quantified in HMC3 cells, as cystine uptake is mediated by an exchange with glutamate via system x_C^-. HMC3 cells were co-cultured with wildtype, xCT KD, or vector control MDA-MB-231 cells to quantitate the direct effect of peripherally-released glutamate on microglial functional system x_C^- activity. The cystine uptake protocol was adapted from previous reports [31] and adjusted to include co-culture conditions. Briefly, microglia and MDA-MB-231 carcinoma cells were seeded in 6-well plates and transwell inserts, respectively. Microglia were either treated with respective agents (LPS, L-glutamic acid) or MDA-MB-231 inserts (wildtype, xCT KD, vector, wildtype + SSZ) were added to microglia cultures. Treated microglia and co-cultures were incubated for 24 h, at which point drugs were aspirated or co-culture inserts were removed, microglia were exposed to ^{14}C-Cystine (0.015 mCi/mL) for 20 min at 37 °C, washed, and cells were lysed (0.1 % Triton-X in

0.1 N NaOH) for 30 min. Lysates (100 µL) were quantified in 1 mL Ecoscint-H scintillation fluid, values were normalized to mg of total protein and compared to ^{14}C-cystine uptake in naïve HMC3 cells from the same experimental run.

Immunocytochemistry

Immunocytochemistry was performed to assess the effect of carcinoma cell-secreted glutamate on microglial activation via morphology and xCT expression. HMC3 microglia were seeded at 10^4 cells/well in 8-well chamber slides (Ibidi, Martinsried, Germany) and treated with LPS (1 µg/mL) or supplemented with complete media from xCT KD or vector-only control cells every 8 h for 24 h. Media supplements were gently aspirated, HMC3 cells were washed, fixed with 10 % neutral buffered formalin, permeabilized with 0.1 % Triton X-100 for 20 min, blocked with 1 % bovine serum albumin for 1 h, incubated in Iba1 and xCT primary antibodies for 1 h each at RT, and visualized using respective secondary antibodies (see Table 1 for antibody details) with DAPI Fluoroshied counterstain (Thermo Fisher, Waltham, MA) using EVOS FL Cell Imaging System.

Western Blotting

HMC3 cells were treated with 1 µg LPS (or PBS) or co-cultured, as above, with MDA-MB-231, xCT KD, or empty vector control, cell inserts for 24 h to

determine the effects of peripheral tumour-secreted glutamate on xCT, interferon regulatory factor 8 (IRF8), signal transducer and activator of transcription 3 (STAT3), and extracellular signal-regulated kinase 1/2 (ERK1/2) protein levels, and quantified by Western blot analysis, as previously described [31]. Briefly, total protein concentrations were determined to ensure equal protein loading of whole cell lysates on 10 % SDS-PAGE gels and subsequent electrophoretic transfer to PVDF membranes (Immobilon-P, Millipore Corporation). Expression levels of target proteins were evaluated using respective primary antibodies with calnexin (90 kDa) as a loading control (see Table 1), with blocking in 5 % skim milk in Tris-buffered saline, 0.1% Tween 20 (TBS-T). Membranes were incubated in respective horseradish peroxidase-conjugated secondary antibodies for 2 h at RT and visualized by enhanced chemiluminescence (ECL-plus kit; GE Healthcare, Chicago, IL) on Amersham Hyperfilm (GE Healthcare). Blots were quantified using densitometry with ImageJ software (US National Institutes of Health), normalized to loading controls, and compared to naïve HMC3 cells.

Statistical Analyses

All *in vitro* data are presented as mean ± SEM from three independent experiments. Individual t-tests were used to assess the effects of functional system x_C^- activity in co-cultures, as measured by ^{14}C-cystine uptake, relative to naïve, LPS-stimulated, and wildtype-co-cultured microglia. For Western Blot analyses, separate t-tests were conducted to assess the effect of LPS and co-culture

conditions on microglial protein levels. For STAT3 and ERK1/2, data are expressed as a percentage of phosphorylated (pSTAT3 and pERK1/2) over respective total protein levels. *In vivo* and *ex vivo* data encompass n = 8/group. For behavioural analysis of nociception, a 2 (treatment) × 2 (test day) repeated measures ANOVA followed by Bonferroni multiple comparisons was conducted on DWB data. Immunocytochemical and immunofluorescent images were qualitatively considered, with representative images presented. All analyses were performed using GraphPad Prism 7.0a software (GraphPad Software, Inc., La Jolla, CA) with $\alpha = 0.05$.

Results

Blockade of System x_C^- with SSZ attenuates CIP

Tumour-bearing mice demonstrated significantly greater nociceptive behaviours relative to sham controls from Day 13 until endpoint, consistent with previously published data from this model [31] and our immunocompromised model of CIP using wildtype MDA-MB-231 carcinoma cells [59]. In accordance with data from immunocompromised MDA-MB-231 tumour-bearing mice, treatment with the system x_C^- inhibitor SSZ delayed behavioural decline in 4T1 tumour-bearing mice, indicated by significantly greater weight borne relative to vehicle-treated tumour-bearing mice from Day 13 through endpoint (Fig. 3.1).

Peripheral Tumour Alters Spinal Microglial Activity

The number of reactive spinal microglia appeared to increase in the L4 dorsal horn ipsilateral to tumour-inoculated limbs relative to sham, with particular density in laminae I-III (Fig. 3.2B). Regional microglia in tumour-bearing mice appeared vivid in colour, indicated by retracted processes and intense immunofluorescence (Fig. 3.2B, inserts v, vi). Several activated microglia in this region also stained positive for xCT in naïve and tumour-bearing mice (Fig. 3.2A&B, inserts iii, vi). Treatment with SSZ abolished xCT in spinal sections confirming the ability of SSZ to reach the target spinal microglia *in vivo,* and regional microglia were characteristically ramified, highly branched in morphology, with weak Iba1 staining (Fig. 3.2C, insert iii).

MDA-MB-231 Carcinoma Cell-released Glutamate Activates Microglia In Vitro

Immunocytochemical fluorescent co-staining of Iba1 and xCT demonstrated that microglia supplemented with MDA-MB-231 cell complete media are activated in a pattern similar to LPS-activated microglia (Fig. 3.3). This activation was attenuated in the presence xCT KD cell complete media, supporting the notion that peripherally-released glutamate contributes to microglial activation. Naïve microglia appeared characteristically ramified, while LPS-stimulated microglial processes were retracted and fluorescent staining of

Iba1 appeared vivid, indicative of increased microglial activation [16]. Activated microglia also exhibited intense xCT staining, with a pattern of increased fluorescence observed directly outside nuclei (Fig. 3.3).

MDA-MB-231 Cell-released Glutamate Increases Microglial Cystine Uptake In Vitro

Treatment with LPS significantly increased ^{14}C-cystine uptake by HMC3 human microglia relative to untreated cultures. Direct stimulation with L-glutamic acid, a quantity analogous to that secreted by MDA-MB-231 carcinoma cells over a 24 h period (data not shown), increased microglial ^{14}C-cystine uptake in a manner comparable to LPS-stimulated microglia. SSZ significantly decreased microglial ^{14}C-cystine uptake relative to naïve cells and abolished LPS-induced increases in microglial ^{14}C-cystine uptake (Fig. 3.4).

In co-cultures, microglial ^{14}C-cystine uptake was significantly increased in the presence of both wildtype and vector control MDA-MB-231 cells, but not with co-cultures of xCT KD or wildtype SSZ-treated MDA-MB-231 cell inserts (Fig. 3.4), suggesting that peripherally-released glutamate may stimulate microglial functional system x_C^- activity.

MDA-MB-231 Carcinoma Cells Alter Microglial Protein Expression In Vitro

The presence of carcinoma cell complete media altered expression of xCT, IRF8, STAT3, and ERK1/2 protein levels in HMC3 microglia (Fig. 3.5). In particular, supplementation with wildtype MDA-MB-231 media increased microglial IRF8, a transcription factor involved in transforming microglia to a reactive state and implicated in microglia-mediated nociception [28]. This effect was attenuated in xCT KD co-cultures. LPS increased microglial xCT protein relative to naïve HMC3 cells; microglia co-cultured with wildtype MDA-MB-231 cells appeared to present marginally more xCT protein than naïve cells, although the effect was insignificant. Similarly, MAPK pathway-related proteins (total/phosphorylated STAT3 and total/phosphorylated ERK1/2) were also marginally affected by LPS and co-cultures, suggesting that MAPK signalling may be involved in xCT regulation in activated microglia, although these effects were slight and insignificant in the present conditions.

Discussion

These studies build on the growing body of literature that implicates microglia in the pain state associated with peripheral tumours. To our knowledge, this is the first study to explore the relationship between tumour-released glutamate and microglial xCT with respect to CIP. Our recent work demonstrated that systemic delivery of the microglial inhibitor with Pexidartinib delayed the onset and severity of spontaneous tumour-induced nociceptive behaviours and prevented behavioural decline of mechanical withdrawal threshold (Miladinovic

et al., 2018, *in press*), and several models have previously demonstrated the role of microglia in CIP [17,18,23,27,61,64]. Our lab has also characterized the importance of system x_C^--released glutamate from tumour cells across various models of CIP [31,44,59].

Electrophysiological work from murine models of CIP in our lab demonstrates sensitization of ascending L4 dorsal root ganglia (DRG) neurons [65–67], afferents which release glutamate onto postsynaptic neurons in the dorsal horn upon activation [7]. Furthermore, we have determined that glutamate directly injected into the himblimb increases excitability in DRG neurons, an effect that was attenuated by the xCT inhibitor SSZ (unpublished data). Thus, the presence of tumour-derived glutamate initiates physiological changes, which include subsequent glutamate release from DRG neurons, and may contribute to CIP through spinal microglial activation.

Research from the present study illustrates the dynamic role of glutamate in microglia-mediated CIP. We have shown that systemically inhibiting system x_C^- activity with SSZ reduces tumour-induced nociceptive behaviours and microglial activation in the dorsal horn. Furthermore, we have demonstrated that extracellular glutamate directly stimulates human HMC3 microglia into their activated state and increases functional system x_C^- activity and expression of xCT, the active antiporter subunit. This activation and functional activity were present

in both glutamate-supplemented microglia and those co-cultured with glutamate-releasing wildtype, but not xCT knockdown carcinoma cells.

Macrophages release neurotoxic levels of glutamate upon activation by LPS, a potent inflammatory stimulus [13,38,39]. This effect has been simulated *in vivo*, in which neurotoxic concentrations of glutamate were released by selectively activated microglia via system x_C^- [21]. In the present study, immunofluorescent co-staining of Iba1 and xCT confirmed the ability of LPS to activate HMC3 human microglia *in vitro*, and demonstrated the parallel state of activation in microglia supplemented with complete media from wildtype, but not xCT KD carcinoma cells, further implicating glutamate in microglial activation. Additionally, activated microglia presented increased xCT protein levels, while microglia supplemented with xCT KD media presented low xCT protein levels, more comparable to naïve microglia than to their wildtype-supplemented counterparts.

Co-culture studies demonstrated that wildtype and vector-only MDA-MB-231 carcinoma cells increased microglial functional system x_C^- activity, and this effect was attenuated by xCT knockdown, suggesting that glutamate released by carcinoma cells may be responsible for microglial activation and oxidative burst. Accordingly, the co-culture of wildtype, but not xCT knockdown cells, increased microglial protein expression of xCT and IRF8, and slightly increased levels of proteins involved in RAS-MAPK signalling. IRF8, a critical regulator of reactivity

in these immune cells, has been previously implicated in microglia-mediated nociception; IRF8-deficient mice are resistant to peripheral nerve injury-induced neuropathic pain, while transferring IRF8-overexpressing microglia spinally to normal mice results in increased nociceptive behaviours [28]. Here, protein levels of IRF8 were dramatically increased in microglial cultures treated with LPS and in those co-cultured with wildtype MDA-MB-231 cells, an effect which was attenuated in xCT KD co-cultures, further supporting the hypothesis that peripherally-derived glutamate is involved in the activation of microglia.

STAT3 is also associated with microglial polarization and activation and macrophage-associated STAT3 has been implicated in tumour progression (reviewed in [47]). MAPK phosphorylates STAT3, which regulates expression of genes, including xCT [22]. In MDA-MB-231 breast cancer cells, the MAPK inhibitor PD098059 has been shown to abolish basal xCT transcriptional activity [22]. Furthermore, sustained treatment with the STAT3 inhibitor SH-4-54 decreases xCT expression and system x_C^- activity [22].

Behavioural data from 4T1 tumour-bearing mice demonstrated progressive nociception, with significant differences between sham and tumour-bearing mice from Day 13 through endpoint. As previously shown by our immunocompromised CIP model [59], treatment with SSZ delayed behavioural decline in tumour-bearing mice. In accordance with this and other reports [14,48,59], data from the

present study confirmed the ability of SSZ to reduce nociception in an immunocompetent 4T1 carcinoma-induced model of CIP.

Tumour-bearing mice that demonstrated nociception at endpoint also presented robust microglial activation in laminae I-III of the L4 dorsal horn with vivid co-staining of xCT. Conversely, L4 dorsal horn microglia in SSZ-treated tumour-bearing mice were characteristically ramified, with low constitutive staining of Iba1 and negligible levels of xCT^+ co-staining. This region of the spinal cord is one in which several microglia-associated factors, including IL-6, IL-1β, phosphorylated 38 MAPK (p38 MAPK), brain-derived neurotrophic factor (BDNF), and toll-like receptor 4 (TLR4) have been previously implicated in CIP, with particular prominence in terminals of laminae I-III [29]. Thus, upregulated xCT in chronically-activated spinal microglial may be one pathway to central microglial-induced glutamate cytotoxicity. SSZ or other system x_C^- targeting agents may therefore represent a potential therapeutic for mitigating chronic spinal microglial activation associated with CIP.

A rapidly growing body of evidence depicts a clear sex difference in immune-mediated pain hypersentivity, such that female mice are often unaffected by microglia-targeting agents which are effective in their male counterparts (reviewed in [50]). The highly heterogeneous state of bone cancer pain is thought to be the consequence of several pathological mechanisms, owing to the unique properties of the affected tissue, including vascularization and rich periosteal

neuronal networks, immune cells, osteoclasts, and osteoblasts. Bone tumour-induced pathologies have been implicated in the sensitization of surrounding nociceptors, including immune-mediated inflammation [2,6], osteoclastogenesis [25], neurogenesis [26,45], demyelination [19], and extracellular acidification [2]. These pathologies may cumulatively contribute to disparity between cancer-induced hyperalgesia and other chronic pain models. Indeed, several studies have demonstrated promising effects of microglial inhibition across models of CIP in both males and females [17,18,23,27,49,61,64]. Minocycline, a commonly used inhibitor of microglial activation, has been shown to inhibit nociceptive behaviours in murine models of mammary carcinoma cell-induced CIP in male and female mice [8,24,49], suggesting the sexual dimorphism commonly observed across several models of chronic pain may not be relevant to CIP.

Neurons of the CNS have limited capacity for cystine uptake, and are reliant primarily on glia for the provision of cysteine for neuronal glutathione production [15]. Relative to neurons, microglia express high levels of the system x_C^- transporter due to a marked need for oxidative protection and are therefore a key source of excitotoxic glutamate. Activated microglia release glutamate via system x_C^- [37], and the vast majority of glutamate exported from activated microglia can be attributed to the system x_C^- exchange mechanism [4,37]. This mechanism becomes extremely active in microglia because it is the primary route of internalizing cystine for the production of glutathione. As microglia produce

abundant ROS, they place themselves under severe oxidative stress. Thus, the microglial oxidative burst creates a glutathione shortage that is alleviated by cystine influx through xCT, extruding glutamate in the balance [5].

In the presence of high extracellular cystine, microglia become neurotoxic effector cells. This toxicity is selective for neurons and dependent on activation of neuronal ionotropic GluRs. The substances released by activated microglia further activate additional nearby astrocytes, microglia, and neurons, creating a positive feedback loop (reviewed in [32]). Thus, once the harmful stimulus has been managed, it is critical that the microglial inflammatory response be dampened. Immunomodulatory mediators inhibit the release of proinflammatory factors, thereby facilitating a return to homeostasis. In a state of chronic microglial activation, such as that seen in cancer, tumour cells constantly secrete toxic levels of glutamate, and disrupt the return to homeostasis. Given the presence of system x_C^- on microglia, nonvesicular glutamate via this antiporter on microglia represents a notable mechanism for glial-neuronal communication.

Data from the present study collectively demonstrate that the system x_C^- antiporter is functionally implicated in CIP and may be particularly relevant to pain progression through microglia. Given the increased spinal microglial activation in the tumour-bearing state, the upregulated presence of xCT on microglia in the presence of glutamate-releasing tumour cells, and the

implications of system x_C^- in the pain state associated with metastatic tumours, this pathway may be a valuable target for mitigating CIP.

Acknowledgements

This work was supported by the Canadian Breast Cancer Foundation to G.S.

Disclosure

The authors declare no conflict of interest.

Acknowledgements

This work was supported by the Canadian Breast Cancer Foundation to G.S.

Disclosure

The authors declare no conflict of interest.

References

[1] Abbadie C, Lindia JA, Cumiskey AM, Peterson LB, Mudgett JS, Bayne EK, DeMartino JA, MacIntyre DE, Forrest MJ. Impaired neuropathic pain responses in mice lacking the chemokine receptor CCR2. Proc. Natl. Acad. Sci. U. S. A. 2003;100:7947–52.

[2] Asai H, Ozaki N, Shinoda M, Nagamine K, Tohnai I, Ueda M, Sugiura Y. Heat and mechanical hyperalgesia in mice model of cancer pain. Pain 2005;117:19–29.

[3] Bannai S. Exchange of cystine and glutamate across plasma membrane of human fibroblasts. J. Biol. Chem. 1986;261:2256–63.

[4] Barger SW, Basile AS. Activation of microglia by secreted amyloid precursor protein evokes release of glutamate by cystine exchange and attenuates synaptic function. J. Neurochem. 2001;76:846–54.

[5] Barger SW, Goodwin ME, Porter MM, Beggs ML. Glutamate release from activated microglia requires the oxidative burst and lipid peroxidation. J. Neurochem. 2007;101:1205–13.

[6] Breese NM, George AC, Pauers LE, Stucky CL. Peripheral inflammation selectively increases TRPV1 function in IB4-positive sensory neurons from adult mouse. Pain 2005;115:37–49.

[7] Broman J, Anderson S, Ottersen OP. Enrichment of glutamate-like immunoreactivity in primary afferent terminals throughout the spinal cord dorsal horn. Eur. J. Neurosci. 1993;5:1050–61.

[8] Bu H, Shu B, Gao F, Liu C, Guan X, Ke C, Cao F, Hinton AO, Xiang H, Yang H, Tian X, Tian Y. Spinal IFN-γ-induced protein-10 (CXCL10) mediates metastatic breast cancer-induced bone pain by activation of microglia in rat models. Breast Cancer Res. Treat. 2014;143:255–63.

[9] Cao H, Zhang Y-Q. Spinal glial activation contributes to pathological pain states. Neurosci. Biobehav. Rev. 2008;32:972–83.

[10] Chen N-F, Huang S-Y, Chen W-F, Chen C-H, Lu C-H, Chen C-L, Yang S-N, Wang H-M, Wen Z-H. TGF-β1 attenuates spinal neuroinflammation and the excitatory amino acid system in rats with neuropathic pain. J. Pain 2013;14:1671–85.

[11] Choi DW. Glutamate neurotoxicity and diseases of the nervous system. Neuron 1988;1:623–34.

[12] De Ciantis K, Henry J, Yashpal G, Singh G. Characterization of a rat model of metastatic prostate cancer bone pain. J. Pain Res. 2010;3:213.

[13] Domercq M, Sánchez-Gómez MV, Sherwin C, Etxebarria E, Fern R, Matute C. System xc- and glutamate transporter inhibition mediates

microglial toxicity to oligodendrocytes. J. Immunol. 2007;178:6549–56.

[14] Doxsee DW, Gout PW, Kurita T, Lo M, Buckley AR, Wang Y, Xue H, Karp CM, Cutz J-C, Cunha GR, Wang Y-Z. Sulfasalazine-induced cystine starvation: potential use for prostate cancer therapy. Prostate 2007;67:162–71.

[15] Dringen R, Pfeiffer B, Hamprecht B. Synthesis of the antioxidant glutathione in neurons: supply by astrocytes of CysGly as precursor for neuronal glutathione. - PubMed - NCBI. J Neurosci 1999;19:562–569.

[16] Hendrickx DAE, van Eden CG, Schuurman KG, Hamann J, Huitinga I. Staining of HLA-DR, Iba1 and CD68 in human microglia reveals partially overlapping expression depending on cellular morphology and pathology. J. Neuroimmunol. 2017;309:12–22.

[17] Hu X-F, He X-T, Zhou K-X, Zhang C, Zhao W-J, Zhang T, Li J-L, Deng J-P, Dong Y-L. The analgesic effects of triptolide in the bone cancer pain rats via inhibiting the upregulation of HDACs in spinal glial cells. J. Neuroinflammation 2017;14:213.

[18] Huo W, Zhang Y, Liu Y, Lei Y, Sun R, Zhang W, Huang Y, Mao Y, Wang C, Ma Z, Gu X. Dehydrocorydaline attenuates bone cancer pain by shifting microglial M1/M2 polarization toward the M2 phenotype. Mol. Pain 2018;14:1744806918781733.

[19] Inoue M, Rashid MH, Fujita R, Contos JJA, Chun J, Ueda H. Initiation of neuropathic pain requires lysophosphatidic acid receptor signaling. Nat. Med. 2004;10:712–8.

[20] Ji R-R, Berta T, Nedergaard M. Glia and pain: Is chronic pain a gliopathy? Pain 2013;154:S10–S28.

[21] Kigerl KA, Ankeny DP, Garg SK, Wei P, Guan Z, Lai W, McTigue DM, Banerjee R, Popovich PG. System xc− regulates microglia and macrophage glutamate excitotoxicity in vivo. Exp. Neurol. 2012;233:333–341.

[22] Linher-Melville K, Haftchenary S, Gunning P, Singh G. Signal transducer and activator of transcription 3 and 5 regulate system Xc- and redox balance in human breast cancer cells. Mol. Cell. Biochem. 2015;405:205–221.

[23] Liu M, Yao M, Wang H, Xu L, Zheng Y, Huang B, Ni H, Xu S, Zhou X, Lian Q. $P2Y_{12}$ receptor-mediated activation of spinal microglia and p38MAPK pathway contribute to cancer-induced bone pain. J. Pain Res. 2017;Volume 10:417–426.

[24] Liu X, Bu H, Liu C, Gao F, Yang H, Tian X, Xu A, Chen Z, Cao F, Tian Y. Inhibition of glial activation in rostral ventromedial medulla attenuates mechanical allodynia in a rat model of cancer-induced bone pain. J. Huazhong Univ. Sci. Technolog. Med. Sci. 2012;32:291–8.

[25] Lozano-Ondoua AN, Symons-Liguori AM, Vanderah TW. Cancer-induced bone pain: Mechanisms and models. Neurosci. Lett. 2013;557 Pt A:52–9.

[26] Mantyh WG, Jimenez-Andrade JM, Stake JI, Bloom AP, Kaczmarska MJ, Taylor RN, Freeman KT, Ghilardi JR, Kuskowski MA, Mantyh PW. Blockade of nerve sprouting and neuroma formation markedly attenuates the development of late stage cancer pain. Neuroscience 2010;171:588–98.

[27] Mao-Ying Q-L, Wang X-W, Yang C-J, Li X, Mi W-L, Wu G-C, Wang Y-Q. Robust spinal neuroinflammation mediates mechanical allodynia in Walker 256 induced bone cancer rats. Mol. Brain 2012;5:16.

[28] Masuda T, Tsuda M, Yoshinaga R, Tozaki-Saitoh H, Ozato K, Tamura T, Inoue K. IRF8 is a critical transcription factor for transforming microglia into a reactive phenotype. Cell Rep. 2012;1:334–340.

[29] Meng X, Gao J, Zuo J-L, Wang L-N, Liu S, Jin X-H, Yao M, Namaka M. Toll-like receptor-4/p38 MAPK signaling in the dorsal horn contributes to P2X4 receptor activation and BDNF over-secretion in cancer induced bone pain. Neurosci. Res. 2017;125:37–45.

[30] Miladinovic T, Nashed MG, Singh G. Overview of glutamatergic dysregulation in central pathologies. Biomolecules 2015;5.

[31] Miladinovic T, Ungard RG, Linher-Melville K, Popovic S, Singh G.

Functional effects of TrkA inhibition on system xC--mediated glutamate release and cancer-induced bone pain. Mol. Pain 2018;14:1–15.

[32] Milligan ED, Watkins LR. Pathological and protective roles of glia in chronic pain. Nat. Rev. Neurosci. 2009;10:23–36.

[33] Murugan M, Ling E-A, Kaur C. Glutamate receptors in microglia. CNS Neurol. Disord. Drug Targets 2013;12:773–84.

[34] Myers RR, Heckman HM, Rodriguez M. Reduced hyperalgesia in nerve-injured WLD mice: relationship to nerve fiber phagocytosis, axonal degeneration, and regeneration in normal mice. Exp. Neurol. 1996;141:94–101.

[35] Niederberger E, Schmidtko A, Coste O, Marian C, Ehnert C, Geisslinger G. The glutamate transporter GLAST is involved in spinal nociceptive processing. Biochem. Biophys. Res. Commun. 2006;346:393–9.

[36] Niederberger E, Schmidtko A, Rothstein JD, Geisslinger G, Tegeder I. Modulation of spinal nociceptive processing through the glutamate transporter GLT-1. Neuroscience 2003;116:81–7.

[37] Piani D, Fontana A. Involvement of the cystine transport system xc- in the macrophage-induced glutamate-dependent cytotoxicity to neurons. J. Immunol. 1994;152:3578–85.

[38] Piani D, Frei K, Do KQ, Cuénod M, Fontana A. Murine brain macrophages induced NMDA receptor mediated neurotoxicity in vitro by secreting glutamate. Neurosci. Lett. 1991;133:159–62.

[39] Piani D, Spranger M, Frei K, Schaffner A, Fontana A. Macrophage-induced cytotoxicity of N-methyl-D-aspartate receptor positive neurons involves excitatory amino acids rather than reactive oxygen intermediates and cytokines. Eur. J. Immunol. 1992;22:2429–36.

[40] Pocock JM, Kettenmann H. Neurotransmitter receptors on microglia. Trends Neurosci. 2007;30:527–35.

[41] Pulaski BA, Ostrand-Rosenberg S. Mouse 4T1 Breast Tumor Model. Current Protocols in Immunology. Hoboken, NJ, USA: John Wiley & Sons, Inc., 2001, Vol. Chapter 20. p. Unit 20.2.

[42] Raghavendra V, Tanga F, DeLeo JA. Inhibition of microglial activation attenuates the development but not existing hypersensitivity in a rat model of neuropathy. J. Pharmacol. Exp. Ther. 2003;306:624–30.

[43] Sato H, Tamba M, Okuno S, Sato K, Keino-Masu K, Masu M, Bannai S. Distribution of cystine/glutamate exchange transporter, system x(c)-, in the mouse brain. J. Neurosci. 2002;22:8028–33.

[44] Seidlitz EP, Sharma MK, Saikali Z, Ghert M, Singh G. Cancer cell lines

release glutamate into the extracellular environment. Clin. Exp. Metastasis 2009;26:781–7.

[45] Sevcik MA, Ghilardi JR, Peters CM, Lindsay TH, Halvorson KG, Jonas BM, Kubota K, Kuskowski MA, Boustany L, Shelton DL, Mantyh PW. Anti-NGF therapy profoundly reduces bone cancer pain and the accompanying increase in markers of peripheral and central sensitization. Pain 2005;115:128–41.

[46] Shan S, Qi-Liang M-Y, Hong C, Tingting L, Mei H, Haili P, Yan-Qing W, Zhi-Qi Z, Yu-Qiu Z. Is functional state of spinal microglia involved in the anti-allodynic and anti-hyperalgesic effects of electroacupuncture in rat model of monoarthritis? Neurobiol. Dis. 2007;26:558–568.

[47] Sica A, Bronte V. Altered macrophage differentiation and immune dysfunction in tumor development. J. Clin. Invest. 2007;117:1155–1166.

[48] Slosky LM, BassiriRad NM, Symons AM, Thompson M, Doyle T, Forte BL, Staatz WD, Bui L, Neumann WL, Mantyh PW, Salvemini D, Largent-Milnes TM, Vanderah TW. The cystine/glutamate antiporter system xc- drives breast tumor cell glutamate release and cancer-induced bone pain. Pain 2016;157:2605–2616.

[49] Song Z-P, Xiong B-R, Guan X-H, Cao F, Manyande A, Zhou Y-Q, Zheng H, Tian Y-K. Minocycline attenuates bone cancer pain in rats by inhibiting

NF-κB in spinal astrocytes. Acta Pharmacol. Sin. 2016;37:753–62.

[50] Sorge RE, Mapplebeck JCS, Rosen S, Beggs S, Taves S, Alexander JK, Martin LJ, Austin J-S, Sotocinal SG, Chen D, Yang M, Shi XQ, Huang H, Pillon NJ, Bilan PJ, Tu Y, Klip A, Ji R-R, Zhang J, Salter MW, Mogil JS. Different immune cells mediate mechanical pain hypersensitivity in male and female mice. Nat. Neurosci. 2015;18:1081–3.

[51] Streit WJ. Microglia as neuroprotective, immunocompetent cells of the CNS. Glia 2002;40:133–9.

[52] Sun S, Cao H, Han M, Li TT, Zhao ZQ, Zhang YQ. Evidence for suppression of electroacupuncture on spinal glial activation and behavioral hypersensitivity in a rat model of monoarthritis. Brain Res. Bull. 2008;75:83–93.

[53] Sweitzer SM, Schubert P, DeLeo JA. Propentofylline, a glial modulating agent, exhibits antiallodynic properties in a rat model of neuropathic pain. J. Pharmacol. Exp. Ther. 2001;297:1210–7.

[54] Tahraoui SL, Marret S, Bodénant C, Leroux P, Dommergues MA, Evrard P, Gressens P. Central role of microglia in neonatal excitotoxic lesions of the murine periventricular white matter. Brain Pathol. 2001;11:56–71.

[55] Tofaris GK, Patterson PH, Jessen KR, Mirsky R. Denervated Schwann

cells attract macrophages by secretion of leukemia inhibitory factor (LIF) and monocyte chemoattractant protein-1 in a process regulated by interleukin-6 and LIF. J. Neurosci. 2002;22:6696–703.

[56] Tsuda M. Microglia in the spinal cord and neuropathic pain. J. Diabetes Investig. 2016;7:17–26.

[57] Tsuda M, Inoue K, Salter MW. Neuropathic pain and spinal microglia: a big problem from molecules in “small” glia. Trends Neurosci. 2005;28:101–7.

[58] Ungard RG, Linher-Melville K, Nashed M, Sharma M, Wen J, Singh G. xCT knockdown in human breast cancer cells delays onset of cancer-induced bone pain. Mol. Pain 2019;15:1–14.

[59] Ungard RG, Seidlitz EP, Singh G. Inhibition of breast cancer-cell glutamate release with sulfasalazine limits cancer-induced bone pain. Pain 2014;155:28–36.

[60] Walter L, Neumann H. Role of microglia in neuronal degeneration and regeneration. Semin. Immunopathol. 2009;31:513–25.

[61] Wang L-N, Yang J-P, Zhan Y, Ji F-H, Wang X-Y, Zuo J-L, Xu Q-N. Minocycline-induced reduction of brain-derived neurotrophic factor expression in relation to cancer-induced bone pain in rats. J. Neurosci. Res.

2012;90:672–81.

[62] Watanabe H, Bannai S. Induction of cystine transport activity in mouse peritoneal macrophages. J. Exp. Med. 1987;165:628–40.

[63] Watkins LR, Martin D, Ulrich P, Tracey KJ, Maier SF. Evidence for the involvement of spinal cord glia in subcutaneous formalin induced hyperalgesia in the rat. Pain 1997;71:225–35.

[64] Yang Y, Li H, Li T-T, Luo H, Gu X-Y, Lü N, Ji R-R, Zhang Y-Q. Delayed activation of spinal microglia contributes to the maintenance of bone cancer pain in female Wistar rats via P2X7 receptor and IL-18. J. Neurosci. 2015;35:7950–63.

[65] Zhu YF, Kwiecien JM, Dabrowski W, Ungard R, Zhu KL, Huizinga JD, Henry JL, Singh G. Cancer pain and neuropathic pain are associated with A β sensory neuronal plasticity in dorsal root ganglia and abnormal sprouting in lumbar spinal cord. Mol. Pain 2018;14:1744806918810099.

[66] Zhu YF, Ungard R, Seidlitz E, Zacal N, Huizinga J, Henry JL, Singh G. Differences in electrophysiological properties of functionally identified nociceptive sensory neurons in an animal model of cancer-induced bone pain. Mol. Pain 2016;12:174480691662877.

[67] Zhu YF, Ungard R, Zacal N, Huizinga JD, Henry JL, Singh G. Rat model

of cancer-induced bone pain: changes in nonnociceptive sensory neurons in vivo. Pain reports 2017;2:e603.

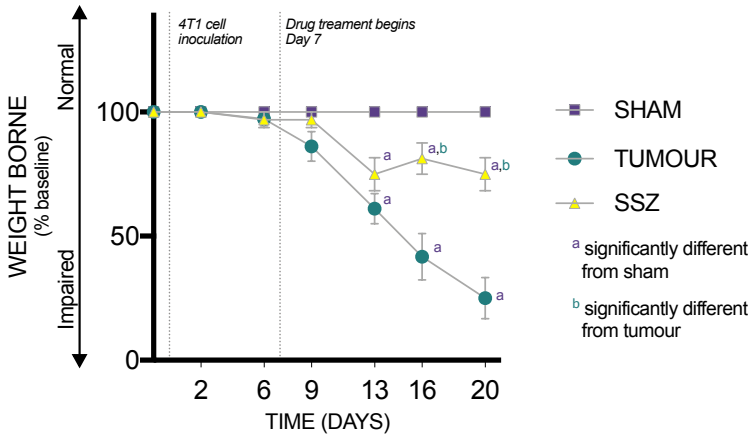

Figure 3.1. Blockade of System xC- with SSZ attenuates CIP.

Nociceptive behaviours were quantitated using the DWB in an effort to confirm the translation of our previously validated murine model of CIP to 4T1 tumour cells. 4T1 tumour-bearing mice demonstrated significantly greater nociceptive behaviours relative to sham controls from Day 13 post-tumour cell inoculation until endpoint, as measured by weight borne in the DWB. This is consistent with previously published data from this model [28] and a similar model of CIP from our lab using wildtype MDA-MB-231 carcinoma cells in immunocompetent mice [50]. In accordance with data from immunocompromised MDA-MB-231 tumour-bearing mice, treatment with the system xC- inhibitor SSZ delayed behavioural decline in 4T1 tumour-bearing mice, as indicated by significantly greater weight borne relative to vehicle-treated mice from Day 13 through endpoint. ($P < 0.05$) significantly different from sham (*) and tumour-bearing mice (°), as determined by ANOVA with Bonferroni multiple comparisons.

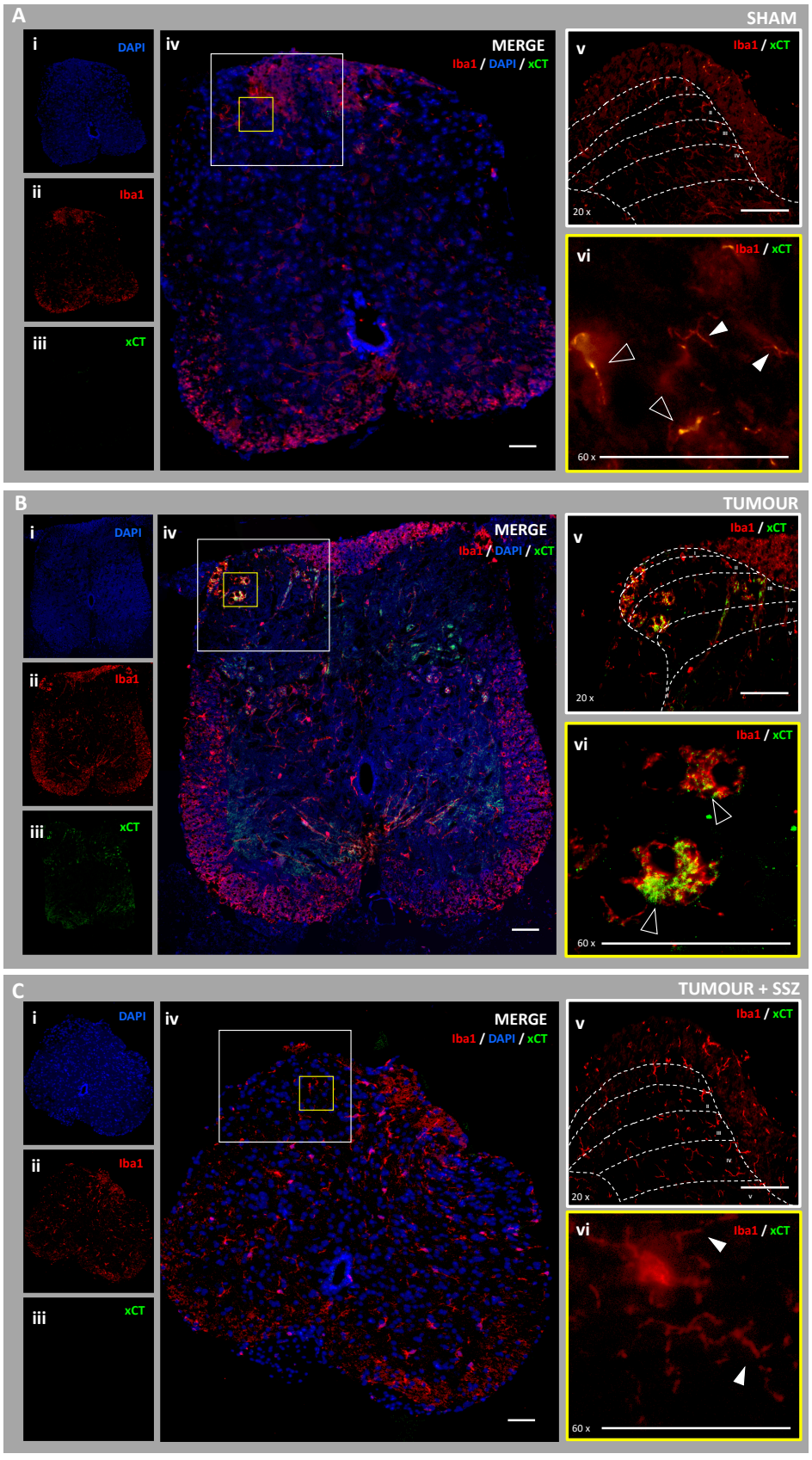
A
SHAM
i DAPI
ii Iba1
iii xCT
iv MERGE
Iba1 / DAPI / xCT
v Iba1 / xCT
20 x
vi Iba1 / xCT
60 x
B
TUMOUR
i DAPI
ii Iba1
iii xCT
iv MERGE
Iba1 / DAPI / xCT
v Iba1 / xCT
20 x
vi Iba1 / xCT
60 x
C
TUMOUR + SSZ
i DAPI
ii Iba1
iii xCT
iv MERGE
Iba1 / DAPI / xCT
v Iba1 / xCT
20 x
vi Iba1 / xCT
60 x

Figure 3.2. Activated spinal microglial xCT increases in the L4 dorsal horn in tumour-bearing mice.

Immunofluorescent staining of nuclei (blue, i) Iba1 (red, ii) and xCT (green, iii), depicting activated microglia and the functional system xC- subunit SLC7A11, respectively, in the lumbar 4 dorsal horn of sham (A), tumour + vehicle (B), and tumour + sulfasalazine (SSZ; C) animals. Captures were collected at endpoint (Day 20 post tumour inoculation) at 10, 20, and 60 × magnification and overlaid for double-label Iba1/xCT immunofluorescence (iv). White box indicates 20 × insert (v), with I-V indicating laminae; yellow box indicates 60 × insert (vi); white arrowheads indicate characteristically ramified microglia, highly branched in morphology; black arrowheads indicate occasions of co-staining of Iba1 and xCT. Scale bars = 50 μm.

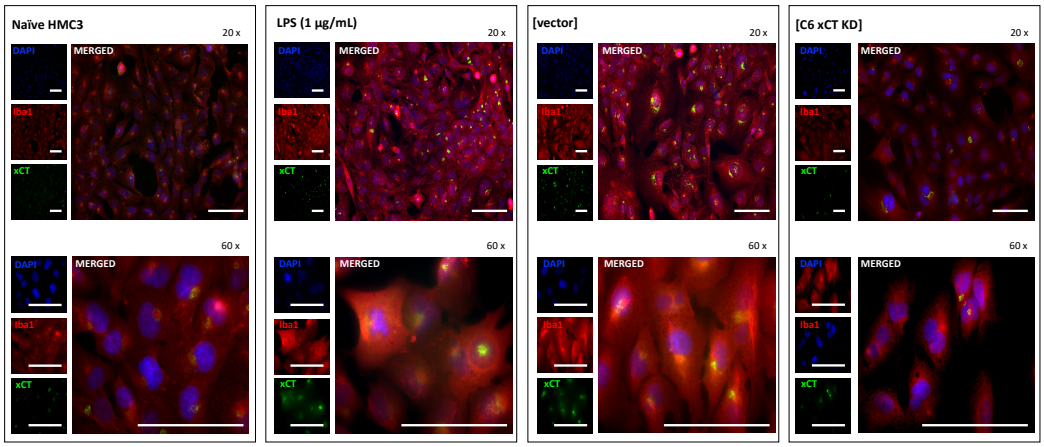

Figure 3.3. Immunocytochemical co-staining of xCT and Iba1 in activated microglia.

HMC3 human microglia are activated in the presence of complete media from wildtype, but not xCT knockdown carcinoma cell complete media. Activated microglia demonstrate increased xCT expression, which is attenuated in microglia supplemented with xCT knockdown cell complete media. Chamber slides were stained for nuclei (blue), Iba1 (red), and xCT (green) and imaged using EVOS FL Cell Imaging System at 20 × dry (top panel) and 60 × oil immersion (bottom panel) lenses. Scale bars = 50 µm.

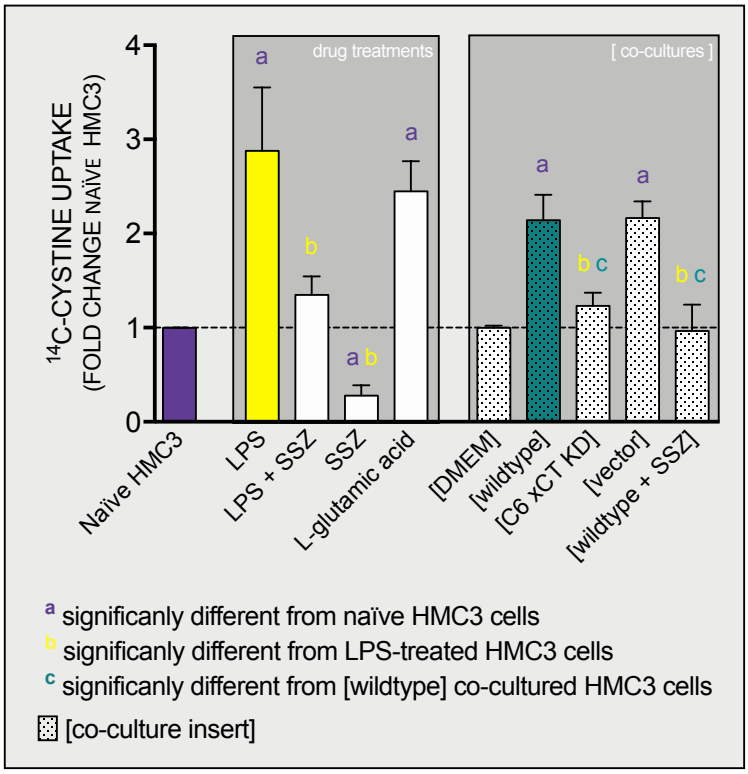

Figure 3.4. Peripherally-released glutamate increases microglial functional system x_C^- activity.

SSZ sterically inhibits constitutive and LPS-induced microglial ^{14C}-cystine uptake in HMC3 human microglia. Treatment with L-glutamic acid increases microglial ^{14C}-cystine uptake comparable to LPS; co-culture with wildtype and vector-only control MDA-MB-231 cells, but not with xCT knockdown cells, increase ^{14C}-cystine uptake in microglia. Inhibiting MDA-MB-231 cell co-cultures with the system x_C^- inhibitor SSZ decreases microglial cystine uptake. ($P < 0.05$) significantly different from naïve (a), LPS-treated (b), and wildtype MDA-MB-231 co-cultured (c) microglia, as determined by respective t-tests.

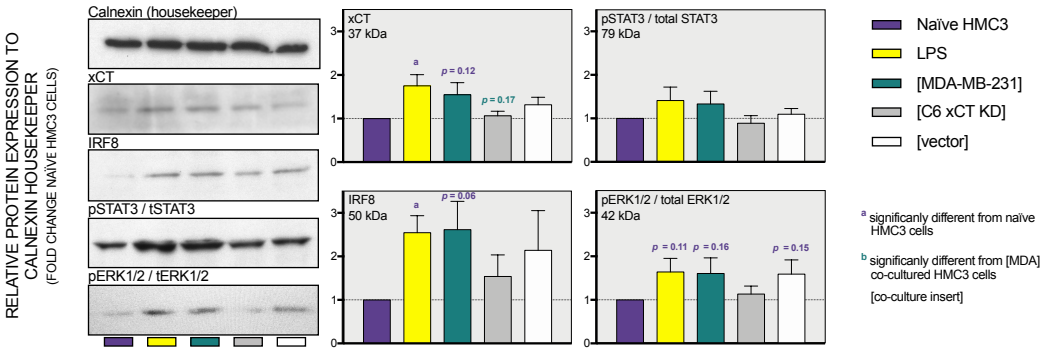

Figure 3.5. LPS alters microglial protein levels.

Western blotting demonstrated the significant increase of microglial IRF8 protein levels in human HMC3 cells stimulated with LPS, with marginal shifts in xCT, pSTAT3, and ERK1/2 protein levels in LPS-stimulated and carcinoma cell co-cultured microglia. Bars represent the mean of three replicates as a fold change relative to naïve HMC3 cells, with error bars indicating SEM; ($P < 0.05$), as determined by planned pairwise comparisons.

Assay	Primary Antibody	Supplier; Catalogue #	[ ]	Secondary Antibody	Notes
Western Blotting	Calnexin	Santa Cruz; SC-11397	1:1000	HRP-conjugated Goat anti-rabbit	
	xCT	Novus Biologicals; 300-318	1:1000	HRP-conjugated Goat anti-rabbit	
	IRF8	Thermo Scientific; PA520088	1:1000	HRP-conjugated Goat anti-rabbit	
	Phospho-STAT3	Cell Signalling; 09145S	1:1000	HRP-conjugated Goat anti-rabbit	
	STAT3	New England Biolabs; 4904P	1:1000	HRP-conjugated Goat anti-rabbit	
	Phospho-ERK1/2	Upstate; 05-797	1:1000	HRP-conjugated Goat anti-rabbit	
	ERK1/2	Cell Signalling; 9122	1:1000	HRP-conjugated Goat anti-rabbit	
	Iba1	Wako; 019-19741	1:1000	HRP-conjugated Goat anti-rabbit	
ICC	xCT	Novus Biologicals; 300-318	1:500	Goat anti-rabbit AF488	
	Iba1	Wako; 019-19741	1:500	Goat anti-rabbit AF647	Blocked with 10% rabbit serum 1h RT
IF	xCT	Novus Biologicals; 300-318	1:200	Goat anti-rabbit AF488	
	Iba1	Wako; 019-19741	1:200	Goat anti-rabbit AF647	Blocked with 10% rabbit serum 1h RT

Table 3.1. Antibodies and respective concentrations ([ ]) utilized for Western Blotting.

Immunocytochemistry (ICC), and Immunofluroescence (IF) assays. RT = room temperature.

CHAPTER 4

Activation of Hippocampal Microglia

in a Murine Model of Cancer-induced Pain

Tanya Miladinovic, Manu Sharma, Andy Phan, Hana Geres,

Robert G Ungard, Katja Linher-Melville, Gurmit Singh

(2019) *Journal of Pain Research, 12*: 1003–1016

Preface

In this chapter, an author-generated version of the manuscript entitled "Activation of Hippocampal Microglia in a Murine Model of Cancer-induced Pain," published in *Journal of Pain Research* March 2019, is presented. This paper is reproduced, with written permission from Dr. Michael E. Schatman, Editor-in-chief of *Journal of Pain Research*.

For this paper, I performed all cell culture and cell treatment, ^{14}C-cystine uptake assay, animal drug treatments, transcardial perfusions and tissue harvesting, processing, and embedding for histological analysis, microtome sectioning, immunofluorescence, photomicroscopy, Western botting, and qPCR assays. I also performed all data analyses, wrote and revised the manuscript, and created all tables and figures therein. Manu Sharma, Andy Phan, and Hana Geres performed behavioural assays. Together with Robert Ungard, I performed the carcinoma cell inoculations. Dr. Gurmit Singh and Dr. Katja Linher-Melville provided intellectual direction and guidance in revising the manuscript. Please note that American spellings are used throughout the article, as required by the journal.

Context and Background Information

The hippocampus, a brain region highly implicated in learning and memory, is deeply altered in various emotional and pain states. These studies

collectively illustrate the important role of affect, or the perceptive complement to nociception, in overall pain experience. These data cumulatively highlight the role of higher-order processing in the pain state associated with peripheral tumours.

The hippocampus may be involved in nociceptive processing, particularly with respect to the affective aspect of pain perception. This work investigated the effect of CIP on the immune response within hippocampal regions and proposed a novel approach to pharmacologically modulating hippocampal microglia in the consideration of the affective component of pain. The hippocampus is involved in multiple cognitive and emotional processes, including the initiation and maintenance of anxiety and depression, and may significantly reduce the efficacy of analgesic agents. Here, I have shown that microglial activation increases in the hippocampi of intrafemoral tumor-bearing mice, and that abolishing microglia with the CSF1R inhibitor Pexidartinib effectively attenuates cancer-induced nociception.

Tumor-induced nociceptive behaviors appeared to progress in parallel with microglial activation in the DG and CA1 regions of the hippocampus, suggesting that regional microglia are implicated in the development and maintenance of CIP. Ablating microglia delayed the onset and severity of IF cancer-induced nociceptive behaviors. Cumulatively, this is the first experimental evidence which demonstrates the effects of peripheral tumor on hippocampal microglial activation in relation to cancer-related nociception in female mice.

However, it is important to appreciate the limitations of this study by recognizing that several other potential mechanisms may be driving CIP, including spinal and non-hippocampal brain microglia. Results of the manuscript presented suggest that hippocampal microglia may be one contributing factor to this pain state. The increase in hippocampal microglia observed in the present study may reflect the emotional and cognitive problems reported by patients with CIP.

This is the first study to assess fluctuations in hippocampal microglial activation patterns in the context of CIP and to address the importance of affective perception as a complement to sensation in driving the pain response in the tumour-bearing state. As such, this manuscript outlines key insights in the field of cancer pain research.

Activation of hippocampal microglia in a murine model of cancer-induced pain

Tanya Miladinovic[1,2], Manu Sharma[1,2], Andy Phan[1,2], Hana Geres[1,2], Robert G Ungard[1,2], Katja Linher-Melville[1,2], Gurmit Singh[1,2]

[1] Michael G. DeGroote Institute for Pain Research and Care, Medicine, McMaster University, 1280 Main St. West, Hamilton, ON L8S 4M1, Canada

[2] Department of Pathology and Molecular Medicine, McMaster University, 1280 Main St. West, Hamilton, ON L8S 4M1, Canada

Correspondence: Dr. Gurmit Singh

Department of Pathology & Molecular Medicine, McMaster University, 1280 Main Street West, Hamilton, ON L8N 3Z5, Canada.

Tel.: +1 905 525 9140 x28144.

E-mail address: singhg@mcmaster.ca (G. Singh).

Abstract

Introduction. Pain is a common and debilitating comorbidity of metastatic breast cancer. The hippocampus has been implicated in nociceptive processing, particularly relating to the subjective aspect of pain. Here, a syngeneic mouse model was used to characterize the effects of peripheral tumors on hippocampal microglial activation in relation to cancer-induced pain (CIP).

Materials and methods. Mice were systemically treated with the colony-stimulating factor 1 receptor inhibitor Pexidartinib prior to intrafemoral (IF) or subcutaneous 4T1 carcinoma cell inoculation. Spontaneous and evoked nociceptive responses were quantitated throughout tumor development, and contralateral hippocampi were collected via endpoint microdissection for RNA analysis. Additionally, IF tumor-bearing animals were sacrificed on days 5, 10, 15, and 20 post 4T1 cell inoculation, and brain sections were immunofluorescently stained for Iba1, a marker of activated microglia.

Results. Ablation of these neuroimmune cells with the CSF1R inhibitor Pexidartinib delayed the onset and severity of cancer-induced nociceptive behaviors in IF tumor-bearing animals, adding to the body of literature that demonstrates microglial contribution to the development and maintenance of CIP. Furthermore, in untreated IF tumor-bearing mice, nociceptive behaviors appeared to progress in parallel with microglial activation in hippocampal regions.

Immuno- fluorescent Iba1+ microglia increased in the dentate gyrus and cornu ammonis 1 hippocampal regions in IF tumor-bearing animals over time, which was confirmed at the mRNA level using relevant microglial markers.

Conclusion. This is the first experimental evidence to demonstrate the effects of peripheral tumor-induced nociception on hippocampal microglial activation. The increase in hippocampal microglia observed in the present study may reflect the emotional and cognitive deficits reported by patients with CIP.

Keywords

Nociception

Hippocampus

Affect

Cancer

4T1

Cancer-induced bone pain

Breast cancer

Microglia

Iba1

Introduction

Pain is a complex, heterogeneous, and subjective phenomenon resulting from integration of sensory, affective, and cognitive experiences. A growing body of literature suggests that chronic pain conditions may be linked to aberrant functioning of neuroimmune circuits implicated in mood and motivation. The hippocampus is involved in multiple cognitive and emotional processes, including the initiation and maintenance of anxiety and depression.[1,2] Clinical studies suggest that such mood conditions are among the factors that prevent recovery from pain, and may significantly reduce the efficacy of analgesic agents.[3] Accordingly, development of pharmacologic interventions for the treatment of chronic pain ought to extend beyond circuits which control sensory transmission, to those which mediate affect. That is, pharmacologic interventions should not only target sensory transmission but should encompass the perceptive pathways involved as well. It is important to consider pathways implicated in the cognitive and affective aspects of pain processing in parallel with ascending and descending sensory pathways in the development of cancer-induced pain (CIP) therapeutics.

Emerging evidence suggests that the hippocampus may be involved in nociceptive processing, particularly with respect to the affective aspect of pain perception.[4–14] The inflammatory response within the hippocampus has been implicated in the perception of pain [15] through the processing and modification of nociceptive stimuli.[16–18] Several experimental studies have found that direct

manipulation of the hippocampus alters nociceptive behavior. For example, hippocampal manipulation has been shown to alter the perception of noxious stimuli: lesion to the ventral hippocampus partially alleviates acute thermal and mechanical nociception in rat pups and adults,[5] while direct injection of the local anesthetic and sodium channel blocker lidocaine to the dentate gyrus (DG) region of the hippocampus produces analgesia.[9,14]

Our lab recently developed a validated murine model of cancer-induced depression (CID) using 4T1 carcinoma cells, in which subcutaneous (SC) tumor burden was associated with increased depressive-like symptoms.[19] RNA-sequencing and real-time RT-PCR analysis of hippocampi revealed considerable overlap between cancer-induced and positive control corticosterone-induced depressive states.[20] Several of the validated hippocampal mRNA targets associated with the depressive-like state in tumor-bearing mice were ionotropic and metabotropic glutamate receptors (GluRs) and glutamatergic modulators,[20] many of which are expressed or secreted by microglia (reviewed in Murugan *et al*[21]).

In the healthy nervous system, the resident immune cells microglia have a highly branched morphology and a downregulated phenotype. Upon activation, microglia release pro-inflammatory cytokines, including interleukin-1 (IL-1), interleukin-6 (IL-6), and tumor necrosis factor-α (TNF-α) (reviewed in Hanisch[25]). However, rising attention is given to chronically-activated microglia,

which release substances inherent to several neurodegenerative disorders, leading to cytotoxicity and neuronal degeneration (reviewed in Tang and Le[26]). Although a complex process, microglial activation may be simplified to the classically activated M1 and alternatively activated M2 states. Thus, M1 microglia, activated by LPS or the proinflammatory cytokine interferon-γ, express antigens including CD68 and CD86, and produce high amounts of oxidative metabolites and proinflammatory cytokines. M2 microglia possess anti-inflammatory properties, express CD206 and arginase, and promote tissue repair and angiogenesis.[22] In animal models of pain, however, this simplified M1/M2 classification may be insufficient, with several intermediate phenotypes present, causing a shift in the M1/M2 balance.[23] In the present study, microglial activation was morphologically characterized by immunohistochemical quantification of ionized calcium binding adaptor molecule 1 (Iba1). Iba1 is a protein expressed by microglia, plays a role in their functional regulation, and is particularly relevant during their activation.[24] Mounting evidence suggests that the immune response may play a significant role in the development of cancer-induced pain (CIP).[27–30]

The present study was designed to further assess the role of the neuroimmune response within the hippocampus in relation to cancer-related nociception. Here, we present data which illustrates the role of hippocampal microglia in the development of tumor-related nociception using a validated murine model of CIP.[31] Spontaneous and evoked nociceptive responses increased

following tumor progression. Immunofluorescent and transcript evidence of microglial activation paralleled development of tumor-induced nociception, and pharmacological microglial inhibition with a colony-stimulating factor 1 receptor (CSF1R) inhibitor attenuated CIP.

Materials and methods

Cell Culture

4T1 triple-negative murine mammary carcinoma cells (American Type Culture Collection, ATCC, Manassas, Virginia) were selected as an analogue to aggressive triple-negative human breast cancer, such as the MDA-MB-231 cell line. Cells were maintained in high glucose RPMI (Life Technologies, Carlsbad, CA), supplemented with 10 % fetal bovine serum (FBS) and 1 % antibiotic/antimycotic (Life Technologies), incubated at 37 °C and 5 % CO_2, and verified to be mycoplasma free before experimental use.

Crystal Violet

To assess potential off-target growth effects of the drug on tumor cells, the selective microglial inhibitor Pexidartinib (PLX3397; Plexxikon Inc, Berkeley, CA, USA), a validated inhibitor of microglial CSF1R,[32] was dissolved in dimethyl sulfoxide (DMSO) for preparation of a 100 mM stock. 4T1 cells were seeded at 5

$\times 10^3$ cells/well in 96-well plates, treated with serial dilutions of Pexidartinib (0.01-100 ng/mL) dissolved in DMSO (maximum final concentration: 0.1 %) or 0.1 % DMSO alone (vehicle control) for 24 h, fixed with 10 % neutral buffered formalin and quantified using 0.1 % Crystal Violet stain in 80 % EtOH based on a standard curve for 4T1 cells. Absorbance was read on an optical plate reader (BioTek) at $\lambda = 570$ nm and expressed as a fold change relative to naïve control wells on the same experimental plate.

Mice

Female BALB/c mice (Charles River Laboratories) aged 4-6 weeks upon arrival were provided *ad libitum* access to food and water and group housed in cages maintained at 24 °C with a 12 h light/dark cycle. Mice were randomly assigned to treatment groups: (1) sham intrafemoral (IF) surgery + vehicle; (2) IF tumor + vehicle; (3) IF tumor + Pexidartinib; (4) SC tumor + vehicle; or (5) SC tumor + Pexidartinib. All animal procedures were reviewed and approved by the *Animal Research Ethics Board* (AREB) of McMaster University and performed according to guidelines established by the Canadian Council on Animal Care.

Experimental Design

Our validated syngeneic mouse models of metastatic IF [31] and SC [19] cancer were utilized to characterize the effects of the CSF1R inhibitor

Pexidartinib on tumor burden and tumor-induced nociception *in vivo*. Experimentally-naïve immunocompetent mice (N=46) were inoculated with either 2×10^4 4T1 cells or frozen/heat killed 4T1 cell sham controls (n=8) percutaneously into the right distal femur (n=28) or subcutaneously at the right hindlimb, lateral to the pelvic-hip joint (n=10) to establish tumors. Animals were systemically treated with the CSF1R inhibitor Pexidartinib administered in pre-absorbed standard rodent chow or control chow for three weeks prior to 4T1 cell inoculation through to experimental endpoint. The behavioral timeline is detailed in Fig. 4.1.

The progression of spontaneous and evoked nociception pre- and post-IF and SC 4T1 cell inoculation was monitored. A blinded experimenter performed all behavioral testing during the animals' light cycle. Animals were randomly assigned to systemic therapies (Pexidartinib or control chow), were acclimated to the behavioral testing environment and equipment one week prior to commencing data recording, and tested twice weekly for the duration of the experiment. Three behavioral tests were performed prior to experimental day 0, which served to establish a stable baseline for the animals' normal locomotive and nociceptive behavior; results are expressed for each animal as a percentage of these baseline scores. A selection of tests for spontaneous and evoked nociception was used to monitor nociceptive responses with tumor progression: Spontaneous Guarding,

Limb Use, and Dynamic Plantar Aesthesiometer (DPA; Ugo Basile, Comerio, Italy).

Spontaneous Nociception

Open Field tests, including time spent spontaneously guarding the affected limb and scored limb use, were used to visually assess ongoing and ambulatory nociception using formerly validated tests.[31,33] The time (s) spent spontaneously guarding the tumor-bearing hindpaw interpreted as representative of ongoing nociception and was recorded during a two-minute open field observation period using a stopwatch. Guarding Time was defined as the time the hindpaw was held aloft while ambulatory. During the 2-minute spontaneous ambulation period, hindlimb use was observed and scored on a scale of 4–0: (4) normal use; (3) pronounced limp; (2) limp and guarding behavior; (1) partial non-use of the limb in locomotor activity; and (0) complete lack of limb use.

Evoked Nociception

The dynamic plantar aesthesiometer (DPA) test, a semi-automated version of the classic von Frey test,[34] was used to quantitate mechanical allodynia and hyperalgesia. A normally non-nociceptive mechanical stimulus was presented individually to the plantar surface of the hind paws and the threshold force and time at which the paw was withdrawn were recorded on a computer. A metal

filament raised by an electrical actuator with variable force and acceleration provided the tactile stimulus. Contralateral hind paws served as a control specific to each animal.

Transcardial Perfusion and Tissue Collection

Throughout tumor development, animals were monitored daily for limb use, overall health status, and body weight. For immunofluorescent staining, animals were euthanized by transcardial perfusion on Day 5, 10, 15 (IF tumor group), or Day 20 (sham/IF/SC tumor groups) post-tumor cell inoculation, or if they no longer bore weight on the afflicted limb. For hippocampal mRNA analysis, animals were euthanized by cervical dislocation under isofluorane anesthetic on or before day 20 post-tumor cell inoculation.

For immunofluorescent histological analysis and quantification of activated hippocampal microglia, untreated and Pexidartinib-treated IF tumor mice and sham controls were sacrificed by transcardial perfusion at Day 5, 10, 15, or 20 post-4T1 cell inoculation (n = 4/day). Animals were sacrificed under sodium pentobarbital anesthetic (90 mg/kg, i.p.) and perfused with 100 mL of PBS, immediately followed by 100 mL of cold 4 % paraformaldehyde (PFA; pH 6.9). Whole brains were dissected, post-fixed in 4 % PFA for 48 h, and paraffin-embedded for immunofluorescent analyses; tumor-bearing femurs and surrounding tissues were post-fixed in 4 % PFA until radiographic analysis.

For RNA investigation, whole brains were immediately dissected on a chilled, RNase-free dish, and preserved in RNAlater Solution (Invitrogen, Carlsbad, CA) at 4 °C for 24 h, then at -80 °C. Each brain was microdissected under stereoscopic microscope to isolate contralateral hippocampi under chilled, RNase-free conditions; the contralateral hemisphere was separated, the cerebellum was removed, and remaining tissue was adjusted with the medial side facing up. Tissue covering the medial surface of the hippocampus was removed using a dissection spatula by inserting below the corpus callosum. The thalamus, septum, and underlying striatum were discarded to clearly reveal the hippocampus. Using forceps to secure the cerebral cortex, a spatula was placed under the ventral part of the hippocampus. Finally, the structure was rolled out to separate the hippocampus from the rest of the cortex. Microdissection technique is detailed in Fig. 4.2.

Radiographic Analysis

Radiographic analysis was used to establish the extent of bone degradation in hindlimbs, indicative of tumor invasion. Radiographs were scored on a scale of 0-3: (0) normal bone, no visible lesion; (1) minor loss of bone density, minimal lesion; (2) moderate to substantial loss of bone density, lesion limited to bone trabecula and cortex; (3) substantial loss of bone density, lesion includes clear periosteal involvement or fracture (See scale development in Ungard *et al*[35]).

Hematoxylin and Eosin

Tumor-bearing hindlimbs were stained to confirm the degree of intrafemoral tumor in animals that demonstrated lytic lesions on X-rays. Following decalcification in 10 % Ethylenediaminetetraacetic acid (EDTA) for 14 days, femurs and surrounding tissues were paraffin-embedded, sagittally sectioned at 5 μm, stained with hematoxylin and eosin, xylene-cleared, and imaged using brightfield microscopy.

Immunofluorescence

Brains were coronally sectioned at 5 μm, slide-mounted, rehydrated, and exposed to antigen retrieval in EDTA (pH 8, 95 °C) for 20 min. Tissues were then blocked (Dako protein block) for 2 h, incubated in respective primary (Wako anti-Iba1, 1:1000, O/N at 4 °C) and fluorescent secondary antibody (Life Technologies AlexaFluor-488 goat anti-rabbit, 1:500, 2 h at RT), or direct conjugate primary antibody (c-Fos D1 AlexaFluor 546: Santa Cruz, 1:200, O/N at 4 °C), counterstained with DAPI, coverslipped, and imaged using EVOS FL Cell Imaging System at 10 × (dry) , 20 × (dry), and 60 × (oil) immersion lenses.

RNA Isolation

Isolated hippocampi were dissociated, preserved in RNAlater, and total RNA was isolated from each sample using the RNeasy Kit (Qiagen), as described previously.[20] Briefly, eluates were DNase-treated using the DNA-free Kit (DNase Treatment and Removal Reagents; Ambion) and RNA quality/purity was quantitated using spectrophotometric analysis at OD_{260}/OD_{280}.

Quantitative Real-time PCR

Relative mRNA levels were quantified using quantitative real-time PCR (qPCR), adopted from previous reports.[20] Briefly, cDNA was synthesized from 400 ng total RNA via reverse transcription using Superscript III kit (Life Technologies) and qPCR assays were performed for each target and reference gene per sample with SsoAdvanced Universal SYBR Green Supermix (BioRad). All target and housekeeping gene primers based on sequences specific for *Mus musculus* were derived from PrimerBank.[36] Official gene symbols, primer sequences (5' to 3'), respective housekeepers, product sizes, and PrimerBank IDs for target gene products are listed in Table 1; specifications of housekeeping genes used in this study (*SDHA*: succinate dehydrogenase complex, subunit A; *Polr2b*: polymerase (RNA) II (DNA directed) polypeptide B; *Taf1b*: TATA box binding protein [Tbp]-associated factor, RNA polymerase I) are summarized in Table 2. Housekeeper genes were selected based on stringent efficiency testing of each target-housekeeper pair. All primers had an annealing temperature of 60 °C. Amplification efficiencies were tested for each primer pair, with efficiency

(E)=[$10^{(-1/S)}$]-1, and relative quantification analysis of gene expression data was conducted according to the 2-ΔΔCT method.[37]

Statistical Analyses

Two-way (tumor × treatment) repeated measures ANOVA with Bonferroni post hoc planned comparisons were used to assess the effect of treatment on all behavioral outcomes. The DPA force recorded at paw withdrawal was expressed as the mean force of the five measurements collected on each test day and normalized to individual animal's baseline values. A reduction in the force in the tumor-bearing limb relative to baseline was considered evidence of increased sensitivity in that limb manifested as an intentional limb withdrawal from the mechanical stimulus.

Chi-square analysis of the proportion of scores within each treatment group was used to assess radiographic analysis of osteolysis. Immunohistochemical staining of hematoxylin and eosin in hind limbs, and immunofluorescent co-staining of c-Fos and Iba1 at endpoint were qualitatively considered. Immunofluorescent staining of Iba1-positive activated microglia in DG and cornu ammonis 1 (CA1) regions of contralateral hippocampi throughout tumor progression was considered qualitatively and quantitated using Image J software;[38] fluorescence levels were determined using the corrected total cell fluorescence (CTCF) method[39] and frequency distributions at each time point

were compared to that of sham controls using the Mann-Whitney U test. qPCR data were analyzed using the 2−ΔΔCT method[37], such that for each of the 14 target genes, the mean ΔCT for the three or four biological replicates in each group being compared was calculated as the mean cycle threshold (CT) of the target gene minus the mean CT of the respective housekeeping gene. For each pairwise comparison, ΔΔCT was then calculated as the mean ΔCT of the experimental group minus the ΔCT of the sham control, and the resulting ΔΔCT value was then converted to 2−ΔΔCT; in all pairwise comparisons of interest (IF tumor vs IF tumor + Pexidartinib; IF tumor vs SC tumor; and SC tumor + SC tumor + Pexidartinib), fold changes were calculated relative to sham control group (n = 1). To determine the overall experimental SEM, SDs derived from the ΔCT values were converted to SEMs, which were used to calculate upper and lower values of 2−ΔΔCT. IF tumor + Pexidartinib; IF Data bars represent the mean (n = 3, SC tumor group; n = 4 IF tumor, IF tumor + Pexidartinib, and SC tumor + Pexidartinib groups) biological replicates relative to sham control, with error bars indicating SEM.

All analyses were performed using GraphPad Prism 7.0a software (GraphPad Software, Inc., La Jolla, CA, USA) and GraphPad QuickCals; α was set at 0.05.

Results

Pexidartinib Does Not Significantly Alter Tumor Cell Growth

Treatment with Pexidartinib (0.01-100 ng/mL) for 24 h did not significantly affect murine 4T1 carcinoma cell number *in vitro* as measured by crystal violet stain (Fig. 4.3), suggesting the effects seen *in vivo* were not attributable to drug effects on tumor cells themselves.

Peripheral Tumor Increases Activated Microglia in DG and CA1

Immunofluorescent staining of Iba1+ cells in the hippocampus demonstrated robust changes in the morphology and number of microglia in the DG and CA1 regions (see Fig. 4.4A-B for representative images of resting and activated state) over the course of IF tumor development (Fig. 4.4B-E). Staining also revealed constituitive expression of Iba1 in sham mice (Fig. 4.4F), with unaltered expression phenotype in SC tumor-bearing mice at day 20 (Fig. 4.4G), and confirmed the ability of Pexidartinib to reach the intended target and ablate hippocampal microglia *in vivo* (Fig. 4.4H). Serial coronal sections through DG and CA1 regions of the hippocampus were collected (approximately 3 mm posterior to Bregma, as detailed in Fig. 4.4I). Quantitatively, the presence of peripheral IF tumors was associated with significant increases in activated microglia on Days 10, 15, and 20 in DG and Days 15 and 20 in CA1 regions (Fig. 4.4J).

Immunocytochemical staining for Iba1+ cells on whole blood smears from Pexidartinib-treated animals confirmed the ability of the drug to ablate peripheral cells of macrophage linage (data not shown). No differences between sham and tumor-inoculated mice were observed in ipsilateral hippo- campi or across prefrontal cortical regions (data not shown), suggesting that brain microgial activation increased in a region- and hemisphere-specific manner.

Peripheral Tumor Decreases Hippocampal Neural Activity

Double-label immunofluorescent staining of Iba1 and c-Fos demonstrated a subtle trend toward lower c-Fos expression in the presence of greater Iba1 expression (Fig. 4.5).The increased level of activated hippocampal microglia seen at endpoint in IF tumor group was associated with lower expression of regional c-Fos than sham and SC tumor groups, suggesting an inverse correlation between activated microglia and functional neural activity in the hippocampus of tumor-bearing animals.

Pexidartinib Attenuates Tumor-induced Nociceptive Behaviors

Intrafemoral tumor-inoculated mice demonstrated significantly greater spontaneous nociception relative to sham controls from Day 9 and 13 post-tumor cell inoculation until endpoint, as measured by Spontaneous Guarding and Limb Use, respectively. Eliminating microglia with Pexidartinib delayed the onset and

severity of spontaneous nociception, as demonstrated by recovered limb use and dramatically reduced guarding behavior relative to untreated mice (Fig. 4.6A,B, respectively). Similarly, in the DPA, tumor-inoculated mice exhibited significantly greater evoked nociceptive behaviors relative to sham controls from Day 9 through endpoint, and ablating microglia with Pexidartinib significantly inhibited tumor-induced behavioral decline, as measured by attenuated hyperalgesia through experimental endpoint (Fig. 4.7).

Pexidartinib Does Not Significantly Alter Tumor Invasion

Radiographic analysis confirmed the presence of bone degradation in cancer cell-inoculated mice at endpoint (See Fig. 4.8A-C for representative images); Pexidartinib did not appear to significantly alter the extent of tumor-induced osteolysis (Chi square=0.896, p=0.484; see Fig. 4.8D). Hematoxylin and eosin staining of affected hindlimbs confirmed the presence of tumor cells in femurs of animals that demonstrated lytic lesions by X-ray; tumor invasion was most frequently observed in the distal epiphysis and diaphysis of affected femurs (data not shown).

Peripheral Tumor Alters Hippocampal mRNA

qPCR confirmed the dramatic increase in hippocampal microglia in tumor-bearing animals at endpoint (Day 20), as demonstrated across multiple microglial

markers at the mRNA level, including AIF1 (Iba1), CD68, and CD11b (Fig. 4.9A-C). Furthermore, IF tumor-bearing mice demonstrated greater levels of hippocampal microglial markers at the mRNA level relative to SC tumor-bearing mice, suggesting that the site of peripheral metastasis contributes to microglial activation in the hippocampus. Treatment with Pexidartinib dramatically reduced hippocampal microglia mRNA across both tumor-bearing models (Fig. 4.9A-C), confirming the ability of the drug to abolish microglia *in vivo*. Hippocampal mRNA levels of the Toll-like receptor 2 (TLR2) and pro-inflammatory cytokine Interleukin 1 beta (IL1-β) were also affected by peripheral tumor, with increases in hippocampal TLR2 and IL1-β mRNA in IF tumor-bearing mice relative to sham, a trend that was abolished by treatment with Pexidartinib (Fig. 9D-E). Pexidartinib also slightly reversed marginal IF and SC tumor-induced decreases in c-Fos mRNA (Fig. 4.9F).

Several mRNA targets previously reported to be related to cancer- and drug-induced depression were affected by peripheral tumor in the present study, demonstrating parallel outcomes to those previously reported in SC tumor-bearing mice,[20] with these effects being amplified in IF tumor-bearing mice. In particular, GluRs and glutamatergic modulators present on microglia (glutamate ionotropic receptor NMDA type subunit 2C: Grin2c, glutamate ionotropic receptor AMPA type subunit 4: Gria4, gamma-aminobutyric acid type A receptor alpha 3 subunit: Gabra3, and glutamate metabotropic receptor 4: Grm4), were reduced across

Pexidartinib- and control-treated IF and SC tumor groups, with the exception of increased Grin2c mRNA in IF tumor-bearing mice relative to sham. Colony stimulating factor 3 Receptor (CSF3r) and transglutaminase 2 (Tgm2) mRNA levels followed a similar pattern across treatment groups, with Pexidartinib abolishing IF and SC tumor-induced increases in mRNA, while gamma-aminobutyric acid type A receptor delta subunit (GABRD) mRNA levels were reduced across all groups relative to sham, and and 5-hydroxytryptamine type 2C receptor (Htr2c) mRNA levels were reduced in IF tumor mice, with Pexidartinib reversing this effect (Fig. 4.10). Given the relatively small group sizes used in this assay (n = 3, SC tumor group; n = 4 IF tumor, IF tumor + Pexidartinib, and SC tumor + Pexidartinib groups), no significant differences were observed within secondary mRNA targets (Grin2c, Gria4, Csf3r, Tgm2, Gabra3, Grm4, Gabrd, and Htr2c), and therefore only trends are offered within these planned comparisons.

Discussion

In the present study, we have demonstrated that activated Iba1+ microglia increase in the hippocampus as IF tumors progress in our validated murine model of CIP. Furthermore, globally eliminating microglia with the CSF1R inhibitor Pexidartinib delays the onset and severity of spontaneous and evoked cancer-induced nociception, and abolishes various tumor-induced aberrancies in microglia-associated mRNA marker levels within the hippocampus.

CSF1R is a key regulator of myeloid lineage cells and is required for microglial survival in the adult brain. Under normal conditions, microglia are the only cell type that express the CSF1R in the brain.[32,40] Chronic treatment with the CSF1R inhibitor Pexidartinib has been shown to transiently eliminate virtually all microglia in the CNS, with no behavioral or cognitive impairments and without compromise of the blood brain barrier. In the present study, immunofluorescent staining of Iba1 confirmed the ability of Pexidartinib to ablate microglia in specific regions of the brain, and qPCR quantification of microglial markers Iba1, CD68, and CD11b from hippocampal mRNA further supported this finding.

In accordance with several murine models of CIP,[31,35,41] intrafemoral inoculation of 4T1 murine mammary carcinoma cells produced dramatic and lasting nociceptive behaviors, while SC inoculation of the same cells did not yield nociception, as assessed by current behavioral assays, suggessting that the host tissue, rather than the mere presence of peripheral tumor, is intimately involved in the development of pain behaviors. It should be noted that the current behavioral assays selected to quantify nociceptive behaviors primarily examine hindlimb nociception, as measured by limb use, paw withdrawal, and limb guarding. As such, SC tumor-bearing mice may have experienced nociception beyond that measured, as skin is highly innervated, and SC tumors were administered directly under the skin.

Inhibition of microglia with Pexidartinib delayed the onset and severity of sustained nociceptive behaviors in IF tumor- bearing mice, adding to the body of literature that implicates microglia in the pain state associated with bone metastasis.[27,28,30,42–44] This is the first study to demonstrate inhibition of CIP by targeting CSF1R. Given that this model utilized breast cancer cells to establish IF and SC tumors, only female mice were used in an effort to translate to a clinically relevant population. However, previous studies have established an immune cell-related sexual dimorphism, such that spinal microglia were required for the development of neuropathic pain hypersensitivity in male, but not female mice.[45] While this effect may be dependent on several elements, including model- and strain-specific factors, additional murine studies in both males and females could further explore the role of region-specific microglial activation across various models of CIP.

Hippocampal microglial activation appeared highly correlated to the development of IF and SC tumors, with the effect being particularly pronounced in IF tumor-bearing mice. Temporal increases in nociceptive behaviors in IF tumor-bearing mice roughly mirrored microglial activation in hippocampal regions, with peak microglial activation occurring on day 15 post tumor cell inoculation, and morphological changes present as early as day 5 following tumor inoculation. Thus, microglial processes appeared retracted (see Fig. 4.4A,B for representative instances), and fluorescent staining of Iba1 appeared brighter as

tumors progressed, indicative of increased microglial activation.[46] Interestingly, microglial activation in the dorsal horn of the spinal cord has been shown to peak two weeks following induction of bone cancer pain in a rat model,[27] and a study assessing the effects of colon carcinoma cell-induced peripheral tumor demonstrated hippocampal dysfunction, including such affective measures as memory impairment and depression-like behaviors.[47] To our knowledge, this is the first study which illustrates the relationship between hippocampal microglia and CIP.

Our lab previously demonstrated overlap in hippocampal mRNA changes within validated murine models of a classic depressive-like state and cancer-induced depression.[19,20] Analysis of hippocampal mRNA from the present model of CIP demonstrated considerable overlap of select mRNA targets with that of mice from models of both corticosterone- and cancer-induced depressive states,[20] including cell signalling and neurotransmission modulators present on microglia.

In the present study, qPCR results demonstrated a dramatic increase in multiple microglial markers in IF tumor-bearing mice relative to sham controls. It has been suggested that Iba1 is most suitable as an early activation marker in considering morphological fluctuations in microglia, as Iba1 staining is inclusive of slender protrusions of ramified microglia, while CD68 and CD11b are widely expressed across various activation stages.[46] Several other hippocampal factors were affected by IF and SC tumor, including TLR2 and IL1-β, both of which

appeared to increase in mice with IF, but not SC tumor. mRNA levels of the immediate early gene c-Fos were also affected by the presence of tumor, such that IF tumor, and to a lesser extent, SC tumor, were associated with lower hippocampal c-Fos expression, a marginal effect which was mitigated by microglial inhibition.

Hippocampal abnormalities, including decreased hippocampal volume, are demonstrated in clinical cases of depression [48] and comorbidity between chronic pain and depression has been repeatedly established.[49–53] One way by which hippocampal volume may be decreased in cases of pain or depression is via nerve death from excitotoxic factors secreted by microglia. That is, in pathological conditions, the state of chronically-activated microglia switches from characteristically neuroprotective to neurotoxic (reviewed in Block *et al*[54]). Indeed, hippocampal expression of the c-Fos protein, a marker of functional neural activity, is dramatically reduced in CA1, CA3, and DG regions of the hippocampus in a formalin-induced model of inflammatory pain, corresponding to increased nociceptive behaviors.[8] Immunofluorescent co-staining of c-Fos and Iba1 from the present study suggest that parallel mechanisms may mediate these pain states.

The present study adds to a growing body of literature that implicates the hippocampus in the nociceptive and affective dimensions of pain. In clinical observation, electrical stimulation of the hippocampus has been shown to evoke

painful sensations in humans,[55] and micro-injection of the local anesthetic lidocaine into the DG mitigates formalin-induced nociception in rats.[9] Furthermore, when injected into DG and CA1 regions, the competitive and non-competitive NMDA receptor antagonists AP5 and MK801 reduce acute and persistent nociceptive behaviors in a model of chronic pain.[10,11] One means by which hippocampal microglia may contribute to nociception is through the secretion of cytotoxic levels of glutamate, which are known to be released by microglia during states of chronic activation.[56,57] Microglia are heterogeneously distributed within the adult mouse brain, with particular density in hippocampal regions,[40] and the hippocampus modulates affective and motivational properties of the nucleus accumbens and forebrain through glutamatergic inputs (reviewed in [15,58]). Future studies may further explore these pathways and their relationship to glutamate-mediated CIP.

In the present study, ablating microglia delayed the onset and severity of IF cancer-induced nociceptive behaviors. Furthermore, tumor-induced nociceptive behaviors appeared to progress in parallel with microglial activation in the DG and CA1 regions of the hippocampus, adding to the body of literature that implicates the hippocampus in the development and maintenance of CIP, and implicating hippocampal microglia in this response. Cumulatively, this is the first experimental evidence that demonstrates the effects of peripheral tumor on hippocampal microglial activation in relation to cancer-related nociception in

female mice. However, it is important to appreciate the limitations of this study; we recognize that several other potential mechanisms may be driving CIP, including spinal and non-hippocampal brain microglia, and we suggest that hippocampal microglia may be one contributing factor to this pain state.

Conclusions

The increase in hippocampal microglia observed in the present study may reflect the emotional and cognitive problems reported by patients with CIP. Given the complexity of CIP and comorbidity between chronic pain conditions and mood disorders, it is essential to consider pathways implicated in the cognitive and affective aspects of pain processing in parallel with ascending and descending sensory pathways in the development of CIP therapeutics.

Acknowledgements

The authors wish to thank Plexxikon for supplying the CSF1R inhibitor Pexidartinib. This work was supported by the Canadian Breast Cancer Foundation to G.S.

Disclosure

The authors report no conflicts of interest in this work.

References

1. Murray F, Smith DW, Hutson PH. Chronic low dose corticosterone exposure decreased hippocampal cell proliferation, volume and induced anxiety and depression like behaviours in mice. *Eur J Pharmacol*. 2008;583(1):115-127. doi:10.1016/j.ejphar.2008.01.014.

2. Eisch AJ, Petrik D. Depression and Hippocampal Neurogenesis: A Road to Remission? *Science (80-)*. 2012;338(6103):72-75. doi:10.1126/science.1222941.

3. Legrain V, Iannetti GD, Plaghki L, Mouraux A. The pain matrix reloaded: a salience detection system for the body. *Prog Neurobiol*. 2011;93(1):111-124. doi:10.1016/j.pneurobio.2010.10.005.

4. Zhao X-Y, Liu M-G, Yuan D-L, *et al*. Nociception-induced spatial and temporal plasticity of synaptic connection and function in the hippocampal formation of rats: a multi-electrode array recording. *Mol Pain*. 2009;5:55. doi:10.1186/1744-8069-5-55.

5. Al Amin HA, Atweh SF, Jabbur SJ, Saadé NE. Effects of ventral hippocampal lesion on thermal and mechanical nociception in neonates and adult rats. *Eur J Neurosci*. 2004;20(11):3027-3034. doi:10.1111/j.1460-9568.2004.03762.x.

6. Echeverry MB, Guimarães FS, Del Bel EA. Acute and delayed restraint stress-induced changes in nitric oxide producing neurons in limbic regions. *Neuroscience*. 2004;125(4):981-993. doi:10.1016/j.neuroscience.2003.12.046.

7. Favaroni Mendes LA, Menescal-de-Oliveira L. Role of cholinergic, opioidergic and GABAergic neurotransmission of the dorsal hippocampus in the modulation of nociception in guinea pigs. *Life Sci*. 2008;83(19-20):644-650. doi:10.1016/j.lfs.2008.09.006.

8. Khanna S, Chang LS, Jiang F, Koh HC. Nociception-driven decreased induction of Fos protein in ventral hippocampus field CA1 of the rat. *Brain Res*. 2004;1004(1-2):167-176. doi:10.1016/j.brainres.2004.01.026.

9. McKenna JE, Melzack R. Analgesia produced by lidocaine microinjection into the dentate gyrus. *Pain*. 1992;49(1):105-112.

10. McKenna JE, Melzack R. Blocking NMDA receptors in the hippocampal dentate gyrus with AP5 produces analgesia in the formalin pain test. *Exp Neurol*. 2001;172(1):92-99. doi:10.1006/exnr.2001.7777.

11. Soleimannejad E, Naghdi N, Semnanian S, Fathollahi Y, Kazemnejad A. Antinociceptive effect of intra-hippocampal CA1 and dentate gyrus injection of MK801 and AP5 in the formalin test in adult male rats. *Eur J Pharmacol*. 2007;562(1-2):39-46. doi:10.1016/j.ejphar.2006.11.051.

12. Soleimannejad E, Semnanian S, Fathollahi Y, Naghdi N. Microinjection of ritanserin into the dorsal hippocampal CA1 and dentate gyrus decrease nociceptive behavior in adult male rat. *Behav Brain Res*. 2006;168(2):221-225. doi:10.1016/j.bbr.2005.11.011.

13. Yamamotová A, Franek M, Vaculín S, St'astný F, Bubeníková-Valesová V, Rokyta R. Different transfer of nociceptive sensitivity from rats with postnatal hippocampal lesions to control rats. *Eur J Neurosci*. 2007;26(2):446-450. doi:10.1111/j.1460-9568.2007.05666.x.

14. McEwen BS. Plasticity of the hippocampus: adaptation to chronic stress and allostatic load. *Ann N Y Acad Sci*. 2001;933:265-277.

15. Fasick V, Spengler RN, Samankan S, Nader ND, Ignatowski TA. The hippocampus and TNF: Common links between chronic pain and depression. *Neurosci Biobehav Rev*. 2015;53:139-159. doi:10.1016/j.neubiorev.2015.03.014.

16. Bushnell MC, Ceko M, Low LA. Cognitive and emotional control of pain and its disruption in chronic pain. *Nat Rev Neurosci*. 2013;14(7):502-511. doi:10.1038/nrn3516.

17. Liu M-G, Chen J. Roles of the hippocampal formation in pain information processing. *Neurosci Bull*. 2009;25(5):237-266. doi:10.1007/s12264-009-0905-4.

18. Simons LE, Elman I, Borsook D. Psychological processing in chronic pain: a neural systems approach. *Neurosci Biobehav Rev*. 2014;39:61-78. doi:10.1016/j.neubiorev.2013.12.006.

19. Nashed MG, Seidlitz EP, Frey BN, Singh G. Depressive-Like Behaviours and Decreased Dendritic Branching in the Medial Prefrontal Cortex of Mice with Tumors: A Novel Validated Model of Cancer-Induced Depression. *Behav Brain Res*. 2015. doi:10.1016/j.bbr.2015.07.040.

20. Nashed MG, Linher-Melville K, Frey BN, Singh G. RNA-sequencing profiles hippocampal gene expression in a validated model of cancer-induced depression. *Genes Brain Behav*. 2016;15(8):711-721. doi:10.1111/gbb.12323.

21. Murugan M, Ling E-A, Kaur C. Glutamate receptors in microglia. *CNS Neurol Disord Drug Targets*. 2013;12(6):773-784.

22. Czeh M, Gressens P, Kaindl AM. The yin and yang of microglia. *Dev Neurosci*. 2011;33(3-4):199-209. doi:10.1159/000328989.

23. Mosser DM, Edwards JP. Exploring the full spectrum of macrophage activation. *Nat Rev Immunol*. 2008;8(12):958-969. doi:10.1038/nri2448.

24. Ito D, Imai Y, Ohsawa K, Nakajima K, Fukuuchi Y, Kohsaka S. Microglia-specific localisation of a novel calcium binding protein, Iba1. *Brain Res*

Mol Brain Res. 1998;57(1):1-9.

25. Hanisch U-K. Microglia as a source and target of cytokines. *Glia*. 2002;40(2):140-155. doi:10.1002/glia.10161.

26. Tang Y, Le W. Differential Roles of M1 and M2 Microglia in Neurodegenerative Diseases. *Mol Neurobiol*. 2016;53(2):1181-1194. doi:10.1007/s12035-014-9070-5.

27. Yang Y, Li H, Li T-T, *et al*. Delayed activation of spinal microglia contributes to the maintenance of bone cancer pain in female Wistar rats via P2X7 receptor and IL-18. *J Neurosci*. 2015;35(20):7950-7963. doi:10.1523/JNEUROSCI.5250-14.2015.

28. Hu J-H, Yang J-P, Liu L, *et al*. Involvement of CX3CR1 in bone cancer pain through the activation of microglia p38 MAPK pathway in the spinal cord. *Brain Res*. 2012;1465:1-9. doi:10.1016/j.brainres.2012.05.020.

29. Bu H, Shu B, Gao F, *et al*. Spinal IFN-γ-induced protein-10 (CXCL10) mediates metastatic breast cancer-induced bone pain by activation of microglia in rat models. *Breast Cancer Res Treat*. 2014;143(2):255-263. doi:10.1007/s10549-013-2807-4.

30. Jin D, Yang J-P, Hu J-H, Wang L-N, Zuo J-L. MCP-1 stimulates spinal microglia via PI3K/Akt pathway in bone cancer pain. *Brain Res*.

2015;1599:158-167. doi:10.1016/j.brainres.2014.12.043.

31. Miladinovic T, Ungard RG, Linher-Melville K, Popovic S, Singh G. Functional effects of TrkA inhibition on system xC--mediated glutamate release and cancer-induced bone pain. *Mol Pain*. 2018;14:1-15. doi:10.1177/1744806918776467.

32. Elmore MRP, Najafi AR, Koike MA, *et al*. Colony-stimulating factor 1 receptor signaling is necessary for microglia viability, unmasking a microglia progenitor cell in the adult brain. *Neuron*. 2014;82(2):380-397. doi:10.1016/j.neuron.2014.02.040.

33. Luger NM, Honore P, Sabino MA, *et al*. Osteoprotegerin diminishes advanced bone cancer pain. *Cancer Res*. 2001;61(10):4038-4047.

34. Nirogi R, Goura V, Shanmuganathan D, Jayarajan P, Abraham R. Comparison of manual and automated filaments for evaluation of neuropathic pain behavior in rats. *J Pharmacol Toxicol Methods*. 2012;66(1):8-13. doi:10.1016/j.vascn.2012.04.006.

35. Ungard RG, Seidlitz EP, Singh G. Inhibition of breast cancer-cell glutamate release with sulfasalazine limits cancer-induced bone pain. *Pain*. 2014;155(1):28-36. doi:10.1016/j.pain.2013.08.030.

36. Wang T, Liang Z-A, Sandford AJ, *et al*. Selection of suitable housekeeping

genes for real-time quantitative PCR in CD4(+) lymphocytes from asthmatics with or without depression. *PLoS One*. 2012;7(10):e48367. doi:10.1371/journal.pone.0048367.

37. Livak KJ, Schmittgen TD. Analysis of relative gene expression data using real-time quantitative PCR and the 2(-Delta Delta C(T)) Method. *Methods*. 2001;25(4):402-408. doi:10.1006/meth.2001.1262.

38. Abramoff MD, Magalhães PJ, Ram SJ. Image processing with ImageJ. *Biophotonics Int*. 2004;11(7):36-41.

39. Jensen EC. Quantitative Analysis of Histological Staining and Fluorescence Using ImageJ. *Anat Rec*. 2013;296(3):378-381. doi:10.1002/ar.22641.

40. Lawson LJ, Perry VH, Dri P, Gordon S. Heterogeneity in the distribution and morphology of microglia in the normal adult mouse brain. *Neuroscience*. 1990;39(1):151-170.

41. Jimenez-Andrade JM, Ghilardi JR, Castañeda-Corral G, Kuskowski MA, Mantyh PW. Preventive or late administration of anti-NGF therapy attenuates tumor-induced nerve sprouting, neuroma formation, and cancer pain. *Pain*. 2011;152(11):2564-2574. doi:10.1016/j.pain.2011.07.020.

42. Hald A, Nedergaard S, Hansen RR, Ding M, Heegaard A-M. Differential

activation of spinal cord glial cells in murine models of neuropathic and cancer pain. *Eur J Pain*. 2009;13(2):138-145. doi:10.1016/j.ejpain.2008.03.014.

43. Zhang R-X, Liu B, Wang L, *et al*. Spinal glial activation in a new rat model of bone cancer pain produced by prostate cancer cell inoculation of the tibia. *Pain*. 2005;118(1-2):125-136. doi:10.1016/j.pain.2005.08.001.

44. Huo W, Zhang Y, Liu Y, *et al*. Dehydrocorydaline attenuates bone cancer pain by shifting microglial M1/M2 polarization toward the M2 phenotype. *Mol Pain*. 2018;14:1744806918781733. doi:10.1177/1744806918781733.

45. Sorge RE, Mapplebeck JCS, Rosen S, *et al*. Different immune cells mediate mechanical pain hypersensitivity in male and female mice. *Nat Neurosci*. 2015;18(8):1081-1083. doi:10.1038/nn.4053.

46. Hendrickx DAE, van Eden CG, Schuurman KG, Hamann J, Huitinga I. Staining of HLA-DR, Iba1 and CD68 in human microglia reveals partially overlapping expression depending on cellular morphology and pathology. *J Neuroimmunol*. 2017;309:12-22. doi:10.1016/j.jneuroim.2017.04.007.

47. Yang M, Kim J, Kim J-S, *et al*. Hippocampal dysfunctions in tumor-bearing mice. *Brain Behav Immun*. 2014;36:147-155. doi:10.1016/j.bbi.2013.10.022.

48. Cole J, Costafreda SG, McGuffin P, Fu CHY. Hippocampal atrophy in first episode depression: A meta-analysis of magnetic resonance imaging studies. *J Affect Disord*. 2011;134(1-3):483-487. doi:10.1016/j.jad.2011.05.057.

49. Gore M, Sadosky A, Stacey BR, Tai K-S, Leslie D. The burden of chronic low back pain: clinical comorbidities, treatment patterns, and health care costs in usual care settings. *Spine (Phila Pa 1976)*. 2012;37(11):E668-77. doi:10.1097/BRS.0b013e318241e5de.

50. Apkarian AV, Mutso AA, Centeno M V, *et al*. Role of adult hippocampal neurogenesis in persistent pain. *Pain*. 2016;157(2):418-428. doi:10.1097/j.pain.0000000000000332.

51. Mutso AA, Radzicki D, Baliki MN, *et al*. Abnormalities in hippocampal functioning with persistent pain. *J Neurosci*. 2012;32(17):5747-5756. doi:10.1523/JNEUROSCI.0587-12.2012.

52. Elman I, Borsook D, Volkow ND. Pain and suicidality: insights from reward and addiction neuroscience. *Prog Neurobiol*. 2013;109:1-27. doi:10.1016/j.pneurobio.2013.06.003.

53. Asmundson GJG, Katz J. Understanding the co-occurrence of anxiety disorders and chronic pain: state-of-the-art. *Depress Anxiety*. 2009;26(10):888-901. doi:10.1002/da.20600.

54. Block ML, Zecca L, Hong J-S. Microglia-mediated neurotoxicity: uncovering the molecular mechanisms. *Nat Rev Neurosci*. 2007;8(1):57-69. doi:10.1038/nrn2038.

55. Halgren E, Walter RD, Cherlow DG, Crandall PH. Mental phenomena evoked by electrical stimulation of the human hippocampal formation and amygdala. *Brain*. 1978;101(1):83-117.

56. Piani D, Frei K, Do KQ, Cuénod M, Fontana A. Murine brain macrophages induced NMDA receptor mediated neurotoxicity in vitro by secreting glutamate. *Neurosci Lett*. 1991;133(2):159-162.

57. Piani D, Spranger M, Frei K, Schaffner A, Fontana A. Macrophage-induced cytotoxicity of N-methyl-D-aspartate receptor positive neurons involves excitatory amino acids rather than reactive oxygen intermediates and cytokines. *Eur J Immunol*. 1992;22(9):2429-2436. doi:10.1002/eji.1830220936.

58. Neugebauer V. Amygdala pain mechanisms. *Handb Exp Pharmacol*. 2015;227:261-284. doi:10.1007/978-3-662-46450-2_13.

59. Paxinos G, Watson C. The Rat Brain in Stereotaxic Coordinates. 6th ed. Cambridge, MA: Academic Press; 2007.

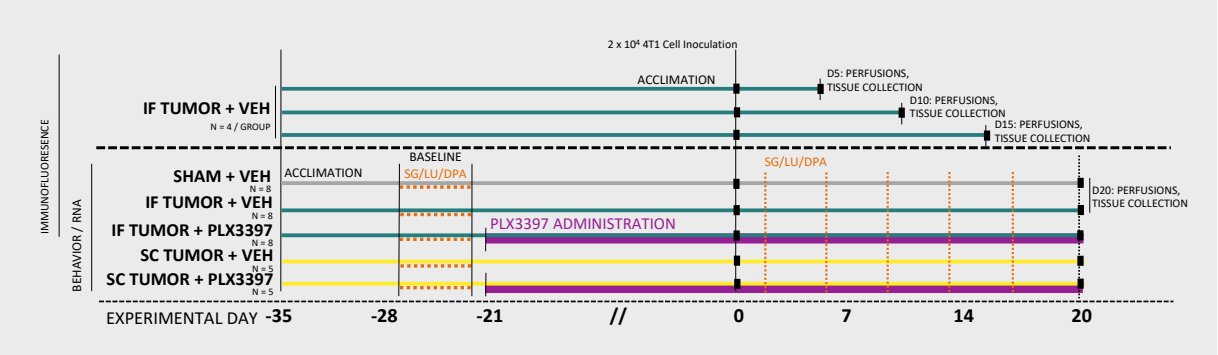

Figure 4.1. Timeline of in vivo experiments.

Procedures for each of the experimental groups are noted along the timeline at the days that they occurred. Day 0 represents the day of IF or SC inoculation. Orange dashed lines indicate days of nociceptive behavior tests; green lines indicate IF tumor group; yellow lines indicate SC tumor group; purple lines indicate period of treatment with Pexidartinib (PlX3397) CSF1R inhibitor. Abbreviations: DPA, dynamic plantar aesthesiometer; IF, intrafemoral; LU, limb use; SC, subcutaneous; SG, spontaneous guarding.

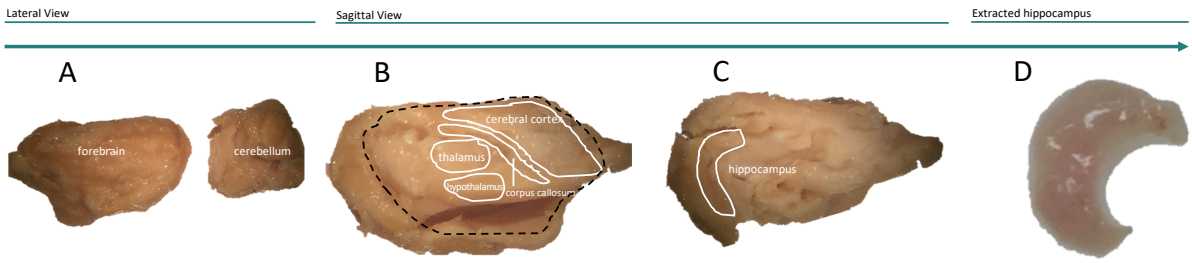

Figure 4.2. Hippocampal Microdissection Methodology.

Following cervical dislocation, contralateral hippocampi were immediately collected by microdissection: contralateral hemisphere was isolated and cerebellum was removed (A), remaining tissue was flipped with medial side facing up (B). Tissue covering the medial surface of hippocampus was removed using dissection spatula (spatula was inserted below corpus callosum; thalamus, septum, and underlying striatum were discarded to clearly reveal hippocampus) (C). Using forceps to secure cerebral cortex, spatula was placed under the ventral part of the hippocampus, and tissue was rolled out to separate the hippocampus from the cortex (D).

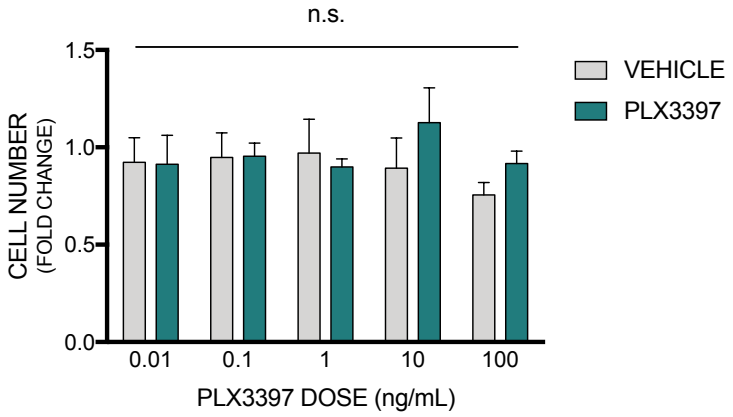

Figure 4.3. CSF1R inhibition does not alter 4T1 breast cancer cell number in vitro.

Cells were treated with Pexidartinib for 24 h. Absorbance was read on a spectrophotometer optical plate reader at λ=570 nm, converted to cell number using a standard curve for 4T1 cells, and expressed as a fold change relative to naïve control wells on the same experimental plate.

Abbreviations: n.s., not significant.

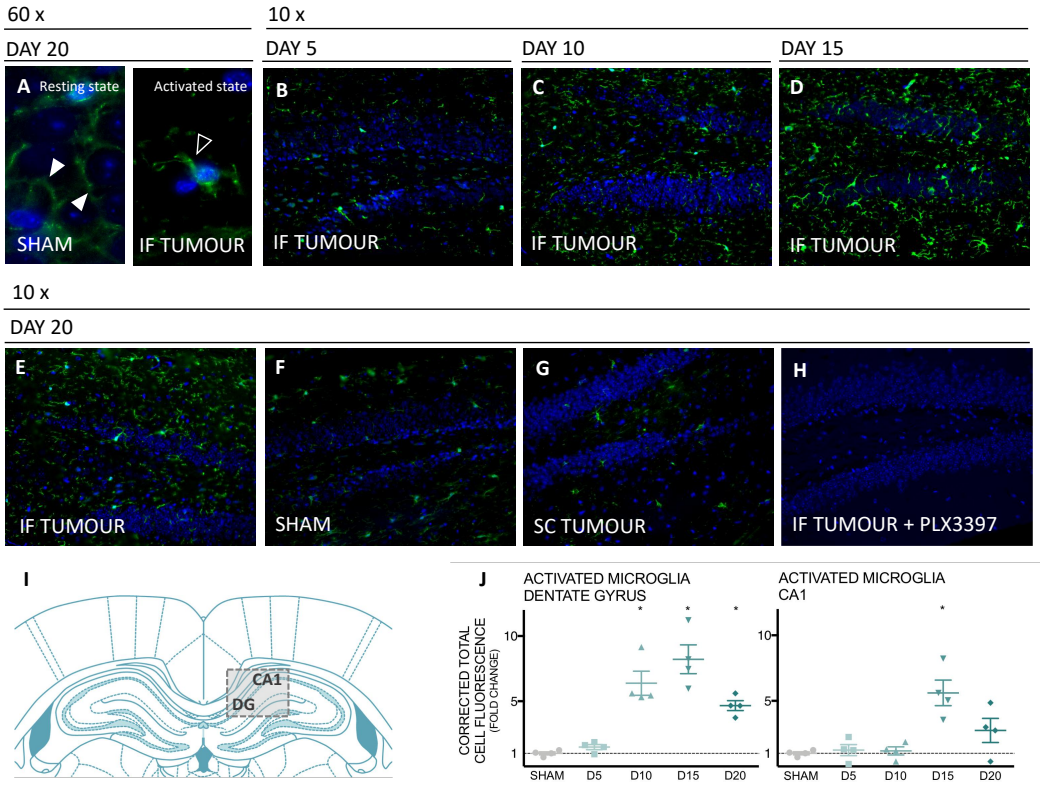

Figure 4.4. Peripheral Tumors Increase Activated Microglia in Hippocampal Regions. Representative immunofluorescent confirmation of resting (A, left) and activated (A, right) microglia in sham and IF tumor-inoculated animals' contralateral hippocampi at 60× magnification, white arrowheads indicate branched processes, characteristic of ramified microglia; black arrowheads indicate retracted processes, characteristic of activated microglia. Representative immunofluorescent staining of contralateral hippocampi throughout IF tumor progression (B–E), and sham (F), SC tumor (G), and IF tumor+ Pexidartinib (H) captures at endpoint (10× magnification). (I) coronal sections through Dg and ca1 regions of the hippocampus were collected (~3 mm posterior to Bregma. (J) Fold

change: activated microglia in Dg (left) and ca1 (right) regions of hippocampus throughout IF tumor progression relative to sham controls. iba1+ staining in each region was quantitated using Image J, with corrected fluorescence levels determined using the CTCF method; n=4/group; points (J) represent cTcF-derived values within specified brain regions from individual animals; **P*<0.05 represents significantly different from sham group, as determined by Mann–Whitney *U* test.

Abbreviations: CA1, cornu ammonis 1; CTCF, corrected total cell fluorescence; DG, dentate gyrus; IF, intrafemoral; SC, subcutaneous.

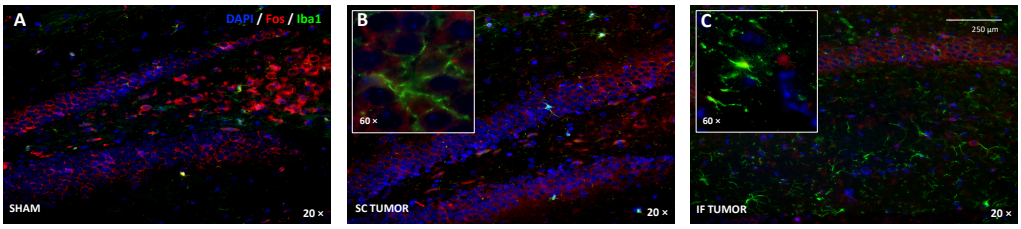

Figure 4.5. Double-label immunofluorescent staining of Iba1 and xCT.

Double-label immunofluorescent staining of Iba1 (green) and c-Fos (red), depicting activated microglia and functional neural activity, respectively, in the contralateral hippocampus of sham (A), SC (B), and IF (C) tumor-bearing animals. Captures were collected at endpoint (day 20 post tumor inoculation) at 20× magnification (inserts depict 60× magnification). Coronal sections through the hippocampus were collected (~3 mm posterior to Bregma using The Rat Brain in stereotaxic coordinates by Paxinos and Watson).[59]

Abbreviations: IF, intrafemoral; SC, subcutaneous.

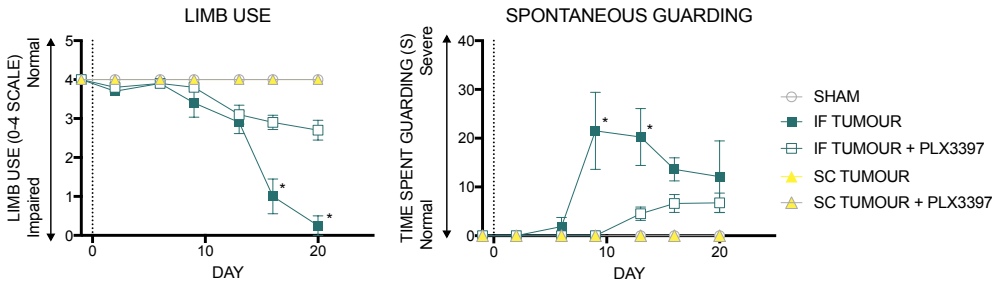

Figure 4.6. Pexidartinib decreases spontaneous nociceptive behaviors.

(A) Quantification of limb use in affected femurs throughout tumor progression. Normal hind limb use during spontaneous ambulation was observed and scored on a scale of 4–0: 4 – normal use, 3 – pronounced limp, 2 – limp and guarding behavior, 1 – partial nonuse of the limb in locomotor activity, and 0 – complete lack of limb use. (B) The time spent spontaneously guarding the hind paw represented ongoing pain and was recorded during a 2-minute open field observation period. Guarding time was defined as the time (s) the hind paw was held aloft while ambulatory. Points indicate mean ± SEM; *significantly different from sham controls, α=0.05; vertical dashed line indicates IF injections (day 0). Abbreviations: IF, intrafemoral; SC, subcutaneous; SEM, standard error of mean.

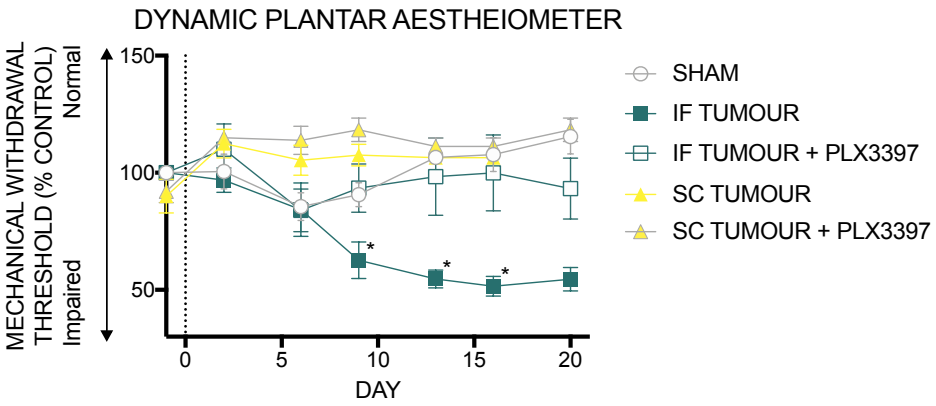

Figure 4.7. Pexidartinib decreases evoked nociceptive behaviors.

The DPA test quantitates evoked nociceptive behaviors by measuring the threshold force at which animals withdraw from a progressive stimulus applied to the plantar surface of the affected hind paw. Thus, 100% on the y-axis is equivalent to baseline behavior prior to tumor inoculation; <100% indicates a decrease in the force withstood by the tumor-bearing limb. Points indicate mean ± SEM; *significantly different from SHAM, α=0.05; vertical dashed lines indicate IF injections (day 0).

Abbreviations: DPA, dynamic plantar aesthesiometer; IF, intrafemoral; SC, subcutaneous; SEM, standard error of mean.

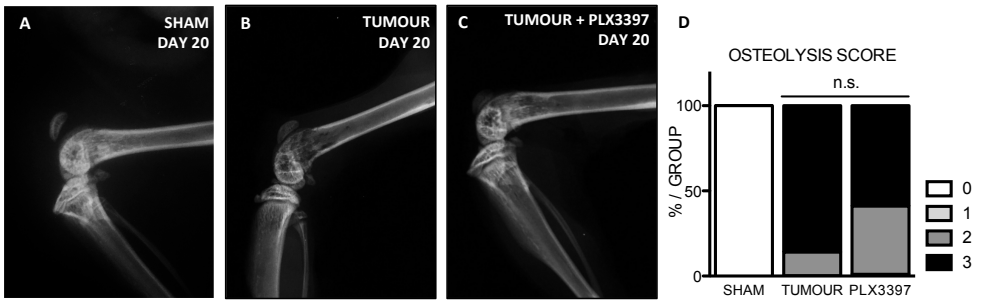

Figure 4.8. Pexidartinib does not alter tumor-induced femoral osteolysis.

(A–D) Quantification of bone osteolysis in tumor-bearing femurs on day 20 post tumor cell inoculation. Representative images indicate advanced tumor growth and consequent bone destruction in sham (A), vehicle- (B), and Pexidartinib-treated (C) tumor-inoculated mice as quantified by a 0–3 numerical scale. Radiographic Lesion Score numbers represent: 0 – normal bone, no visible lesion; 1 – minor loss of bone density, minimal lesion; 2 – moderate to substantial loss of bone density, lesion limited to bone trabeculae and cortex; 3 – substantial loss of bone density, lesion includes clear periosteal involvement and/or fracture. (D) Osteolytic scores expressed as total percent per treatment group in each score category at endpoint. *P<0.05, as determined by chi-square analysis, α=0.05; n=8/group. Abbreviation: n.s., not significant.

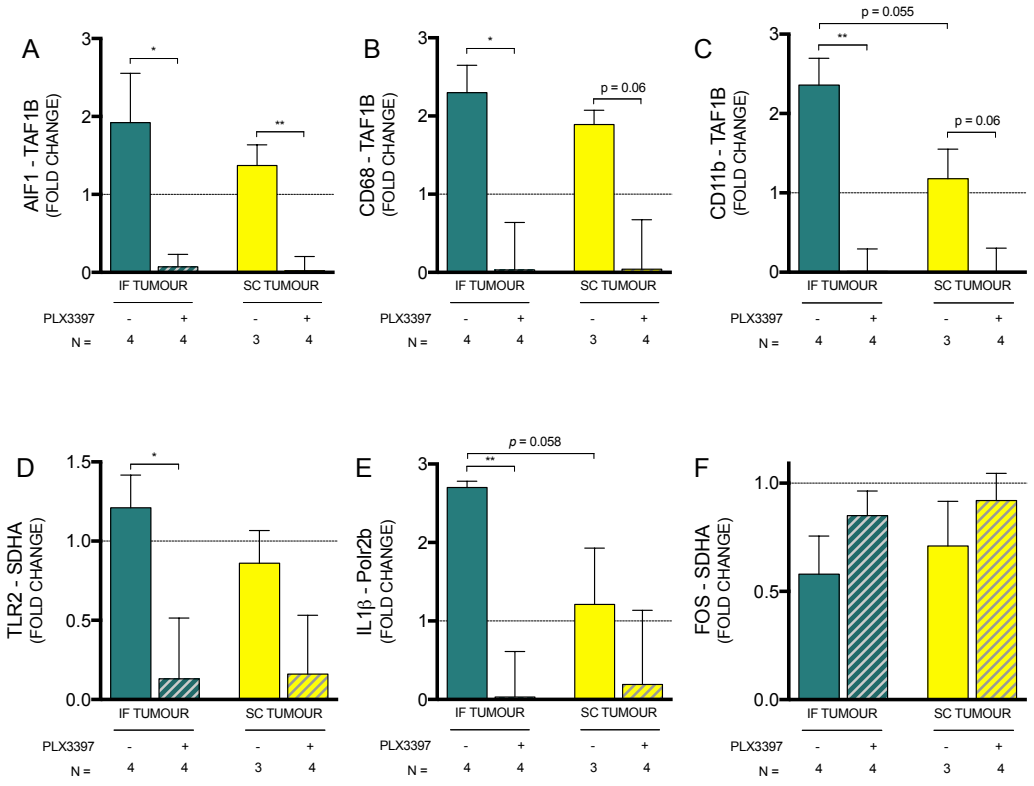

Figure 4.9. Intrafemoral tumors increase hippocampal microglial markers.

(A–C) qPCR confirmed the dramatic increase of hippocampal microglia in tumor-bearing mice, as demonstrated by microglial markers allograft inflammatory factor 1/ionized calcium-binding adapter molecule 1 (AIF1/Iba1), cD68, and cD11b; treatment with the csF1R inhibitor Pexidartinib dramatically reduced hippocampal microglia across IF and SC tumor-bearing models. IF tumor-bearing mice demonstrated significantly higher levels of hippocampal microglial mRNA relative to SC tumor-bearing mice. (D–F) Factors associated with microglial activation were also affected by peripheral tumor, including TLR2, iL-1β, and the

immediate-early gene c-Fos. Bars represent the mean of three or four biological replicates as a fold change relative to sham (n=1), with error bars indicating SE<M. *P<0.05 and **P<0.01, as determined by planned pairwise comparisons.

Abbreviations: IF, intrafemoral; SC, subcutaneous; SEM, standard error of mean; TLR2, toll-like receptor 2.

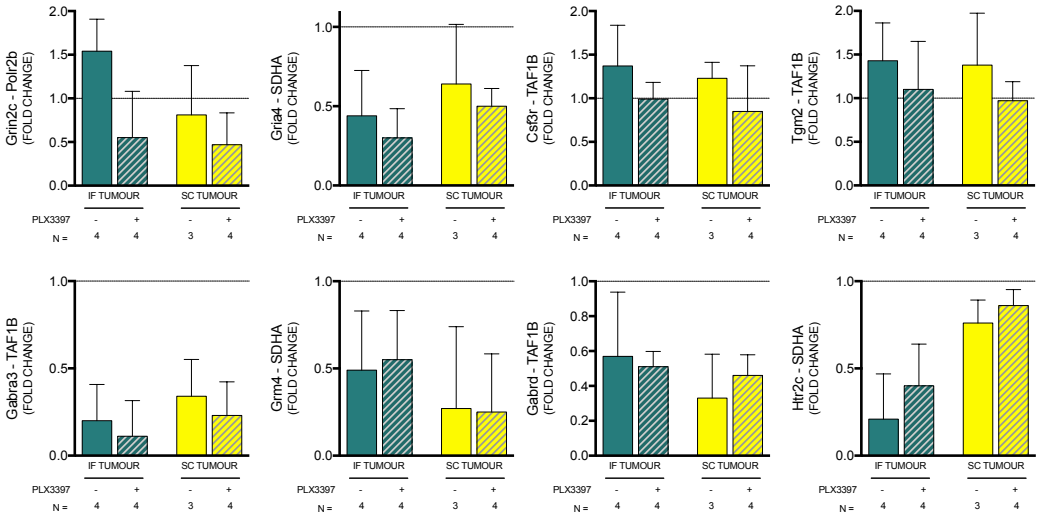

Figure 4.10. Peripheral tumors alter select hippocampal mRNA.

Secondary mRNA targets are affected by IF and SC tumors (glutamate ionotropic receptor NMDA type subunit 2c, GRIN2c; glutamate ionotropic receptor AMPA type subunit 4, GRIA4; colony stimulating factor 3 receptor, CSF3R; gamma-aminobutyric acid type a receptor alpha 3 subunit, GABRA3; transglutaminase 2, TGM2; glutamate metabotropic receptor 4, GRM4; gamma-aminobutyric acid type a receptor delta subunit, GABRD; 5-hydroxytryptamine type 2c receptor, HTR2C). Bars represent the mean of three or four biological replicates as a fold change relative to sham (n=1), with error bars indicating SEM.

Abbreviations: IF, intrafemoral; SC, subcutaneous; SEM, standard error of mean.

Gene Symbol		Primer Sequence (5' to 3')	Housekeeper	Product Size (bp)	PrimerBank ID
AIF1	FWD REV	ATCAACAAGCAATTCCTCGATGA CAGCATTCGCTTCAAGGACATA	mTBP	144	9506379a1
CD68	FWD REV	CCATCCTTCACGATGACACCT GGCAGGGTTATGAGTGACAGTT	mTBP	138	6753351c2
CD11b	FWD REV	CCATGACCTTCCAAGAGAATGC ACCGGCTTGTGCTGTAGTC	mTBP	147	132626288c1
TLR2	FWD REV	CACCACTGCCCGTAGATGAAG AGGGTACAGTCGTCGAACTCT	mSDHA	148	158749637c3
IL1-β	FWD REV	GAAATGCCACCTTTTGACAGTG TGGATGCTCTCATCAGGACAG	mPOLR2b	116	118130747c1
c-FOS	FWD REV	CGGGTTTCAACGCCGACTA TGGCACTAGAGACGGACAGAT	mSDHA	165	31560587c1
GRIN2C	FWD REV	GGGATCTGCCATAACGAGAAG GCACTGAGTGTCGAAGTTTCCA	mPOLR2b	157	7110609a1
GRIA4	FWD REV	TTTGCAGGCAGATTGTCTTG GGGGCTGGTGTTATGAAGAA	mSDHA	153	164419754c1
GABRA3	FWD REV	AGACAGACATGGCATGATGAAAG GGTGTGGTCATATTGTGAGCC	mSDHA	146	247269170c3
GRM4	FWD REV	GACCGCATCAACAACGACC GTGCCGTCCTTCTCGATGAG	mSDHA	137	62945391c1
CSF3R	FWD REV	CTGATCTTCTTGCTACTCCCCA GGTGTAGTTCAAGTGAGGCAG	mTBP	249	6681051a1
TGM2	FWD REV	GACAATGTGGAGGAGGGATCT CTCTAGGCTGAGACGGTACAG	mTBP	120	6678329a1
GABRD	FWD REV	CCAGCATTGACCATATCTCAGAG TCATGGAACCAGGCAGATTTG	mTBP	190	160707922c2
HTR2C	FWD REV	TGCTGGTGGGACTACTTGTCA GACGCAGTTGAAAATAGCACATC	mSDHA	124	160358830c3

Table 4.1. Primers used for relative qPCR analysis.

Gene Symbol		Primer Sequence (5' to 3')	Product Size (bp)
SDHA	FWD REV	GATTTGCCTCGTTTCCCAGAC GCCATAGCCTGCACATCATATT	215
Polr2b	FWD REV	ATGGCTTAACAGATCGTGACCT GCGACATTCTCCTGTATAGGCA	176
TAF1B	FWD REV	GATTTGCCTCGTTTCCCAGAC GCCATAGCCTGCACATCATATT	215

Table 4.2. Housekeeping gene primers used for relative qPCR analysis.

CHAPTER 5

Summary and Future Directions

Summary

In this dissertation, I have tested the hypothesis that:

Cancer can induce pain through defined biological mechanisms, including ***activated microglia****. Chronically-activated* ***microglia release excess glutamate*** *through system* x_C^-*. Therefore, pharmacologically targeting microglia will* ***reduce cancer pain through xCT****-mediated glutamate release.*

From this hypothesis, three related, but distinct testable objectives were formulated. These objectives represent the main body of the experimental work presented in this dissertation. The key studies contributing to each manuscript, as well as the significant results from each objective, will be summarized here, and major conclusions will be drawn for each body of experimental work. The implications of each of these specific objectives will be addressed individually in this final chapter and discussed as they relate to existing literature in the field and to each other. Finally, overall implications of the data will be cumulatively considered and notes on future directions of research will be discussed.

Objective 1. *Examine the effects of TrkA inhibition on functional system* x_C^- *activity and CIP.*

Several key findings contributed to the fundamental hypothesis that was investigated in this objective, as follows:

1. Biologically-active NGF is excessively synthesized and released by breast cancer cells, an effect which is blocked by the TrkA inhibitor K252, indicating the existence of an NGF autocrine loop (Dollé *et al*., 2003).

2. Pre-clinical models of nociception demonstrate hypoalgesia in NGF- and TrkA-knockout mice (Crowley *et al*., 1994; Smeyne *et al*., 1994).

3. Pre-clinical evidence suggests a functional relationship between glutamate and some neurotrophins (X. Liu *et al*., 2012; Taylor *et al*., 2003; Xiong *et al*., 2002); NGF (Dollé *et al*., 2003), TrkA (Lagadec *et al*., 2009), and xCT (Seidlitz *et al*., 2009; Sharma *et al*., 2010) are upregulated in breast cancer cells.

4. NGF activates mitogen-activated protein kinase (MAPK) signalling through TrkA (Huang & Reichardt, 2003); MAPK phosphorylates signal transducer and activator of transcription 3 (STAT3) (Linher-Melville *et al*., 2016; Linher-Melville, Haftchenary, Gunning, & Singh, 2015; Linher-Melville & Singh, 2017), which regulates

expression of xCT (Linher-Melville *et al*., 2015); the MAPK inhibitor PD098059 abolishes xCT transcriptional activity (Linher-Melville *et al*., 2015) and the STAT3 inhibitor SH-4-54 decreases xCT expression and system x_C^- activity (Linher-Melville *et al*., 2015).

These findings contributed to the hypothesis: *inhibiting the actions of NGF on TrkA may reduce CIP by decreasing functional system x_C^- activity.* This objective built on existing literature and these studies cumulatively addressed CIP at the site of the tumour, with particular focus on inhibiting excess glutamate release from carcinoma cells within the bone microenvironment. If excess glutamate released from cancer cells contributes to the pain state associated with intrafemoral tumour burden, it is reasonable to expect an indirect inhibitor of system x_C^- to prevent the development of nociceptive behaviours in this model of CIP.

To confirm the appropriateness of 4T1 murine carcinoma cells for this model of CIP, *in vitro* experiments were first performed to confirm expression of xCT and functional activity of system x_C^- in these cells in comparison with MDA-MB-231 human carcinoma cells. These characteristics had been previously confirmed in an immunocompromised model of CIP, which utilized MDA-MB-231 cells in BALB/c nu/nu mice (Seidlitz *et al*., 2009; Ungard *et al*., 2014). Once confirmed, 4T1 cells were stimulated with β-NGF and/or treated with the specific TrkA inhibitor AG879 to assess the downstream effects of NGF on functional

system x_C^- activity in cultured cells. Overall, an interesting trend was observed, such that inhibiting carcinoma cells with the TrkA antagonist reduced xCT at the protein level in addition to reducing functional system x_C^- activity, while stimulating cells with β-NGF increased system x_C^- functional activity and protein levels.

After these cells had been established as a suitable medium for a model of CIP, mice were intrafemorally inoculated with live or sham control 4T1 carcinoma cells. Tumour growth *in vivo* was rapid, with tumour size swiftly surpassing that of our lab's previously validated MDA-MB-231 immunocompromised model, and several carcinoma cells leaked out of the bone, potentially contributing to nociception beyond that specific to the bone microenvironment. As such, subsequent studies comprising this dissertation report on *CIP*, rather than cancer-induced *bone* pain (CIBP), to encompass nociceptive behaviours related to factors beyond bone-specific processes. Cancer-induced nociceptive behaviours progressed rapidly, reaching maximum nociception and behavioural endpoint within three weeks of bearing tumours. Systemic treatment with AG879 dramatically reduced nociception in this model, a model which utilized cells that behave similarly to MDA-MB-231 cells *in vitro*, giving reason to believe this treatment would translate organically to clinical cases of breast cancer.

Objective 2. *Examine the nociceptive relationship between peripherally-released glutamate and microglial xCT.*

Several key findings contributed to the central hypothesis that was investigated in this objective, as follows:

1. Spinal microglial activation is well documented in chronic pain (Cao & Zhang, 2008; Ji *et al*., 2013; Shan *et al*., 2007; Sun *et al*., 2008) and CIP (X.-F. Hu *et al*., 2017; Huo *et al*., 2018; M. Liu *et al*., 2017; Mao-Ying *et al*., 2012; Wang *et al*., 2012; Yang *et al*., 2015).

2. Chronically activated microglia produce and release harmful substances, including excess glutamate, causing cytotoxicity (S W Barger & Basile, 2001; Steven W Barger *et al*., 2007; Piani & Fontana, 1994; Walter & Neumann, 2009).

3. Microglia express glutamate receptors (GluRs) (Pocock & Kettenmann, 2007; Tahraoui *et al*., 2001) and are activated by exogenous glutamate (Murugan *et al*., 2013).

These findings led to the hypothesis: *spinal microglia contribute to cancer-induced pain through system x_C^--mediated glutamate release.* Through this objective, two important concepts were established: (1) microglia are activated by carcinoma cell-released glutamate, and (2) in turn, microglia upregulate xCT in this glutamate-induced activated state.

This objective addressed an important aspect of cancer pain signalling; it is known that activated microglia increase in tumour-bearing mice experiencing nociception (X.-F. Hu *et al*., 2017; Huo *et al*., 2018; M. Liu *et al*., 2017; Mao-Ying *et al*., 2012; Wang *et al*., 2012; Yang *et al*., 2015), but the mechanism(s) driving this activation, and the consequences of it, are poorly understood. The first important finding from this study – microglia are activated by glutamate released by MDA-MB-231 carcinoma cells – was established by utilizing co-culture studies and immunofluorescent imaging to explore the response from inflammatory immune spinal microglial cells as a first-line response to peripherally-released glutamate. The direct relationship between carcinoma cell-released glutamate and reactive spinal microglia was apparent *in vitro*, with wildtype carcinoma cells eliciting a robust pattern of microglial activation (retracted processes and vivid immunofluorescent staining), a phenomenon that was absent in clone C6 xCT knockdown (xCT KD) co-cultured microglia.

The second noteworthy finding from this study – microglia upregulate xCT in the activated state associated with carcinoma cell-released glutamate – was established by quantifying xCT protein by Western blot analysis and immunocytochemistry. Microglia activated by direct LPS and by glutamate-releasing carcinoma cells expressed greater levels of the xCT protein in their activated state. Functional system x_C^- activity supported this finding, demonstrating increased ^{14}C-cystine uptake by microglia co-cultured with

wildtype, but not xCT KD MDA-MB-231 cells. This *in vitro* trend translated to an animal model of CIP, such that animals bearing glutamate-releasing 4T1 tumours demonstrated sustained nociceptive behaviours throughout the experimental timeline and increased xCT expression in activated spinal microglia at endpoint.

In the presence of high extracellular cystine, microglia become neurotoxic effector cells, and this toxicity is selective for neurons and dependent on activation of neuronal ionotropic GluRs. The substances released by activated microglia further activate additional nearby astrocytes, microglia, and neurons to aid in this process, creating a positive feedback loop (reviewed in (Milligan & Watkins, 2009)). Thus, once the harmful stimulus has been managed, it is critical that the microglial inflammatory response be dampened.

Peripheral nerve injury produces a sustained shift in dorsal horn glutamate release and uptake (Inquimbert *et al*., 2012), further supporting the notion that aberrant glutamate regulation within the spinal cord is an important driver of nociception. Glutamate is the major transmitter of primary sensory nociceptive afferents (Basbaum, Bautista, Scherrer, & Julius, 2009; Miller, Hoffman, Sutharshan, & Schechter, 2011) and excitatory dorsal horn interneurons (Todd, 2010). Given that the superficial dorsal horn is the first relay station for somatosensory input, maintaining regional glutamate homeostasis at these synapses is essential to the effective transfer of nociceptive information to the CNS.

Objective 3. *Evaluate the activation pattern of hippocampal microglia in a syngeneic model of CIP and the anti-nociceptive effects of microglial inhibition.*

Several key findings contributed to the fundamental hypothesis that was investigated in this final objective, as follows:

1. Clinical reports estimate that nearly half of patients with chronic pain also present with symptoms characteristic of clinical depression (Dworkin & Gitlin, 1991); mood conditions are among the factors that prevent recovery from pain, and may significantly reduce the efficacy of analgesic agents (Legrain *et al*., 2011).

2. The hippocampus is involved in several emotional processes, including the initiation and maintenance of depression (Eisch & Petrik, 2012; Murray *et al*., 2008).

3. Pre-clinical data suggests that the hippocampus is involved in nociceptive processing, particularly with respect to the affective aspect of pain perception (Al Amin *et al*., 2004; Echeverry *et al*., 2004; Favaroni Mendes & Menescal-de-Oliveira, 2008; Khanna *et al*., 2004; McEwen, 2001; McKenna & Melzack, 1992, 2001; E Soleimannejad *et al*., 2006; Elaheh Soleimannejad *et al*., 2007; Yamamotová *et al*., 2007; Zhao *et al*., 2009).

4. The inflammatory response within the hippocampus has been implicated in the perception of pain (Fasick *et al*., 2015).

The effects of pain and depression seemingly converge in higher brain centres sensitive to both types of stimuli. Thus, the following hypothesis was developed: *activated hippocampal microglia contribute to the inflammatory response associated with central processing of tumour-induced nociception.* This objective provided novel information on the inflammatory response in the progressive presence of peripheral tumour. As tumours progressed, regional immune cells demonstrated increasingly vivid immunofluorescent staining of Iba1, a marker of activated microglia. To my knowledge, this is the first study to temporally examine the hippocampal immune response to tumour burden in the context of CIP.

Pain is the cumulative interpretation of sensation and perception, which involves the integration of sensory input with existing memories and emotional responses. Clinical evidence demonstrates comorbidity between chronic pain and depression, emphasizing the impact of the affective or emotional component of pain (Duric & McCarson, 2006). The hippocampus is a brain region implicated in learning and memory and has recently been implicated in depression and nociceptive processing. As a key component of the limbic system, this brain region is intimately involved in mood regulation, and is one of several brain regions capable of continuous cell proliferation and neurogenesis throughout adulthood (Gross, 2000). In the dentate gyrus region of hippocampus, neurogenesis is dramatically reduced after long-term inflammatory nociception

(Duric & McCarson, 2006). Immunofluorescent labelling of the early immediate gene c-Fos in the present study provided an estimate of the magnitude of neuronal excitation. Co-staining of c-Fos with the microglial marker Iba1 supported previous literature, with an inverse relationship observed in the present study, such that higher levels of Iba1 were associated with lower levels of c-Fos-positive cells.

Various activators of nociception-induced spinal central sensitization are intimately associated with depression-related processes in the limbic system (Duric & McCarson, 2006). Preclinical data suggests that antidepressant-induced reduction in analgesia is mediated by the inhibition of the microglia-released pro-inflammatory cytokine tumor necrosis factor-α (TNF-α). Thus, microinfusion of recombinant TNF-α into the cerebroventricular space adjacent to the hippocampus produces nociception in naïve animals (Ignatowski, Sud, Reynolds, Knight, & Spengler, 2005; Sud, Spengler, Nader, & Ignatowski, 2008), further implicating the hippocampus in microglia-related nociception.

Future Directions

The preceding chapters collectively outline the complex role of glutamate and microglial cells in cancer pain signalling. These studies represent a milestone to understanding the pathophysiology of this complex disease and the perception of pain that accompanies sensory nociceptive signalling induced by tumours. However, it is important to address the limitations inherent to animal models of complex cancer pain states and discuss potential paths to mitigate these hurdles in light of this research.

The 4T1 mammary carcinoma cell line was selected for use across these studies, as this cell line is highly tumourigenic and invasive. The growth and metastatic spread of these cells in BALB/c mice very closely mimic human breast cancer in its proliferative and metastatic characteristics (Pulaski & Ostrand-Rosenberg, 2001), therefore, this tumour cell line was used as an animal model for stage IV human breast cancer. While this strain of mouse is robust and generally capable of enduring surgical procedures to reach advanced disease state, these mice are immunocompetent and thus present a reactive immune response upon injection of any non-murine (*i.e.*, human) cancer cell lines. This is a limitation in that we cannot assess the true effects of *human* cancer cells (for example, the MDA-MB-231 human carcinoma cell line used in the *in vitro* studies of Chapters 2 and 4). Rather, immunocompetent mice may only be inoculated with their murine analogue cells. Our lab has generated stable system x_C^-

knockdown breast cancer cells, which have effectively been delivered to immunocompromised BALB/c nu/nu mice. However, illness and subsequent attrition were high in these groups, particularly when tumour cells were injected intrafemorally, and cellular growth of C6 xCT KD and vector-only cells was markedly slowed compared to naïve MDA-MB-231 cells, significantly increasing experimental timelines and limiting comparability to wildtypes. Based on early experimental data from our lab, it may not be feasible to perform the battery of behavioural tests used in the previous chapters on immunodeficient mouse strains inoculated with xCT KD tumour cells. While this method may introduce additional confounds relating to altered cell physiology, *in vivo* cellular growth, ability to metastasize, etc., these studies would nevertheless theoretically provide evidence of cancer-derived glutamate being physiologically necessary to the development of CIP and subsequent immune processes. Conversely, the subcutaneous or intrafemoral implantation of glutamate pellets, or inoculation with high/low glutamate-releasing tumour cells, would provide evidence of peripherally-released glutamate being sufficient to induce nociceptive symptoms. Moreover, these studies would cumulatively provide more direct evidence of peripherally-/tumour-released glutamate on (1) xCT expression in activated spinal microglia, and (2) hippocampal microglial activation. Additionally, the use of xCT knockout mice (*i.e.*, Hideyo Sato *et al*., 2005) in a similar intrafemoral model of CIP would provide the platform to isolate the role of resident xCT in nociception, although the knockout of this gene may introduce confounds, such as

impaired spatial working memory (De Bundel *et al*., 2011) and decreased reproductive performance (Hamashima *et al*., 2017), etc., and would not be specific to microglial xCT.

As discussed in Chapter 2, NGF is a significant driver of CIP. This neurotrophin binds to its cognate tyrosine kinase receptor, TrkA, through which it activates several signalling pathways, including RAS-MAPK signalling, which has been shown to regulate xCT gene expression (Linher-Melville *et al*., 2015). While Chapter 2 explored this relationship within cancer cells, specifically, this phenomenon may also translate to microglia, as these immune cells express TrkA receptors (Alexaki *et al*., 2018), express xCT (Domercq *et al*., 2016; H Sato *et al*., 1999), and secrete NGF (Nakajima *et al*., 2001). Microglia are an important contributor to NGF secretion in chronic pain conditions (Popiolek-Barczyk & Mika, 2016). Given the evidence for an NGF autocrine loop (Dollé *et al*., 2003)., it is important to explore the role of NGF in microglial activation and associated system x_C^--mediated glutamate release.

The collection of microglia at experimental endpoint for primary culture would provide the opportunity to assess group differences in protein expression *ex vivo*. For example, if there is a difference in IRF8 protein expression from isolated spinal microglia between untreated tumour-bearing mice and those treated with SSZ (or other systemic analgesic(s)), we may conclude that the ability of peripheral tumour-released glutamate to activate microglia (as demonstrated in

Chapter 3) translates to an *in vivo* model. Functional cellular assays, including MTT (3-(4,5-dimethylthiazol-2-yl)-2,5-diphenyltetrazolium bromide) and cystine uptake assays, could also be performed in primary microglial cultures from different experimental groups to quantitate cellular metabolism and system x_C^- activity, respectively. This would add value to the existing findings presented in this dissertation, as the co-culture studies performed in Chapter 3 were completed under the assumption that effects of glutamate released from cancer cells in the periphery extend to central microglia. In reality, glutamate does not readily cross the BBB *in vivo*. However, there is evidence of increased circulating glutamate in the presence of peripheral tumours and under pathological conditions, such as cancer, the BBB is disrupted, increasing its permeability. That said, the co-culture model employed in the present studies do not account for any level of permeability and as such, do not completely demonstrate what may occur *in vivo*. The use of *ex vivo* primary microglial cultures, rather than a co-culture model, would more completely illustrate this phenomenon.

Chapter 4 outlined the dramatic increase in hippocampal microglial activation as a consequence of peripheral tumour-induced nociception. The concept of studying affect in animal models is difficult to define, as pain is the amalgamation of sensory and perceptive processes which may reciprocally influence each other. Future studies could further explore the specific *role* of the hippocampus in pain processing, rather than the *effects* of nociception on this

brain region, as we have performed in Chapter 4. This could be achieved through direct manipulation to the hippocampus, via cannula administration of the inhibitory PLX3397 or stimulatory LPS, or by microsurgical implantation of glutamate-releasing tumour cells (*i.e.*, glioblastoma cells) or glutamate pellets directly into this region.

In the current studies (Chapters 3 and 4), PLX33397 was administered systemically, and thus reduced microglial activation across peripheral tissues and the peripheral and central nervous systems, including the spinal cord, brainstem, thalamus, cerebral cortex, etc. Direct manipulation of hippocampal microglia in our CIP model, in which PLX3397 would be directly and selectively administered to the hippocampus, would provide a better understanding of hippocampal microglia, specifically, in this disease state.

Conclusions

The work presented in this dissertation explored the dynamic role of glutamate and microglia in CIP. An immunocompetent murine model of 4T1 tumour-induced nociception was first used to demonstrate the relationship between NGF and glutamate released from breast cancer cells by system x_C^- in the context of CIP. Pharmacologically inhibiting the actions of NGF on TrkA attenuated functional system x_C^- activity *in vitro* and mitigated CIP *in vivo*. Direct co-culture of human MDA-MD-231 wildtype and xCT KD cells with microglia

then revealed that glutamate released from tumour cells increased microglial activation and system x_C^- activity *in vitro*. In addition, the presence of peripheral tumours and cancer-induced nociception were associated with increased microglial activation in distinct hippocampal regions implicated in pain states and mood disorders. This dissertation contributed to the understanding of glutamate's role in cancer pain signalling with particular emphasis on the immune component of the CNS. Additionally, this research provided early evidence of increased hippocampal microglial activation in the pain state associated with peripheral tumour. Investigating the effects of tumour- and centrally-released glutamate will propel a better understanding of this signalling molecule as a driver of tumour-induced nociception.

References

Abbadie, C., Lindia, J. A., Cumiskey, A. M., Peterson, L. B., Mudgett, J. S., Bayne, E. K., … Forrest, M. J. (2003). Impaired neuropathic pain responses in mice lacking the chemokine receptor CCR2. *Proceedings of the National Academy of Sciences of the United States of America*, *100*(13), 7947–52. http://doi.org/10.1073/pnas.1331358100

Al Amin, H. A., Atweh, S. F., Jabbur, S. J., & Saadé, N. E. (2004). Effects of ventral hippocampal lesion on thermal and mechanical nociception in neonates and adult rats. *The European Journal of Neuroscience*, *20*(11), 3027–34. http://doi.org/10.1111/j.1460-9568.2004.03762.x

Albertini, G., Deneyer, L., Ottestad-Hansen, S., Zhou, Y., Ates, G., Walrave, L., … Smolders, I. (2018). Genetic deletion of xCT attenuates peripheral and central inflammation and mitigates LPS-induced sickness and depressive-like behavior in mice. *Glia*. http://doi.org/10.1002/glia.23343

Alexaki, V. I., Fodelianaki, G., Neuwirth, A., Mund, C., Kourgiantaki, A., Ieronimaki, E., … Chavakis, T. (2018). DHEA inhibits acute microglia-mediated inflammation through activation of the TrkA-Akt1/2-CREB-Jmjd3 pathway. *Molecular Psychiatry*, *23*(6), 1410–1420. http://doi.org/10.1038/mp.2017.167

Aloe, L., Tuveri, M. A., Carcassi, U., & Levi-Montalcini, R. (1992). Nerve growth factor in the synovial fluid of patients with chronic arthritis. *Arthritis and Rheumatism*, *35*(3), 351–5.

Arriza, J. L., Eliasof, S., Kavanaugh, M. P., & Amara, S. G. (1997). Excitatory amino acid transporter 5, a retinal glutamate transporter coupled to a chloride conductance. *Proceedings of the National Academy of Sciences of the United States of America*, *94*(8), 4155–60.

Asai, H., Ozaki, N., Shinoda, M., Nagamine, K., Tohnai, I., Ueda, M., & Sugiura, Y. (2005). Heat and mechanical hyperalgesia in mice model of cancer pain. *Pain*, *117*(1–2), 19–29. http://doi.org/10.1016/j.pain.2005.05.010

Baker, D. A., Xi, Z.-X., Shen, H., Swanson, C. J., & Kalivas, P. W. (2002). The origin and neuronal function of in vivo nonsynaptic glutamate. *The Journal of Neuroscience : The Official Journal of the Society for Neuroscience*, *22*(20), 9134–41.

Banks, W. A., Gray, A. M., Erickson, M. A., Salameh, T. S., Damodarasamy, M., Sheibani, N., … Reed, M. J. (2015). Lipopolysaccharide-induced blood-brain barrier disruption: roles of cyclooxygenase, oxidative stress, neuroinflammation, and elements of the neurovascular unit. *Journal of Neuroinflammation*, *12*(1), 223. http://doi.org/10.1186/s12974-015-0434-1

Bannai, S. (1986). Exchange of cystine and glutamate across plasma membrane of human fibroblasts. *The Journal of Biological Chemistry*, *261*(5), 2256–63.

Bar-Peled, O., Ben-Hur, H., Biegon, A., Groner, Y., Dewhurst, S., Furuta, A., & Rothstein, J. D. (1997). Distribution of glutamate transporter subtypes during human brain development. *Journal of Neurochemistry*, *69*(6), 2571–80.

Barger, S. W., & Basile, A. S. (2001). Activation of microglia by secreted amyloid precursor protein evokes release of glutamate by cystine exchange and attenuates synaptic function. *Journal of Neurochemistry*, *76*(3), 846–54.

Barger, S. W., Goodwin, M. E., Porter, M. M., & Beggs, M. L. (2007). Glutamate release from activated microglia requires the oxidative burst and lipid peroxidation. *Journal of Neurochemistry*, *101*(5), 1205–13. http://doi.org/10.1111/j.1471-4159.2007.04487.x

Basbaum, A. I., Bautista, D. M., Scherrer, G., & Julius, D. (2009). Cellular and Molecular Mechanisms of Pain. *Cell*, *139*(2), 267–284. http://doi.org/10.1016/j.cell.2009.09.028

Bentea, E., Demuyser, T., Van Liefferinge, J., Albertini, G., Deneyer, L., Nys, J., … Smolders, I. (2015). Absence of system xc- in mice decreases anxiety and depressive-like behavior without affecting sensorimotor function or spatial vision. *Prog Neuropsychopharmacol Biol Psychiatry*, *59C*, 49–58.

http://doi.org/10.1016/j.pnpbp.2015.01.010

Bloom, A. P., Jimenez-Andrade, J. M., Taylor, R. N., Castañeda-Corral, G., Kaczmarska, M. J., Freeman, K. T., … Mantyh, P. W. (2011). Breast cancer-induced bone remodeling, skeletal pain, and sprouting of sensory nerve fibers. *The Journal of Pain : Official Journal of the American Pain Society*, *12*(6), 698–711. http://doi.org/10.1016/j.jpain.2010.12.016

Borges, K., & Dingledine, R. (1998). AMPA receptors: molecular and functional diversity. *Progress in Brain Research*, *116*, 153–70.

Breese, N. M., George, A. C., Pauers, L. E., & Stucky, C. L. (2005). Peripheral inflammation selectively increases TRPV1 function in IB4-positive sensory neurons from adult mouse. *Pain*, *115*(1–2), 37–49. http://doi.org/10.1016/j.pain.2005.02.010

Bu, H., Shu, B., Gao, F., Liu, C., Guan, X., Ke, C., … Tian, Y. (2014). Spinal IFN-γ-induced protein-10 (CXCL10) mediates metastatic breast cancer-induced bone pain by activation of microglia in rat models. *Breast Cancer Research and Treatment*, *143*(2), 255–63. http://doi.org/10.1007/s10549-013-2807-4

Bushnell, M. C., Ceko, M., & Low, L. A. (2013). Cognitive and emotional control of pain and its disruption in chronic pain. *Nature Reviews. Neuroscience*,

14(7), 502–11. http://doi.org/10.1038/nrn3516

Cao, H., & Zhang, Y.-Q. (2008). Spinal glial activation contributes to pathological pain states. *Neuroscience and Biobehavioral Reviews*, *32*(5), 972–83. http://doi.org/10.1016/j.neubiorev.2008.03.009

Castañeda-Corral, G., Jimenez-Andrade, J. M., Bloom, A. P., Taylor, R. N., Mantyh, W. G., Kaczmarska, M. J., … Mantyh, P. W. (2011). The majority of myelinated and unmyelinated sensory nerve fibers that innervate bone express the tropomyosin receptor kinase A. *Neuroscience*, *178*, 196–207. http://doi.org/10.1016/j.neuroscience.2011.01.039

Choi, D. W. (1994). Glutamate receptors and the induction of excitotoxic neuronal death. *Progress in Brain Research*, *100*, 47–51.

Choi, D. W., Maulucci-Gedde, M., & Kriegstein, A. R. (1987). Glutamate neurotoxicity in cortical cell culture. *The Journal of Neuroscience : The Official Journal of the Society for Neuroscience*, *7*(2), 357–68.

Colburn, R. W., DeLeo, J. A., Rickman, A. J., Yeager, M. P., Kwon, P., & Hickey, W. F. (1997). Dissociation of microglial activation and neuropathic pain behaviors following peripheral nerve injury in the rat. *Journal of Neuroimmunology*, *79*(2), 163–75.

Coleman, R. E. (1997). Skeletal complications of malignancy. *Cancer*, *80*(8 Suppl), 1588–1594.

Crowley, C., Spencer, S. D., Nishimura, M. C., Chen, K. S., Pitts-Meek, S., Armanini, M. P., … Levinson, A. D. (1994). Mice lacking nerve growth factor display perinatal loss of sensory and sympathetic neurons yet develop basal forebrain cholinergic neurons. *Cell*, *76*(6), 1001–11.

Danbolt, N. C. (2001). Glutamate uptake. *Progress in Neurobiology*, *65*(1), 1–105.

Davis, B. M., Lewin, G. R., Mendell, L. M., Jones, M. E., & Albers, K. M. (1993). Altered expression of nerve growth factor in the skin of transgenic mice leads to changes in response to mechanical stimuli. *Neuroscience*, *56*(4), 789–92.

De Bundel, D., Schallier, A., Loyens, E., Fernando, R., Miyashita, H., Van Liefferinge, J., … Massie, A. (2011). Loss of System xFormula Does Not Induce Oxidative Stress But Decreases Extracellular Glutamate in Hippocampus and Influences Spatial Working Memory and Limbic Seizure Susceptibility. *Journal of Neuroscience*, *31*(15), 5792–5803. http://doi.org/10.1523/JNEUROSCI.5465-10.2011

Descamps, S., Lebourhis, X., Delehedde, M., Boilly, B., & Hondermarck, H.

(1998). Nerve growth factor is mitogenic for cancerous but not normal human breast epithelial cells. *The Journal of Biological Chemistry*, *273*(27), 16659–62.

Descamps, S., Toillon, R. A., Adriaenssens, E., Pawlowski, V., Cool, S. M., Nurcombe, V., … Hondermarck, H. (2001). Nerve growth factor stimulates proliferation and survival of human breast cancer cells through two distinct signaling pathways. *The Journal of Biological Chemistry*, *276*(21), 17864–70. http://doi.org/10.1074/jbc.M010499200

Dollé, L., El Yazidi-Belkoura, I., Adriaenssens, E., Nurcombe, V., & Hondermarck, H. (2003). Nerve growth factor overexpression and autocrine loop in breast cancer cells. *Oncogene*, *22*(36), 5592–601. http://doi.org/10.1038/sj.onc.1206805

Domercq, M., Szczupak, B., Gejo, J., Gómez-Vallejo, V., Padro, D., Gona, K. B., … Martín, A. (2016). PET Imaging with [(18)F]FSPG Evidences the Role of System xc(-) on Brain Inflammation Following Cerebral Ischemia in Rats. *Theranostics*, *6*(11), 1753–67. http://doi.org/10.7150/thno.15616

Dougherty, K. D., Dreyfus, C. F., & Black, I. B. (2000). Brain-derived neurotrophic factor in astrocytes, oligodendrocytes, and microglia/macrophages after spinal cord injury. *Neurobiology of Disease*,

7(6 Pt B), 574–85. http://doi.org/10.1006/nbdi.2000.0318

Dringen, R., Pfeiffer, B., & Hamprecht, B. (1999). Synthesis of the antioxidant glutathione in neurons: supply by astrocytes of CysGly as precursor for neuronal glutathione. - PubMed - NCBI. *J Neurosci*, *19*(2), 562–569.

Duric, V., & McCarson, K. (2006). Persistent Pain Produces Stress-like Alterations in Hippocampal Neurogenesis and Gene Expression. *The Journal of Pain*, *7*(8), 544–555. http://doi.org/10.1016/j.jpain.2006.01.458

Dworkin, R. H., & Gitlin, M. J. (1991). Clinical aspects of depression in chronic pain patients. *The Clinical Journal of Pain*, *7*(2), 79–94.

Echeverry, M. B., Guimarães, F. S., & Del Bel, E. A. (2004). Acute and delayed restraint stress-induced changes in nitric oxide producing neurons in limbic regions. *Neuroscience*, *125*(4), 981–93. http://doi.org/10.1016/j.neuroscience.2003.12.046

Eisch, A. J., & Petrik, D. (2012). Depression and Hippocampal Neurogenesis: A Road to Remission? *Science*, *338*(6103), 72–75. http://doi.org/10.1126/science.1222941

Elmore, M. R. P., Najafi, A. R., Koike, M. A., Dagher, N. N., Spangenberg, E. E., Rice, R. A., … Green, K. N. (2014). Colony-stimulating factor 1 receptor

signaling is necessary for microglia viability, unmasking a microglia progenitor cell in the adult brain. *Neuron*, *82*(2), 380–97. http://doi.org/10.1016/j.neuron.2014.02.040

Eulenburg, V., & Gomeza, J. (2010). Neurotransmitter transporters expressed in glial cells as regulators of synapse function. *Brain Research Reviews*, *63*(1–2), 103–112. http://doi.org/10.1016/j.brainresrev.2010.01.003

Fasick, V., Spengler, R. N., Samankan, S., Nader, N. D., & Ignatowski, T. A. (2015). The hippocampus and TNF: Common links between chronic pain and depression. *Neuroscience & Biobehavioral Reviews*, *53*, 139–159. http://doi.org/10.1016/j.neubiorev.2015.03.014

Favaroni Mendes, L. A., & Menescal-de-Oliveira, L. (2008). Role of cholinergic, opioidergic and GABAergic neurotransmission of the dorsal hippocampus in the modulation of nociception in guinea pigs. *Life Sciences*, *83*(19–20), 644–50. http://doi.org/10.1016/j.lfs.2008.09.006

Fonnum, F. (1984). Glutamate: a neurotransmitter in mammalian brain. *Journal of Neurochemistry*, *42*(1), 1–11.

Friess, H., Zhu, Z. W., di Mola, F. F., Kulli, C., Graber, H. U., Andren-Sandberg, A., … Büchler, M. W. (1999). Nerve growth factor and its high-affinity receptor in chronic pancreatitis. *Annals of Surgery*, *230*(5), 615–24.

Furuta, A., Martin, L. J., Lin, C. L., Dykes-Hoberg, M., & Rothstein, J. D. (1997). Cellular and synaptic localization of the neuronal glutamate transporters excitatory amino acid transporter 3 and 4. *Neuroscience*, *81*(4), 1031–42.

Graeber, M. B., Tetzlaff, W., Streit, W. J., & Kreutzberg, G. W. (1988). Microglial cells but not astrocytes undergo mitosis following rat facial nerve axotomy. *Neuroscience Letters*, *85*(3), 317–21.

Grewer, C., & Rauen, T. (2005). Electrogenic glutamate transporters in the CNS: molecular mechanism, pre-steady-state kinetics, and their impact on synaptic signaling. *The Journal of Membrane Biology*, *203*(1), 1–20. http://doi.org/10.1007/s00232-004-0731-6

Gross, C. G. (2000). Neurogenesis in the adult brain: death of a dogma. *Nature Reviews. Neuroscience*, *1*(1), 67–73. http://doi.org/10.1038/35036235

Guise, T. (2010). Examining the metastatic niche: targeting the microenvironment. *Semin Oncol*, *37 Suppl 2*, S2-14. http://doi.org/10.1053/j.seminoncol.2010.10.007

Hagino, Y., Kariura, Y., Manago, Y., Amano, T., Wang, B., Sekiguchi, M., … Noda, M. (2004). Heterogeneity and potentiation of AMPA type of glutamate receptors in rat cultured microglia. *Glia*, *47*(1), 68–77. http://doi.org/10.1002/glia.20034

Halliday, D. A., Zettler, C., Rush, R. A., Scicchitano, R., & McNeil, J. D. (1998). Elevated nerve growth factor levels in the synovial fluid of patients with inflammatory joint disease. *Neurochemical Research*, *23*(6), 919–22.

Halvorson, K. G. (2005). A Blocking Antibody to Nerve Growth Factor Attenuates Skeletal Pain Induced by Prostate Tumor Cells Growing in Bone. *Cancer Research*, *65*(20), 9426–9435. http://doi.org/10.1158/0008-5472.CAN-05-0826

Hamashima, S., Homma, T., Kobayashi, S., Ishii, N., Kurahashi, T., Watanabe, R., … Fujii, J. (2017). Decreased reproductive performance in xCT-knockout male mice. *Free Radical Research*, *51*(9–10), 851–860. http://doi.org/10.1080/10715762.2017.1388504

Hardingham, G. E., & Bading, H. (2010). Synaptic versus extrasynaptic NMDA receptor signalling: implications for neurodegenerative disorders. *Nature Reviews. Neuroscience*, *11*(10), 682–96. http://doi.org/10.1038/nrn2911

Hinoi, E., Takarada, T., Ueshima, T., Tsuchihashi, Y., & Yoneda, Y. (2004). Glutamate signaling in peripheral tissues. *European Journal of Biochemistry*, *271*(1), 1–13.

Hollmann, M., & Heinemann, S. (1994). Cloned Glutamate Receptors. *Annual Review of Neuroscience*, *17*(1), 31–108.

http://doi.org/10.1146/annurev.ne.17.030194.000335

Hu, J.-H., Yang, J.-P., Liu, L., Li, C.-F., Wang, L.-N., Ji, F.-H., & Cheng, H. (2012). Involvement of CX3CR1 in bone cancer pain through the activation of microglia p38 MAPK pathway in the spinal cord. *Brain Research*, *1465*, 1–9. http://doi.org/10.1016/j.brainres.2012.05.020

Hu, X.-F., He, X.-T., Zhou, K.-X., Zhang, C., Zhao, W.-J., Zhang, T., … Dong, Y.-L. (2017). The analgesic effects of triptolide in the bone cancer pain rats via inhibiting the upregulation of HDACs in spinal glial cells. *Journal of Neuroinflammation*, *14*(1), 213. http://doi.org/10.1186/s12974-017-0988-1

Huang, E. J., & Reichardt, L. F. (2003). Trk receptors: roles in neuronal signal transduction. *Annual Review of Biochemistry*, *72*(1), 609–42. http://doi.org/10.1146/annurev.biochem.72.121801.161629

Huo, W., Zhang, Y., Liu, Y., Lei, Y., Sun, R., Zhang, W., … Gu, X. (2018). Dehydrocorydaline attenuates bone cancer pain by shifting microglial M1/M2 polarization toward the M2 phenotype. *Molecular Pain*, *14*, 1744806918781733. http://doi.org/10.1177/1744806918781733

Ignatowski, T. A., Sud, R., Reynolds, J. L., Knight, P. R., & Spengler, R. N. (2005). The dissipation of neuropathic pain paradoxically involves the presence of tumor necrosis factor-alpha (TNF). *Neuropharmacology*, *48*(3),

448–60. http://doi.org/10.1016/j.neuropharm.2004.11.001

Inoue, M., Rashid, M. H., Fujita, R., Contos, J. J. A., Chun, J., & Ueda, H. (2004). Initiation of neuropathic pain requires lysophosphatidic acid receptor signaling. *Nature Medicine*, *10*(7), 712–8. http://doi.org/10.1038/nm1060

Inquimbert, P., Bartels, K., Babaniyi, O. B., Barrett, L. B., Tegeder, I., & Scholz, J. (2012). Peripheral nerve injury produces a sustained shift in the balance between glutamate release and uptake in the dorsal horn of the spinal cord. *Pain*, *153*(12), 2422–31. http://doi.org/10.1016/j.pain.2012.08.011

Jang, J. H., Kim, D.-W., Sang Nam, T., Se Paik, K., & Leem, J. W. (2004). Peripheral glutamate receptors contribute to mechanical hyperalgesia in a neuropathic pain model of the rat. *Neuroscience*, *128*(1), 169–76. http://doi.org/10.1016/j.neuroscience.2004.06.040

Ji, R.-R., Berta, T., & Nedergaard, M. (2013). Glia and pain: Is chronic pain a gliopathy? *Pain*, *154*, S10–S28. http://doi.org/10.1016/j.pain.2013.06.022

Jimenez-Andrade, J. M., Bloom, A. P., Stake, J. I., Mantyh, W. G., Taylor, R. N., Freeman, K. T., … Mantyh, P. W. (2010). Pathological sprouting of adult nociceptors in chronic prostate cancer-induced bone pain. *The Journal of Neuroscience : The Official Journal of the Society for Neuroscience*, *30*(44), 14649–56. http://doi.org/10.1523/JNEUROSCI.3300-10.2010

Jimenez-Andrade, J. M., Ghilardi, J. R., Castañeda-Corral, G., Kuskowski, M. A., & Mantyh, P. W. (2011). Preventive or late administration of anti-NGF therapy attenuates tumor-induced nerve sprouting, neuroma formation, and cancer pain. *Pain*, *152*(11), 2564–74. http://doi.org/10.1016/j.pain.2011.07.020

Jimenez-Andrade, J. M., Martin, C. D., Koewler, N. J., Freeman, K. T., Sullivan, L. J., Halvorson, K. G., … Mantyh, P. W. (2007). Nerve growth factor sequestering therapy attenuates non-malignant skeletal pain following fracture. *Pain*, *133*(1), 183–196. http://doi.org/10.1016/j.pain.2007.06.016

Jin, D., Yang, J.-P., Hu, J.-H., Wang, L.-N., & Zuo, J.-L. (2015). MCP-1 stimulates spinal microglia via PI3K/Akt pathway in bone cancer pain. *Brain Research*, *1599*, 158–67. http://doi.org/10.1016/j.brainres.2014.12.043

Kanai, Y., & Hediger, M. A. (1992). Primary structure and functional characterization of a high-affinity glutamate transporter. *Nature*, *360*(6403), 467–71. http://doi.org/10.1038/360467a0

Kew, J. N. C., & Kemp, J. A. (2005). Ionotropic and metabotropic glutamate receptor structure and pharmacology. *Psychopharmacology*, *179*(1), 4–29. http://doi.org/10.1007/s00213-005-2200-z

Khanna, S., Chang, L. S., Jiang, F., & Koh, H. C. (2004). Nociception-driven

decreased induction of Fos protein in ventral hippocampus field CA1 of the rat. *Brain Research*, *1004*(1–2), 167–76. http://doi.org/10.1016/j.brainres.2004.01.026

Kigerl, K. A., Ankeny, D. P., Garg, S. K., Wei, P., Guan, Z., Lai, W., … Popovich, P. G. (2012). System xc− regulates microglia and macrophage glutamate excitotoxicity in vivo. *Experimental Neurology*, *233*(1), 333–341. http://doi.org/10.1016/j.expneurol.2011.10.025

Lagadec, C., Meignan, S., Adriaenssens, E., Foveau, B., Vanhecke, E., Romon, R., … Le Bourhis, X. (2009). TrkA overexpression enhances growth and metastasis of breast cancer cells. *Oncogene*, *28*(18), 1960–70. http://doi.org/10.1038/onc.2009.61

Lawson, L. J., Perry, V. H., Dri, P., & Gordon, S. (1990). Heterogeneity in the distribution and morphology of microglia in the normal adult mouse brain. *Neuroscience*, *39*(1), 151–70.

Legrain, V., Iannetti, G. D., Plaghki, L., & Mouraux, A. (2011). The pain matrix reloaded: a salience detection system for the body. *Progress in Neurobiology*, *93*(1), 111–24. http://doi.org/10.1016/j.pneurobio.2010.10.005

Linher-Melville, K., Haftchenary, S., Gunning, P., & Singh, G. (2015). Signal

transducer and activator of transcription 3 and 5 regulate system Xc- and redox balance in human breast cancer cells. *Molecular and Cellular Biochemistry*, *405*(1–2), 205–221. http://doi.org/10.1007/s11010-015-2412-4

Linher-Melville, K., Nashed, M. G., Ungard, R. G., Haftchenary, S., Rosa, D. A., Gunning, P. T., & Singh, G. (2016). Chronic Inhibition of STAT3/STAT5 in Treatment-Resistant Human Breast Cancer Cell Subtypes: Convergence on the ROS/SUMO Pathway and Its Effects on xCT Expression and System xc- Activity. *PLOS ONE*, *11*(8), e0161202.

Linher-Melville, K., & Singh, G. (2017). The complex roles of STAT3 and STAT5 in maintaining redox balance: Lessons from STAT-mediated xCT expression in cancer cells. *Molecular and Cellular Endocrinology*. http://doi.org/10.1016/j.mce.2017.02.014

Liu, G. J., Kalous, A., Werry, E. L., & Bennett, M. R. (2006). Purine release from spinal cord microglia after elevation of calcium by glutamate. *Molecular Pharmacology*, *70*(3), 851–9. http://doi.org/10.1124/mol.105.021436

Liu, M.-G., & Chen, J. (2009). Roles of the hippocampal formation in pain information processing. *Neuroscience Bulletin*, *25*(5), 237–66. http://doi.org/10.1007/s12264-009-0905-4

Liu, M., Yao, M., Wang, H., Xu, L., Zheng, Y., Huang, B., … Lian, Q. (2017).

$P2Y_{12}$ receptor-mediated activation of spinal microglia and p38MAPK pathway contribute to cancer-induced bone pain. *Journal of Pain Research*, *Volume 10*, 417–426. http://doi.org/10.2147/JPR.S124326

Liu, X., Resch, J., Rush, T., & Lobner, D. (2012). Functional upregulation of system xc- by fibroblast growth factor-2. *Neuropharmacology*, *62*(2), 901–6. http://doi.org/10.1016/j.neuropharm.2011.09.019

Lo, M., Wang, Y. Z., & Gout, P. W. (2008). The x(c)- cystine/glutamate antiporter: a potential target for therapy of cancer and other diseases. *J Cell Physiol*, *215*(3), 593–602. http://doi.org/10.1002/jcp.21366

Lowe, E. M., Anand, P., Terenghi, G., Williams-Chestnut, R. E., Sinicropi, D. V, & Osborne, J. L. (1997). Increased nerve growth factor levels in the urinary bladder of women with idiopathic sensory urgency and interstitial cystitis. *British Journal of Urology*, *79*(4), 572–7.

Lozano-Ondoua, A. N., Symons-Liguori, A. M., & Vanderah, T. W. (2013). Cancer-induced bone pain: Mechanisms and models. *Neuroscience Letters*, *557 Pt A*, 52–9. http://doi.org/10.1016/j.neulet.2013.08.003

Mantyh, P. W., Koltzenburg, M., Mendell, L. M., Tive, L., & Shelton, D. L. (2011). Antagonism of nerve growth factor-TrkA signaling and the relief of pain. *Anesthesiology*, *115*(1), 189–204.

http://doi.org/10.1097/ALN.0b013e31821b1ac5

Mantyh, W. G., Jimenez-Andrade, J. M., Stake, J. I., Bloom, A. P., Kaczmarska, M. J., Taylor, R. N., … Mantyh, P. W. (2010). Blockade of nerve sprouting and neuroma formation markedly attenuates the development of late stage cancer pain. *Neuroscience*, *171*(2), 588–98. http://doi.org/10.1016/j.neuroscience.2010.08.056

Mao-Ying, Q.-L., Wang, X.-W., Yang, C.-J., Li, X., Mi, W.-L., Wu, G.-C., & Wang, Y.-Q. (2012). Robust spinal neuroinflammation mediates mechanical allodynia in Walker 256 induced bone cancer rats. *Molecular Brain*, *5*(1), 16. http://doi.org/10.1186/1756-6606-5-16

McBean, G. J. (2002). Cerebral cystine uptake: a tale of two transporters. *Trends in Pharmacological Sciences*, *23*(7), 299–302.

McEwen, B. S. (2001). Plasticity of the hippocampus: adaptation to chronic stress and allostatic load. *Annals of the New York Academy of Sciences*, *933*, 265–77.

McKenna, J. E., & Melzack, R. (1992). Analgesia produced by lidocaine microinjection into the dentate gyrus. *Pain*, *49*(1), 105–12.

McKenna, J. E., & Melzack, R. (2001). Blocking NMDA receptors in the

hippocampal dentate gyrus with AP5 produces analgesia in the formalin pain test. *Experimental Neurology*, *172*(1), 92–9. http://doi.org/10.1006/exnr.2001.7777

McNamee, K. E., Burleigh, A., Gompels, L. L., Feldmann, M., Allen, S. J., Williams, R. O., … Inglis, J. J. (2010). Treatment of murine osteoarthritis with TrkAd5 reveals a pivotal role for nerve growth factor in non-inflammatory joint pain. *Pain*, *149*(2), 386–392. http://doi.org/10.1016/j.pain.2010.03.002

Meldrum, B. S. (2000). Glutamate as a neurotransmitter in the brain: review of physiology and pathology. *The Journal of Nutrition*, *130*(4S Suppl), 1007S–15S. http://doi.org/10.1093/jn/130.4.1007S

Mesci, P., Zaïdi, S., Lobsiger, C. S., Millecamps, S., Escartin, C., Seilhean, D., … Boillée, S. (2015). System xC− is a mediator of microglial function and its deletion slows symptoms in amyotrophic lateral sclerosis mice. *Brain*, *138*(1), 53–68. http://doi.org/10.1093/brain/awu312

Miladinovic, T., Nashed, M. G., & Singh, G. (2015). Overview of Glutamatergic Dysregulation in Central Pathologies. *Biomolecules*, *5*(4), 3112–41. http://doi.org/10.3390/biom5043112

Miladinovic, T., Ungard, R. G., Linher-Melville, K., Popovic, S., & Singh, G.

(2018). Functional effects of TrkA inhibition on system xC--mediated glutamate release and cancer-induced bone pain. *Molecular Pain*, *14*, 1–15. http://doi.org/10.1177/1744806918776467

Miller, K. E., Hoffman, E. M., Sutharshan, M., & Schechter, R. (2011). Glutamate pharmacology and metabolism in peripheral primary afferents: Physiological and pathophysiological mechanisms. *Pharmacology & Therapeutics*, *130*(3), 283–309. http://doi.org/10.1016/j.pharmthera.2011.01.005

Milligan, E. D., & Watkins, L. R. (2009). Pathological and protective roles of glia in chronic pain. *Nature Reviews. Neuroscience*, *10*(1), 23–36. http://doi.org/10.1038/nrn2533

Mundy, G. R. (2002). Metastasis to bone: causes, consequences and therapeutic opportunities. *Nat Rev Cancer*, *2*(8), 584–593. http://doi.org/10.1038/nrc867

Murray, F., Smith, D. W., & Hutson, P. H. (2008). Chronic low dose corticosterone exposure decreased hippocampal cell proliferation, volume and induced anxiety and depression like behaviours in mice. *European Journal of Pharmacology*, *583*(1), 115–27. http://doi.org/10.1016/j.ejphar.2008.01.014

Murugan, M., Ling, E.-A., & Kaur, C. (2013). Glutamate receptors in microglia. *CNS & Neurological Disorders Drug Targets*, *12*(6), 773–84.

Mutso, A. A., Radzicki, D., Baliki, M. N., Huang, L., Banisadr, G., Centeno, M. V, … Apkarian, A. V. (2012). Abnormalities in hippocampal functioning with persistent pain. *The Journal of Neuroscience : The Official Journal of the Society for Neuroscience*, *32*(17), 5747–56. http://doi.org/10.1523/JNEUROSCI.0587-12.2012

Myers, R. R., Heckman, H. M., & Rodriguez, M. (1996). Reduced hyperalgesia in nerve-injured WLD mice: relationship to nerve fiber phagocytosis, axonal degeneration, and regeneration in normal mice. *Experimental Neurology*, *141*(1), 94–101. http://doi.org/10.1006/exnr.1996.0142

Nakajima, K., Honda, S., Tohyama, Y., Imai, Y., Kohsaka, S., & Kurihara, T. (2001). Neurotrophin secretion from cultured microglia. *Journal of Neuroscience Research*, *65*(4), 322–331. http://doi.org/10.1002/jnr.1157

Nicholls, D., & Attwell, D. (1990). The release and uptake of excitatory amino acids. *Trends in Pharmacological Sciences*, *11*(11), 462–8.

Ottestad-Hansen, S., Hu, Q. X., Follin-Arbelet, V. V., Bentea, E., Sato, H., Massie, A., … Danbolt, N. C. (2018). The cystine-glutamate exchanger (xCT, Slc7a11) is expressed in significant concentrations in a subpopulation of astrocytes in the mouse brain. *Glia*, *66*(5), 951–970. http://doi.org/10.1002/glia.23294

Peng, J., Gu, N., Zhou, L., B Eyo, U., Murugan, M., Gan, W.-B., & Wu, L.-J. (2016). Microglia and monocytes synergistically promote the transition from acute to chronic pain after nerve injury. *Nature Communications*, *7*, 12029. http://doi.org/10.1038/ncomms12029

Piani, D., & Fontana, A. (1994). Involvement of the cystine transport system xc- in the macrophage-induced glutamate-dependent cytotoxicity to neurons. *Journal of Immunology (Baltimore, Md. : 1950)*, *152*(7), 3578–85.

Piani, D., Frei, K., Do, K. Q., Cuénod, M., & Fontana, A. (1991). Murine brain macrophages induced NMDA receptor mediated neurotoxicity in vitro by secreting glutamate. *Neuroscience Letters*, *133*(2), 159–62.

Pines, G., Danbolt, N. C., Bjørås, M., Zhang, Y., Bendahan, A., Eide, L., … Kanner, B. I. (1992). Cloning and expression of a rat brain L-glutamate transporter. *Nature*, *360*(6403), 464–7. http://doi.org/10.1038/360464a0

Pocock, J. M., & Kettenmann, H. (2007). Neurotransmitter receptors on microglia. *Trends in Neurosciences*, *30*(10), 527–35. http://doi.org/10.1016/j.tins.2007.07.007

Popiolek-Barczyk, K., & Mika, J. (2016). Targeting the Microglial Signaling Pathways: New Insights in the Modulation of Neuropathic Pain. *Current Medicinal Chemistry*, *23*(26), 2908–2928.

Pulaski, B. A., & Ostrand-Rosenberg, S. (2001). Mouse 4T1 Breast Tumor Model. In *Current Protocols in Immunology* (Vol. Chapter 20, p. Unit 20.2). Hoboken, NJ, USA: John Wiley & Sons, Inc. http://doi.org/10.1002/0471142735.im2002s39

Qin, L., Wu, X., Block, M. L., Liu, Y., Breese, G. R., Hong, J.-S., … Crews, F. T. (2007). Systemic LPS causes chronic neuroinflammation and progressive neurodegeneration. *Glia*, *55*(5), 453–62. http://doi.org/10.1002/glia.20467

Raghavendra, V., Tanga, F., & DeLeo, J. A. (2003). Inhibition of microglial activation attenuates the development but not existing hypersensitivity in a rat model of neuropathy. *The Journal of Pharmacology and Experimental Therapeutics*, *306*(2), 624–30. http://doi.org/10.1124/jpet.103.052407

Reissner, K. J., & Kalivas, P. W. (2010). Using glutamate homeostasis as a target for treating addictive disorders. *Behavioural Pharmacology*, *21*(5–6), 514–22. http://doi.org/10.1097/FBP.0b013e32833d41b2

Rigillo, G., Vilella, A., Benatti, C., Schaeffer, L., Brunello, N., Blom, J. M. C., … Tascedda, F. (2018). LPS-induced histone H3 phospho(Ser10)-acetylation(Lys14) regulates neuronal and microglial neuroinflammatory response. *Brain, Behavior, and Immunity*. http://doi.org/10.1016/j.bbi.2018.09.019

Sagara, J. I., Miura, K., & Bannai, S. (1993). Maintenance of neuronal glutathione by glial cells. *Journal of Neurochemistry*, *61*(5), 1672–6.

Sato, H., Shiiya, A., Kimata, M., Maebara, K., Tamba, M., Sakakura, Y., … Bannai, S. (2005). Redox imbalance in cystine/glutamate transporter-deficient mice. *The Journal of Biological Chemistry*, *280*(45), 37423–9. http://doi.org/10.1074/jbc.M506439200

Sato, H., Tamba, M., Ishii, T., & Bannai, S. (1999). Cloning and expression of a plasma membrane cystine/glutamate exchange transporter composed of two distinct proteins. *The Journal of Biological Chemistry*, *274*(17), 11455–8.

Schoepfer, R., Monyer, H., Sommer, B., Wisden, W., Sprengel, R., Kuner, T., … Burnashev, N. (1994). Molecular biology of glutamate receptors. *Progress in Neurobiology*, *42*(2), 353–7.

Schousboe, A. (1981). Transport and metabolism of glutamate and GABA in neuron and glial cells. *International Review of Neurobiology*, *22*, 1–45.

Seidlitz, E. P., Sharma, M. K., Saikali, Z., Ghert, M., & Singh, G. (2009). Cancer cell lines release glutamate into the extracellular environment. *Clinical & Experimental Metastasis*, *26*(7), 781–7. http://doi.org/10.1007/s10585-009-9277-4

Seidlitz, E. P., Sharma, M. K., & Singh, G. (2010). Extracellular glutamate alters mature osteoclast and osteoblast functions. *Canadian Journal of Physiology and Pharmacology*, *88*(9), 929–36. http://doi.org/10.1139/y10-070

Sevcik, M. A., Ghilardi, J. R., Peters, C. M., Lindsay, T. H., Halvorson, K. G., Jonas, B. M., … Mantyh, P. W. (2005). Anti-NGF therapy profoundly reduces bone cancer pain and the accompanying increase in markers of peripheral and central sensitization. *Pain*, *115*(1–2), 128–41. http://doi.org/10.1016/j.pain.2005.02.022

Shan, S., Qi-Liang, M.-Y., Hong, C., Tingting, L., Mei, H., Haili, P., … Yu-Qiu, Z. (2007). Is functional state of spinal microglia involved in the anti-allodynic and anti-hyperalgesic effects of electroacupuncture in rat model of monoarthritis? *Neurobiology of Disease*, *26*(3), 558–568. http://doi.org/10.1016/j.nbd.2007.02.007

Sharma, M. K., Seidlitz, E. P., & Singh, G. (2010). Cancer cells release glutamate via the cystine/glutamate antiporter. *Biochemical and Biophysical Research Communications*, *391*(1), 91–5. http://doi.org/10.1016/j.bbrc.2009.10.168

Shih, A. Y., Erb, H., Sun, X., Toda, S., Kalivas, P. W., & Murphy, T. H. (2006). Cystine/glutamate exchange modulates glutathione supply for neuroprotection from oxidative stress and cell proliferation. *The Journal of*

Neuroscience : The Official Journal of the Society for Neuroscience, *26*(41), 10514–23. http://doi.org/10.1523/JNEUROSCI.3178-06.2006

Simons, L. E., Elman, I., & Borsook, D. (2014). Psychological processing in chronic pain: a neural systems approach. *Neuroscience and Biobehavioral Reviews*, *39*, 61–78. http://doi.org/10.1016/j.neubiorev.2013.12.006

Skelly, D. T., Hennessy, E., Dansereau, M.-A., & Cunningham, C. (2013). A systematic analysis of the peripheral and CNS effects of systemic LPS, IL-1β, [corrected] TNF-α and IL-6 challenges in C57BL/6 mice. *PloS One*, *8*(7), e69123. http://doi.org/10.1371/journal.pone.0069123

Slosky, L. M., BassiriRad, N. M., Symons, A. M., Thompson, M., Doyle, T., Forte, B. L., … Vanderah, T. W. (2016). The cystine/glutamate antiporter system xc- drives breast tumor cell glutamate release and cancer-induced bone pain. *Pain*, *157*(11), 2605–2616. http://doi.org/10.1097/j.pain.0000000000000681

Smeyne, R. J., Klein, R., Schnapp, A., Long, L. K., Bryant, S., Lewin, A., … Barbacid, M. (1994). Severe sensory and sympathetic neuropathies in mice carrying a disrupted Trk/NGF receptor gene. *Nature*, *368*(6468), 246–9. http://doi.org/10.1038/368246a0

Soleimannejad, E., Naghdi, N., Semnanian, S., Fathollahi, Y., & Kazemnejad, A.

(2007). Antinociceptive effect of intra-hippocampal CA1 and dentate gyrus injection of MK801 and AP5 in the formalin test in adult male rats. *European Journal of Pharmacology*, *562*(1–2), 39–46. http://doi.org/10.1016/j.ejphar.2006.11.051

Soleimannejad, E., Semnanian, S., Fathollahi, Y., & Naghdi, N. (2006). Microinjection of ritanserin into the dorsal hippocampal CA1 and dentate gyrus decrease nociceptive behavior in adult male rat. *Behavioural Brain Research*, *168*(2), 221–5. http://doi.org/10.1016/j.bbr.2005.11.011

Stoll, G., & Jander, S. (1999). The role of microglia and macrophages in the pathophysiology of the CNS. *Progress in Neurobiology*, *58*(3), 233–47.

Storck, T., Schulte, S., Hofmann, K., & Stoffel, W. (1992). Structure, expression, and functional analysis of a Na(+)-dependent glutamate/aspartate transporter from rat brain. *Proceedings of the National Academy of Sciences of the United States of America*, *89*(22), 10955–9.

Streit, W. J. (2002). Microglia as neuroprotective, immunocompetent cells of the CNS. *Glia*, *40*(2), 133–9. http://doi.org/10.1002/glia.10154

Stucky, C. L., Koltzenburg, M., Schneider, M., Engle, M. G., Albers, K. M., & Davis, B. M. (1999). Overexpression of nerve growth factor in skin selectively affects the survival and functional properties of nociceptors. *The*

Journal of Neuroscience : The Official Journal of the Society for Neuroscience, *19*(19), 8509–16.

Sud, R., Spengler, R. N., Nader, N. D., & Ignatowski, T. A. (2008). Antinociception occurs with a reversal in alpha 2-adrenoceptor regulation of TNF production by peripheral monocytes/macrophages from pro- to anti-inflammatory. *European Journal of Pharmacology*, *588*(2–3), 217–31. http://doi.org/10.1016/j.ejphar.2008.04.043

Sun, S., Cao, H., Han, M., Li, T. T., Zhao, Z. Q., & Zhang, Y. Q. (2008). Evidence for suppression of electroacupuncture on spinal glial activation and behavioral hypersensitivity in a rat model of monoarthritis. *Brain Research Bulletin*, *75*(1), 83–93. http://doi.org/10.1016/j.brainresbull.2007.07.027

Sweitzer, S. M., Schubert, P., & DeLeo, J. A. (2001). Propentofylline, a glial modulating agent, exhibits antiallodynic properties in a rat model of neuropathic pain. *The Journal of Pharmacology and Experimental Therapeutics*, *297*(3), 1210–7.

Tahraoui, S. L., Marret, S., Bodénant, C., Leroux, P., Dommergues, M. A., Evrard, P., & Gressens, P. (2001). Central role of microglia in neonatal excitotoxic lesions of the murine periventricular white matter. *Brain Pathology (Zurich, Switzerland)*, *11*(1), 56–71.

Tang, Y., & Le, W. (2016). Differential Roles of M1 and M2 Microglia in Neurodegenerative Diseases. *Molecular Neurobiology*, *53*(2), 1181–1194. http://doi.org/10.1007/s12035-014-9070-5

Taylor, S., Srinivasan, B., Wordinger, R. J., & Roque, R. S. (2003). Glutamate stimulates neurotrophin expression in cultured Müller cells. *Molecular Brain Research*, *111*(1–2), 189–197. http://doi.org/10.1016/S0169-328X(03)00030-5

Todd, A. J. (2010). Neuronal circuitry for pain processing in the dorsal horn. *Nature Reviews Neuroscience*, *11*(12), 823–836. http://doi.org/10.1038/nrn2947

Tofaris, G. K., Patterson, P. H., Jessen, K. R., & Mirsky, R. (2002). Denervated Schwann cells attract macrophages by secretion of leukemia inhibitory factor (LIF) and monocyte chemoattractant protein-1 in a process regulated by interleukin-6 and LIF. *The Journal of Neuroscience : The Official Journal of the Society for Neuroscience*, *22*(15), 6696–703. http://doi.org/20026699

Tsuda, M., Inoue, K., & Salter, M. W. (2005). Neuropathic pain and spinal microglia: a big problem from molecules in “small” glia. *Trends in Neurosciences*, *28*(2), 101–7. http://doi.org/10.1016/j.tins.2004.12.002

Tzingounis, A. V, & Wadiche, J. I. (2007). Glutamate transporters: confining

runaway excitation by shaping synaptic transmission. *Nature Reviews. Neuroscience*, *8*(12), 935–47. http://doi.org/10.1038/nrn2274

Ungard, R. G., Linher-Melville, K., Nashed, M., Sharma, M., Wen, J., & Singh, G. (2019). xCT knockdown in human breast cancer cells delays onset of cancer-induced bone pain. *Molecular Pain*, *15*, 1–14. http://doi.org/10.1177/1744806918822185

Ungard, R. G., Seidlitz, E. P., & Singh, G. (2014). Inhibition of breast cancer-cell glutamate release with sulfasalazine limits cancer-induced bone pain. *Pain*, *155*(1), 28–36. http://doi.org/10.1016/j.pain.2013.08.030

Vandenberg, R. J., & Ryan, R. M. (2013). Mechanisms of glutamate transport. *Physiological Reviews*, *93*(4), 1621–57. http://doi.org/10.1152/physrev.00007.2013

Vaure, C., & Liu, Y. (2014). A comparative review of toll-like receptor 4 expression and functionality in different animal species. *Frontiers in Immunology*, *5*, 316. http://doi.org/10.3389/fimmu.2014.00316

Walter, L., & Neumann, H. (2009). Role of microglia in neuronal degeneration and regeneration. *Seminars in Immunopathology*, *31*(4), 513–25. http://doi.org/10.1007/s00281-009-0180-5

Wang, L.-N., Yang, J.-P., Zhan, Y., Ji, F.-H., Wang, X.-Y., Zuo, J.-L., & Xu, Q.-N. (2012). Minocycline-induced reduction of brain-derived neurotrophic factor expression in relation to cancer-induced bone pain in rats. *Journal of Neuroscience Research*, *90*(3), 672–81. http://doi.org/10.1002/jnr.22788

Watanabe, H., & Bannai, S. (1987). Induction of cystine transport activity in mouse peritoneal macrophages. *The Journal of Experimental Medicine*, *165*(3), 628–40.

Watkins, L. R., Martin, D., Ulrich, P., Tracey, K. J., & Maier, S. F. (1997). Evidence for the involvement of spinal cord glia in subcutaneous formalin induced hyperalgesia in the rat. *Pain*, *71*(3), 225–35.

Xiong, H., Futamura, T., Jourdi, H., Zhou, H., Takei, N., Diverse-Pierluissi, M., … Nawa, H. (2002). Neurotrophins induce BDNF expression through the glutamate receptor pathway in neocortical neurons. *Neuropharmacology*, *42*(7), 903–912. http://doi.org/10.1016/S0028-3908(02)00043-6

Yamamotová, A., Franek, M., Vaculín, S., St'astný, F., Bubeníková-Valesová, V., & Rokyta, R. (2007). Different transfer of nociceptive sensitivity from rats with postnatal hippocampal lesions to control rats. *The European Journal of Neuroscience*, *26*(2), 446–50. http://doi.org/10.1111/j.1460-9568.2007.05666.x

Yang, Y., Li, H., Li, T.-T., Luo, H., Gu, X.-Y., Lü, N., … Zhang, Y.-Q. (2015). Delayed activation of spinal microglia contributes to the maintenance of bone cancer pain in female Wistar rats via P2X7 receptor and IL-18. *The Journal of Neuroscience : The Official Journal of the Society for Neuroscience*, *35*(20), 7950–63. http://doi.org/10.1523/JNEUROSCI.5250-14.2015

Zhao, X.-Y., Liu, M.-G., Yuan, D.-L., Wang, Y., He, Y., Wang, D.-D., … Chen, J. (2009). Nociception-induced spatial and temporal plasticity of synaptic connection and function in the hippocampal formation of rats: a multi-electrode array recording. *Molecular Pain*, *5*, 55. http://doi.org/10.1186/1744-8069-5-55

Zhuo, M., Wu, G., & Wu, L.-J. (2011). Neuronal and microglial mechanisms of neuropathic pain. *Molecular Brain*, *4*(1), 31. http://doi.org/10.1186/1756-6606-4-31

APPENDIX 1

General Materials and Methods

Preface

The purpose of this section is to provide additional details for central methodologies. Journal article length restrictions did not allow for these details to be presented in the original articles. Details are not provided for methods that directly followed manufacturer manuals, such as RNA isolation and osmotic pump loading and implantation. In addition, details are not provided for lengthy methods that directly followed protocols previously detailed in published manuscripts. For example, the battery of tests for nociceptive behaviours is extensively outlined by Ungard *et al.*, in their 2014 paper "Inhibition of breast cancer-cell glutamate release with sulfasalazine limits cancer-induced bone pain" published in PAIN.

Cell Cultures and Treatments

Several cell lines were used in these studies, including human (MDA-MB-231) and murine (4T1, T47D) triple-negative murine carcinoma cells and human microglia cells (HMC3). All cells were ordered from American Type Culture Collection (ATCC).

As per supplier instructions, 4T1 triple-negative murine mammary gland carcinoma cells were maintained in high glucose Roswell Park Memorial Institute medium (RPMI-1640; Life Technologies); T47D triple-negative human breast carcinoma cells were maintained in high glucose RPMI (Life Technologies); MDA-MB-231 triple-negative human breast carcinoma cells were maintained in high glucose DMEM (Life Technologies). All carcinoma cells were supplemented with 10 % fetal bovine serum (FBS) and 1 % antibiotic/antimycotic (Life Technologies) incubated at 37 °C and 5 % CO_2 and verified to be mycoplasma free before experimental use.

Our lab recently developed shRNA-generated C6 xCT knockdown clones (C6 xCT KD), and pLK01 empty vector control cells (See (Ungard *et al*., 2019)). Briefly, stable system x_C^- knockdown breast cancer cells were generated using a shRNA approach with a puromycin-selectable mammalian expression vector carrying either a shRNA cassette specifically targeting the human xCT gene SLC7A11 or an empty-vector control.

MDA-MB-231 cells were transfected with the shRNA vector V2LHS-C6 (Open Biosystems, Thermo Scientific) using Lipofectamine 2000 (Life Technologies; 2 µg shRNA + 10 µl lipofectamine 2000 /well of 6 well plate). Puromycin (5 µg/ml) was added to growth media for selection after 48-hour transfection, and media was refreshed every 2-3 days until cell colonies were formed 3-4 weeks later. All cell colonies for each shRNA vector were pooled and proliferated to enough cells for further analysis. These obtained stable knockdown cell lines were named G1, C6, A12 and F12, respectively, and C6 was selected for further studies based on several growth characteristics. Following knockdown generation, cells were maintained in high glucose DMEM (Life Technologies, Carlsbad, CA). To maintain xCT knockdown, growth media for C6 xCT KD clones (and empty vector control cells) were supplemented with Puromycin (1 µg/mL) daily.

HMC3 human microglia cells were purchased from ATCC and were maintained in EMEM (Life Technologies, Carlsbad, CA). As per supplier instructions, microglia cells were supplemented with 10 % fetal bovine serum (FBS) and carcinoma cells were supplemented with 10 % FBS and 1 % antibiotic/antimycotic.

Cells were grown in incubators with 5% CO_2 at 37 °C, and were regularly subcultured once confluent. To subculture, cells were first washed with 5 mL of 1 × PBS followed by trypsinization with approximately 1-2 mL (dependent on cell

confluency and culture dish size) of 2 × 0.1% EDTA-trypsin. Cells were placed into the incubator for approximately 4 minutes to allow cells to detach from the flask. Fresh culture media was then added to the flask to de-activate the trypsin. Excess cells were then removed, counted with a Haemocytometer slide, and a calculated fraction of cells added to a new flask with fresh culture medium.

Co-cultures

HMC3 human microglia were co-cultured with or without wildtype, C6 xCT KD, or empty vector control MDA-MB-231 carcinoma cells as an *in vitro* model of peripheral tumour-released glutamate on microglial activation. HMC3 cells were seeded at 5 x 10^5 cells/well in 6-well plates. All MDA-MB-231 cells were seeded at 5 x 10^5 cells/insert in 4 μM pore transwell inserts (Corning, Tewksbury, MA). Cells were allowed to adhere to inserts or wells in respective media for 2 h. Once adhered, MDA-MB-231 transwell inserts were added to HMC3 plates and co-cultured for 24 h, with EMEM+ and DMEM+/+ media-only negative controls. See Fig. 1.2. for schematic representation of the co-culture system. See below section outlining co-culture ^{14}C-cystine uptake for assay-specific details.

^{14}C-Cystine Uptake

This protocol was adapted by Jennifer Fazzari and Natalie Zacal from the following papers:

Lutgen *et al*, 2013, Psychopharmacology, 226:531-540.

Shih *et al*, 2006, The Journal of Neuroscience, 26(41):10514-10523.

The cellular uptake of radiolabeled ^{14}C-cystine was quantified in MDA-MB-231 and T47D human breast cancer cells and 4T1 murine adenocarcinoma cells, as cystine uptake is mediated by an exchange with glutamate via system x_C^-. The following steps were performed:

A. Seed cells in a 6-well plate and let the cells adhere overnight or min 4 h.

B. Drug-treat the cells in 300 µl of HBSS for 20 minutes at 37°C.

C. Do not aspirate drug + HBSS. Instead, add the cystine directly to the HBSS and drug on the cells. Make a master mix using 0.45 µl of stock radioactive ^{14}C-cystine per well plus 4.55 µl HBSS per well to bump the volume of radioactive cystine up to 5 µl per well. Multiply these volumes by the number of samples or wells (plus one extra volume) you have to make your master mix.

D. Add 5 µl of the master mix to each well and incubate for 20 minutes in 37°C incubator. Stock radioactive ^{14}C-L-Cystine is 10 µCi in 500 µl or 20 µCi/ml Perkin Elmer Catalog number: NEC845010UC.

E. Quickly wash each well 3x in ice cold HBSS (2 mL per well).

F. Lyse cells in 220 µL of lysis buffer (0.1N NaOH containing 0.1% Triton-X) for 30 minutes.

G. Collect cell lysates into 1.5 mL microtubes.

H. Put 100 µl of each cell lysate into 1 mL of Ecoscint-H solution in a 5 mL plastic scintillation vial. Make a blank using 100ul of lysis buffer in 1 mL of Ecoscint-H solution.

I. Go to the High Throughput Screening Facility to do a scintillation count of your samples using the Beckman LS6500 scintillation counter. Put the scintillation vials into the blue plastic holder (Put the blank in the first position, leave a space, and then load your samples) and load the racks in the machine starting closest to you on the right-hand side in the following order: first the blue holder with the “HALT” card facing you, then another blue holder that you have put your samples into. Hit the 3sec button on the printer until the “Pause” light goes off and make sure the printer is loaded with paper. Using the control buttons on the Beckman counter, select: “Main

Menu", "Count Single Rack", Select "User Program", Enter "15" for 14C with 3-minute reads, hit *Select*, *Select* again, and hit *Start*.

J. Do a Bio-Rad assay of the cell lysate to determine protein concentration for normalizing CPM per mg of protein. Perform a Bio-Rad assay using the cell lysate (or a 1:2 or a 1:3 dilution if appropriate) in a 10ul volume in duplicate or triplicates of a 96-well plate.

Bio-Rad Protein Assay

The Bio-rad protein assay protocol was developed by Dr. Eric Seidlitz and is used to determine protein content in aqueous samples.

A. Label eppendorf tubes for BSA standards and sample dilutions.

B. Prepare the BSA standard by making a stock of ~10 mg/mL BSA powder (in common refrigerator) with Milli-Q water.

C. Make BSA standard dilutions:

a. 2.0 mg/mL

b. 1.0 mg/mL

c. 0.5 mg/mL

d. 0.250 mg/mL

e. 0.125 mg/mL

f. 0.0625 mg/mL

g. 0.0313 mg/mL

D. Prepare BioRad solution in a 1:4 dilution with Milli-Q water (e.g. 3 + 12 mL; 2+8 mL; 2.5+10 mL, etc.).

E. Using a 96-well plate, add 10 µL of each BSA standard (in triplicate) with 3 wells of Milli-Q water as a blank (rows A, B, and C will therefore have 3 blanks plus the 7 different BSA concentrations from wells 4-10).

F. Add 10 μL of each test sample and each dilution (1:10 and 1:100 are usually sufficient) in triplicate to the plate.

G. Add 240 μL of BioRad 1:4 solution to each well; remove unwanted bubbles from the wells.

H. Read plate in BioTek PowerWave XL plate reader at 570 nm (using Eric – BioRad protein protocol)

I. Export data file to Excel then save this file on a 3.5" floppy disc

J. Using Excel, copy the raw absorbance values then Paste Special…Values into the protein measurement template file (v.3) at the appropriate location – the standard curves and equations will be automatically generated.

K. Select the appropriate dilution for each sample that falls within the linear range of thestandard curve and perform the final protein concentration calculation using the equation y=mx+b where x is the average absorbance of the triplicate sample and both m and b are derived from the linear equation generated by Excel from the standard curve.

Amplex Red

Immediately prior to ^{14}C-cystine uptake quantification, growth media samples from 6-well plates were collected and stored at 4 °C. Glutamate release was quantified using the AMPLEX Red glutamic acid assay kit (Invitrogen/Molecular Probes, Eugene, OR, USA). This assay quantitates the fluorescent reaction product resorufin, which is produced in proportion to glutamate, for analysis on a CytoFluor Series 4000 Fluorescence Multi-Well Plate Reader (PerSeptive Biosystems, Framingham, MA, USA). To optimize this assay for measurement of media glutamate concentrations beyond 0.5 μM and eliminate the repeated cycling of glutamate and α-ketoglutarate, L-alanine and L-glutamate pyruvate transaminase were omitted from the reaction mixture [142]. Background glutamate from a media-only control well was subtracted from extracellular glutamate levels in culture media and values were normalized to total protein using the Bradford protein assay, as above. In detail, the following steps were followed:

A. Standard Curve. Complete standard curve using a 96-well place following concentrations in Table 1.1.

B. Assay Plate. Dispense 25 μL of each of the above glutamate concentration tubes into triplicate wells of the assay plate, as per scheme in Fig. 1.1.

C. Sample preparation. Map out sample location on plate, planning for triplicates of each sample. Prepare samples by diluting in 1× reaction buffer (0.5M Tris - pH 7.5). A of 1:5 dilution is recommended, with the aim to bring the sample concentration to within the range of the standard curve. Prepare at least 85 ul (3 x 25 µL plus slight extra) of each sample for triplicates. Pipette 25 µL to each well of the assay plate, as indicated on scheme above. Also pipette 25 µL of 10 µM H_2O_2 into triplicate wells (A1-A3) of the assay plate according to scheme above as a positive control.

D. Assay preparation and initiation for 1 plate. Prepare an assay mix for 100 reactions (2.75 ml) according to the Table 1.2, which will result in the following concentrations of each component:

Amplex Red comes in a 5 mg bottle. To create working stock, add 1923 µl of DMSO to the 5 mg bottle from now on to make 25 µl aliquots of 2.6 µg/µl and then use the entire 25 µl aliquot in the Assay Mix Tube and adjust the 1 × reaction buffer volume accordingly. Pour all of the assay mix into a reagent reservoir (non-sterile). Using a multichannel pipettor, add 25 µL of assay mix to each well of the assay plate, mixing gently by pipetting. Incubate at 37°C for 30 min. Measure fluorescence using an excitation wavelength of 530-560 nm and emission wavelength of ~590 nm (530/25 nm and 580/50 nm in the CytoFluor in room 4-68, with gain set at 40). Plot a standard curve: Fluorescent units on Y-axis versus Glutamate Concentration (µM) on X-axis and find the equation of the

line. Use that formula and the absorbance values for your unknown samples to find their corresponding glutamate concentrations.

Co-Culture ^{14}C-Cystine Uptake

The cellular uptake of radiolabeled ^{14}C-cystine was quantified in HMC3 cells, as cystine uptake is mediated by an exchange with glutamate via system x_C^-. HMC3 cells were co-cultured with wildtype, xCT KD, or vector control MDA-MB-231 cells to quantitate the direct effect of peripherally-released glutamate on microglial functional system x_C^- activity. Specific treatments and co-culture inserts are listed below, with co-culture conditions indicated by square brackets (*i.e.*, [MDA-MB-231]):

A. Naïve HMC3 (media only insert)

B. HMC3 + LPS (1 μg/mL; positive control: microglial activation)

C. HMC3 + LPS + SSZ (200 μM)

D. HMC3 + SSZ (negative control: xCT inhibition, microglia)

E. HMC3 + L-glutamic acid (300 mM, positive control: glutamate)

F. HMC3 + [wildtype MDA-MB-231]

G. HMC3 + [MDA-MB-231 C6 xCT KD]

H. HMC3 + [MDA-MB-231 pLK01 vector only]

I. HMC3 + [MDA-MB-231 + SSZ] (negative control: xCT inhibition, tumour)

The cystine uptake protocol was adapted from previous reports (Miladinovic, Ungard, Linher-Melville, Popovic, & Singh, 2018) and adjusted to include co-culture conditions. Briefly, 2×10^5 HMC3 human microglia cells and wildtype, xCT KD, or vector control MDA-MB-231 carcinoma cells were seeded in respective media in 6-well plates (microglia) or 4 μM pore transwell inserts (carcinoma cells), and allowed to adhere for 2 h. Microglia were then treated with respective agents (LPS, L-glutamic acid) or MDA-MB-231 carcinoma cell inserts (wildtype, C6 xCT KD, vector only, wildtype + SSZ) were added to microglia cultures.

Microglia/carcinoma cell insert co-cultures were incubated together for 24 h, at which point drugs were aspirated or co-culture inserts were removed, microglia plates were washed and exposed to ^{14}C-Cystine (0.015 mCi/mL) for 20 min at 37 °C, excess cystine was washed, and cells were lysed in 220 μL of lysis buffer (0.1 % Triton-X in 0.1 N NaOH) for 30 min. Cell lysates (100 μL) were quantified in 1 mL Ecoscint-H scintillation fluid, values were normalized to mg of total protein using the Bradford protein assay (BioRad) and compared to ^{14}C-cystine uptake in naïve wildtype MDA-MB-231 cells from the same experimental run.

Quantitative Real-Time RT-PCR

In Chapters 3 and 4, total RNA was isolated from each cell lysate and tissue sample using the Qiagen RNAeasy Kit. 400 ng of total RNA was reverse transcribed into cDNA using the SuperScript III kit. Briefly, RNA in the presence of 1 µL of 50 µM oligo(dT)20 and 1 µL of 10 mM dNTP mix (final volume of 13 µL) was incubated on a thermocycler at 65°C for 5 min. Reactions were place on ice prior to adding 4 µL of 5X first strand buffer, 1 µL of 0.1 M DTT, 1 µL RNaseOUT Recombinant RNase Inhibitor, and 1 µL SuperScript III reverse transcriptase for a final volume of 20 µL. Reactions were then incubated at 50 °C for 50 min and 70 °C for 15 min. The resulting cDNA was diluted to a final volume of 60 µL through addition of nuclease-free water and stored at -20°C.

Relative mRNA levels were evaluated by qRT-PCR. Each 12.5 µL reaction contained 2 µL of diluted cDNA, 6.25 µL of SYBR Green premix, and 0.5 µL of 10 µM forward (FOR) and reverse (REV) primer. All target and housekeeping gene primers based on sequences specific for *Mus Musculus* were derived from PrimerBank, with annealing temperatures of 60°C. Official gene symbols, primer sequences, product sizes, and specific melting peaks for each target gene product are listed in Table S1 of Chapter 4. The specifications of the three housekeeping genes used in this study are summarized in Table S2 of Chapter 4. A MiniOpticon 48-well Real-Time PCR System linked to CFX Manager software was programmed with the following cycling parameters: 95°C

for 1 min, 40 cycles of 95°C for 10 sec and 60°C for 25 sec, and a final melting peak determination (95°C for 15 sec, followed by incremental 0.5°C increases of 5 sec from 65°C to 95°C). Reactions for target genes were run in duplicate for each cDNA sample. Parallel duplicate reactions for the appropriate housekeeping gene were carried out to calculate relative mRNA levels using the $2^{-\Delta\Delta C}$ Efficiency testing was achieved by evaluating the slopes derived from plotting the log of a 2-fold serial dilution of murine brain cDNA (template) versus the C_T of each target gene compared to three different possible housekeepers at each template dilution. This test resulted in parallel lines, with slopes of well-matched targets and housekeepers being equivalent and optimally >3. A further test was carried out by plotting ΔC_T values (target C_T at each template dilution minus housekeeper C_T at the equivalent dilution) across the dilution series, which yielded a straight line with a slope close to 0 (< 0.1). Amplification efficiencies were tested for each primer pair, with efficiency (E) = [10 raised to (-1/S)] - 1 (E should be close to 1), and the integrity of each product was verified by gel electrophoresis to validate expected product sizes.

Fluorescent Immunocytochemistry

In Chapter 2, MDA-MB-231 human mammary carcinoma cells and 4T1 murine carcinoma cells were fluorescently stained for xCT with DAPI counterstain using immunocytochemistry. In Chapter 4, HMC3 human microglia calls were fluorescently co-stained for xCT and Iba1 with DAPI counterstain. The protocol below was optimized for each cell line and antigen of interest to minimize background fluorescence and autofluorescence over several optimization attempts.

A. Seed 10^4 cells/well in 8-well chamber slides (Ibidi, Martinsried, Germany). Allow to adhere overnight at 37 °C.

B. Gently aspirate media from chambers (use pipette for gentler approach than glass aspirater), wash with PBS.

C. Fix with 10% formalin, gently wash cells with PBS.

D. Permeabilize with 400 µL 0.1% Triton X-100, 10 min; wash 3 ×

E. Block with 1% bovina serum albumin (BSA) in PBS 20 min

F. Primary antibody incubation: 1:1000 anti-Iba1, 2 h at RT; wash 3×

G. Secondary antibody incubation: 1:1000 AF647, 12 h at 4 °C; wash 3×

H. Block: 10 % rabbit serum; 1 h at RT

I. Primary antibody incubation: 1:1000 anti-xCT, 2 h at RT; wash 3 ×

J. Secondary antibody incubation: 1:1000 AF488, 12 h at 4 °C; wash 3 ×

K. Coverslip with DAPI anti-fade, cure overnight, seal and store in the dark at 4 °C for several months (image immediately if possible for optimal fluorescent signal)

Tissue Collection and Preservation / *Ex Vivo* Immunofluorescence

In Chapters 2, 3, and 4, select *ex vivo* tissues were processed and immunofluorescently stained for antigens of interest (Chapter 2: xCT and cytokeratin 7 in tumour-bearing femurs; Chapter 3: Iba1 and xCT in spinal cord, lumbar vertebrae 4; Chapter 4, Iba1 in contralateral hippocampi dentate gyrus and Cornu Ammonis 1 regions) with DAPI counterstain.

Under sodium pentobarbital anesthetic (90 mg/kg, i.p.), animals were perfused with 100 mL cold PBS, immediately followed by 100 mL freshly prepared cold 4 % paraformaldehyde (PFA). Tissue of interest were microdissected, post-fixed in 4 % PFA for at least 48 h, and decalcified in 10 % Ethylenediaminetetraacetic acid (EDTA) for 14 days with EDTA replaced every 2-3 days. Once decalcification was confirmed, tissues were dehydrated under the protocol found in Table 1.3. using the Shandon Citadel 2000 Paraffin Processing System, and paraffin-embedded for histological analyses. Following Paraffin processing, tissues were microtome sectioned at 5 μm and slide mounted on Superfrost Plus charged microscope slides (Thermo Fisher Scientific), baked at 60 °C for 2 h, and cooled. Slides were then rehydrated using the following schedule:

A. Xylene I: 4 min

B. Xylene II: 4 min

C. Xylene III: 4 min

D. Xylene IV: 4 min

E. 100 % EtOH I: 10 min

F. 100 % EtOH II: 10 min

G. 95 % EtOH: 5 min

H. 70 % EtOH: 5 min

I. 50 % EtOH: 5 min

J. ddH_2O

Slides were then subjected to the following steps for fluorescent staining:

A. Antigen retrieval in EDTA (pH 8, 95 °C) for 20-30 min (allow 10 min to cool for delicate tissues), wash 3 × with TBS-T.

B. Draw hydrophobic barrier, as necessary, to separate contol from experimental tissue on the same slide. Block using DAKO protein block, 20 min at RT.

C. Probe for select primary antibody (*i.e.*, rabbit anti-xCT, Novus Biologicals, NB300-318) at a concentration of 1:1000 (to be otimized for each antibody/tissue combination, diluted in TBS-T, 2 h at RT (minimum) or up to overinight at 4 °C; wash 3 × with TBS-T. Omit primary antibody for control

tissue; replace with respective isotype control at the same dilution (*i.e.*, 1:1000 rabbit IgG in TBS-T).

D. Incubate with respective secondary antibody (*i.e.*, goat anti-rabbit AF488), diluted in TBS-T, 2 h at RT or up to overinight at 4 °C; wash 3 × with TBS-T. NB: from this step forward, slides are light-sensitive. Protect from ambient light exposure to avoid fluorescence fading.

E. If co-labelling several antigens of interest, repeat steps C-D as required. NB: Effort should be made to select primary antibodies raised in different species. However, primary antibodies are frequently raised in rabbit. If it is not possible to select antibodies raised in different species, tissues must first be blocked with rabbit serum following the first primary-secondary antibody pair to prevent nonspecific staining (*i.e.*, first antibody pair: rabbit anti-xCT primary antibody, goat anti rabbit AF488 (FITC), **block with 10% rabbit serum 2 h**; proceed to second antibody pair: rabbit anti-Iba1 primary antibody, goat anti rabbit AF647 (far red), **block with 10% rabbit serum 2 h**; proceed to third antibody pair, etc.). Following final primary-secondary antobody pair, proceed to step F.

F. Wash 3 × TBS-T, 1 × ddH_2O, gently dry slide with kim wipe, avoiding tissue area. Remove hydrophobic barrier with cotton tip, if necessary. Coverslip with small amount of antifade medium, avoiding any air between slide and coverslip, and allow to cure overnight in the dark at RT. Seal with nail polish,

dry, and image using EVOS Imaging System (McMaster Biophotonics Facility). Protect from light; store at 4 °C for several months.

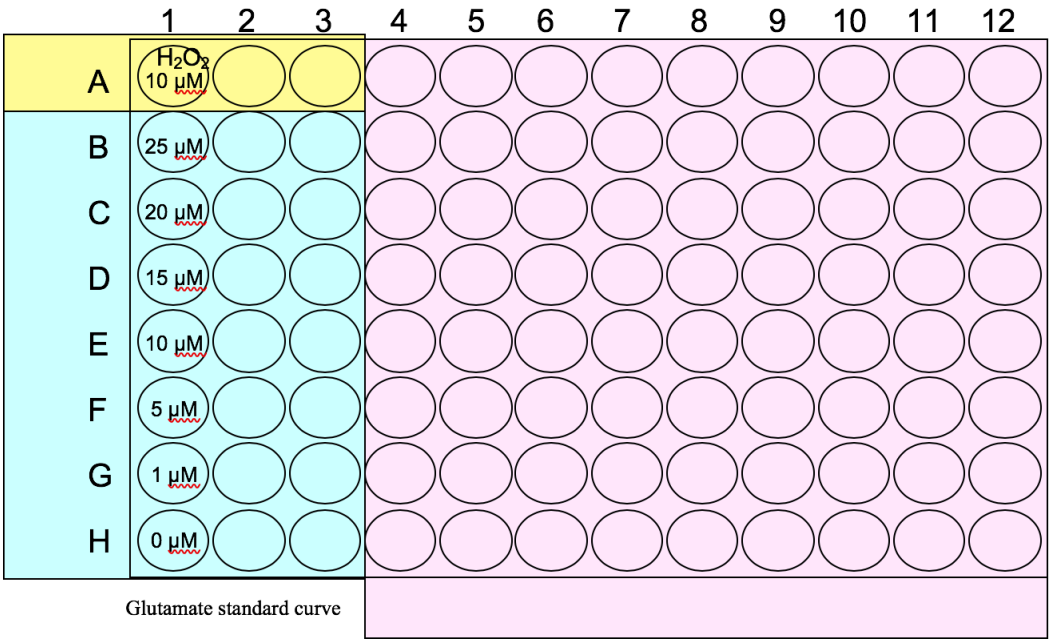

Figure 1.1. Assay Plate for Amplex Red.

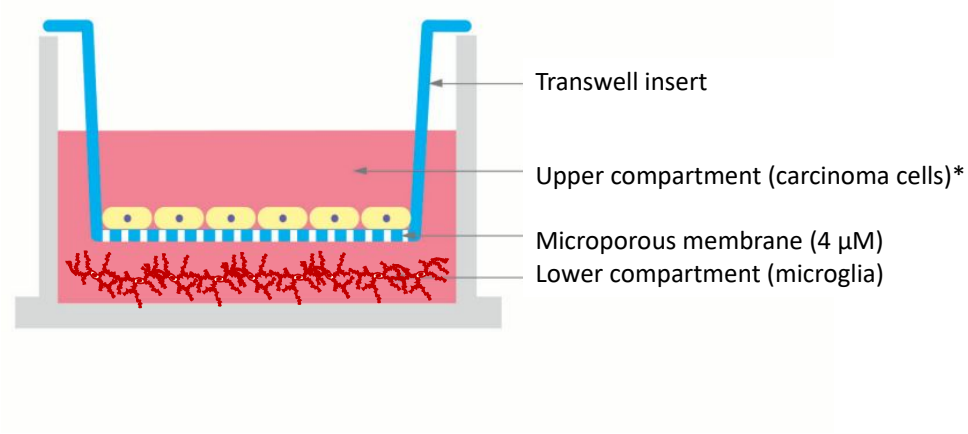

Figure 1.2. Co-culture system. Transwell inserts (4 µM pore size) were plated with MDA-MB-231 carcinoma cells and added to 6-well plates previously plated with HMC3 human microglia to create co-culture conditions. * refers to all MDA-MB-231 carcinoma cells, including: naïve MDA-MB-231, MDA-MB-231 + sulfasalazine, MDA-MB-231 C6 xCT KD, MDA-MB-231 vector only (negative control) and media only control. Figure adapted from supplier materials (Corning, New York, United States).

[Glutamate]	Volume of 25uM Glutamate Solution	Volume of 1x Reaction Buffer
25 uM	100 ul	0 ul
20 uM	80 ul	20 ul
15 uM	60 ul	40 ul
10 uM	40 ul	60 ul
5 uM	20 ul	80 ul
1 uM	4 ul	96 ul
0	0 ul	100 ul

Table 1.1. Glutamate concentrations for Amplex Red standard curve.

Reagent	Volume to Add to Assay Mix Tube	Final Concentration in Assay Mix Tube	Final Concentration in Assay Plate
1x Reaction Buffer	2694 ul	-	-
HRP, **100 U/ml**	6.9 ul	0.25 U/ml	0.125 U/ml
L-Glutamate Oxidase, **5 U/ml**	44 ul	0.08 U/ml	0.04 U/ml
Amplex Red	4.65 ul (or the entire 5 ul Amplex Red aliquot)	0.026 ug/ul	0.013 ug/ul

Table 1.3. Amplex Red Assay Mix Preparation.

STEP	SOLUTION	Program A: Processing Time (hr:min)	Program D: Processing Time (hr:min)
1	PBS	0:30	0:30
2	50% Ethanol	0:30	0:30
3	70% Ethanol	1:00	1:00
4	90% Ethanol	1:00	1:00
5	100% Ethanol I	1:00	1:00
6	100% Ethanol II	2:00	2:00
7	100% Ethanol III	2:00	2:00
8	Histoclear I	1:00	1:00
9	Histoclear II	1:30	1:30
10	Histoclear III	1:30	1:30
11	Paraffin I	2:00	PASS
12	Paraffin II (Vacuum)	3:00	3:00
	Total time	*17:00*	*15:00*

Table 1.3. Dehydration processing schedule for immunohistochemistry for small (Program A) and large (Program D) tissues.

APPENDIX 2

Co-authored Papers

and Other Published Works

Oncodynamics: Effects of Cancer Cells on the Body

Together with several other members of the Singh Lab, the textbook *Oncodynamics: Effects of Cancer Cells on the Body* was published in 2016. This literature served to introduce new terminology to the field of oncology, subdividing it into oncokinetics—the mechanics of the tumor cells as they arise and spread throughout the body—and oncodynamics—the impact of abnormal cues generated by tumors on the physiological functioning of the body. This textbook outlined the importance of oncodynamics from both a cancer patient's and a caregiver's perspectives, stressing its significant impact on cancer patient functionality and the opportunity that cancer researchers will have to develop cross-disciplinary interactions and predict potential consequences of tumors and/or treatment. I am primary author of Chapter Three: *Cancer-induced Neurogenesis*; this publication (2016) can be found here: https://www.springer.com/gp/book/9783319285566.

Glutamate Dysregulation in Central Pathologies

This review served to discuss the role of glutamate dysregulation across several pathological states, including CIP. As the major excitatory neurotransmitter in the mammalian central nervous system, glutamate plays a key role in many central pathologies, including gliomas, psychiatric, neurodevelopmental, and neurodegenerative disorders. Post-mortem and serological studies have implicated glutamatergic dysregulation in these pathologies, and pharmacological modulation of glutamate receptors and transporters has provided further validation for the involvement of glutamate. Furthermore, efforts from genetic, in vitro, and animal studies are actively elucidating the specific glutamatergic mechanisms that contribute to the aetiology of central pathologies. However, details regarding specific mechanisms remain sparse and progress in effectively modulating glutamate to alleviate symptoms or inhibit disease states has been relatively slow. In this report, we review what is currently known about glutamate signalling in central pathologies. We also discuss glutamate's mediating role in comorbidities, specifically cancer-induced bone pain and depression. This work has been published in Biomolecules (2015) and is available in full here: https://www.ncbi.nlm.nih.gov/pubmed/26569330.

Preparation of tetrazine-containing [2 + 1] complexes of ^{99}mTc and in vivo targeting using bioorthogonal inverse electron demand Diels-Alder chemistry.

The aim of this work was to synthesize and evaluate [2 + 1] ^{99m}Tc(i) polypyridine complexes containing tetrazines, which along with the corresponding Re(i) complexes, represent a new class of isostructural nuclear and turn-on luminescent probes that can be derivatized and targeted using bioorthogonal chemistry. To this end, [2 + 1] complexes of ^{99m}Tc(i) of the type [^{99m}Tc(CO)$_3$(N^N)(L)] (N^N = bathophenanthroline disulfonate (BPS) or 2,2'-bipyridine (bipy)), where the monodentate ligand (L) was a tetrazine linked to the metal through an imidazole derivative, were prepared. The desired products were obtained in nearly quantitative radiochemical yield by adding [^{99m}Tc(CO)$_3$(N^N)(OH$_2$)]^n to the imidazole-tetrazine ligand and heating at 60 °C for 30 min. Measurement of the reaction kinetics between the tetrazine and (E)-cyclooct-4-enol revealed a second-order rate constant of 8.6×10^3 M^{-1} s^{-1} at 37 °C, which is suitable for in vivo applications that require rapid coupling. Stability studies showed that the metal complexes were resistant to ligand challenge and exhibited reasonable protein binding in vitro. Biodistribution studies of the more water-soluble BPS derivative in normal mice, one hour after administration of a bisphosphonate derivative of trans-cyclooctene (TCO-BP), revealed high activity concentrations in the knee (9.3 ± 0.3 %ID g^{-1}) and shoulder (5.3 ± 0.7 %ID g^{-1}).

Using the same pretargeting approach, SPECT/CT imaging showed that the [2 + 1] tetrazine complex localized to implanted skeletal tumors. This is the first report of the preparation of ^{99m}Tc complexes of BPS and demonstration that their tetrazine derivatives can be used to prepare targeted imaging probes by employing bioorthogonal chemistry. This work has been published in Biomolecules (2017) and is available in full here: https://www.ncbi.nlm.nih.gov/pubmed/28640297.